UNIVERSITY OF SOUTHAMPTON

FACULTY OF NATURAL AND ENVIRONMENTAL SCIENCES

Ocean and Earth Science

Beyond the Tipping Point: Temporary Resilience of the Atlantic Meridional Overturning Circulation

by

Rosalind K. Haskins

Thesis for the degree of Doctor of Philosophy

April 2019

UNIVERSITY OF SOUTHAMPTON

ABSTRACT

FACULTY OF NATURAL AND ENVIRONMENTAL SCIENCES

Ocean and Earth Science

Doctor of Philosophy

BEYOND THE TIPPING POINT: TEMPORARY RESILIENCE OF THE ATLANTIC MERIDIONAL OVERTURNING CIRCULATION

By Rosalind K. Haskins

The Atlantic meridional overturning circulation (AMOC) is projected to weaken due to anthropogenic climate change, partially due to ice melt freshening the North Atlantic Ocean. In order to successfully mitigate climate change it is important to consider the reversibility of temporary forcing and explore longer-term changes to the ocean state. We apply freshwater forcing to the North Atlantic and Arctic regions for various durations in global climate models (GCMs) to understand the impacts on North Atlantic density and AMOC strength. Firstly, the processes and timescales of the recovery phase were explored by considering the roles of salinity and temperature in AMOC recovery following a weakening. The behaviour of the AMOC was well reconstructed by applying 'rotated geostrophy' to meridional density gradient profiles between 50°N and 30°S. This makes it possible to determine the role of ocean and surface fluxes in the North and South Atlantic. Changes at 50°N dominate the weakening and early recovery. The magnitude of the overshoot to high AMOC transports in the recovery phase was related to density changes in the South Atlantic. This method was then applied to permanent hosing simulations in 2 GCMs in order to establish the changing mechanisms of AMOC weakening as the freshwater input increased. A change in AMOC weakening mechanism was found to coincide with the 'tipping point' for non-recovery. To explore this, a range of temporarily forced simulations was used to understand the role of feedbacks in the recovering and non-recovering ocean states. A positive salt advective feedback was found for the region 30°N in the Atlantic to the Bering Strait. However more locally to the region of convection, changes to the surface freshwater flux resulted in a positive freshwater feedback – which partially compensated for the removal of freshwater forcing and so supported the weak AMOC state.

Table of Contents

Table of Tables

Table of Figures

Academic Thesis: Declaration Of Authorship

I, Rosalind K. Haskins, declare that this thesis and the work presented in it are my own and have been generated by me as the result of my own original research.

Beyond the Tipping Point: Temporary Resilience of the Atlantic Meridional Overturning Circulation

I confirm that:

1. This work was done wholly or mainly while in candidature for a research degree at this University;
2. Where any part of this thesis has previously been submitted for a degree or any other qualification at this University or any other institution, this has been clearly stated;
3. Where I have consulted the published work of others, this is always clearly attributed;
4. Where I have quoted from the work of others, the source is always given. With the exception of such quotations, this thesis is entirely my own work;
5. I have acknowledged all main sources of help;
6. Where the thesis is based on work done by myself jointly with others, I have made clear exactly what was done by others and what I have contributed myself;
7. Parts of this work have been published as:

Haskins RK, Oliver, KIC, Jackson LC, Drijfhout SS, Wood RA (2018) Explaining asymmetry between weakening and recovery of the AMOC in a coupled climate model. Clim Dyn, 0(0):1–13. http://doi.org/10.1007/s00382-018-4570-z

Haskins RK, Oliver KIC, Jackson LC, Wood RA, Drijfhout SS (2019) Temperature domination of AMOC weakening due to freshwater hosing in two GCMs. Clim Dyn 0(0):1–14. https://doi.org/10.1007/s00382-019-04998-5

Signed: 

Date: 14.12.19

Acknowledgements

First and foremost I would like to express my gratitude to my supervisory team, who advised me through the many iterations of written work and mountains of figures until I got my bearing, at which point they allowed me the freedom to direct my own research. The first 2 results chapters also benefitted from the feedback of 2 anonymous reviewers, whose suggestions led to significant improvements. I would also like to thank my initial Panel Chair Gerard McCarthy for his attention to detail in his feedback on my early written work and helping me to get on a research cruise. Thanks are also due to Jeremy Grist for stepping in to be my Panel Chair for the final year.

I would also like to state my appreciation for Jeff Blundell spending hours with me in the Linux Suite teaching me to use the command line interface, to hack code, and for introducing me to the world of high-performance clusters. I am also very grateful to Robin Smith for his assistance in the running of FAMOUS, and for his patience through our extensive troubleshooting emails.

I'd like to thank my NOCS colleagues Ella Mcknight, Neela Moraji, IT Rob (Jones), Xiaodong Yang and Johnny Harrison for their comradeship, humour, and constant willingness to raise a drink to the highs and lows of PhD life. Finally, I'd like to recognise the huge contribution made over the years by my partner Gavin Haughton, who went through every step of the PhD with me, feed me coffee, and made me a daily pack lunch. Gavin made it a happier, healthier, and less stressful experience than it would otherwise have been.

Definitions and Abbreviations

AABW	Antarctic bottom water
AMOC	Atlantic meridional overturning circulation
APE	Available potential energy
D-O	Dansgaard–Oeschger
GCM	Global climate model
ITCZ	Intertropical convergence zone
KE	Kinetic energy
MLD	Mixed layer depth
NADW	North Atlantic deep water

Chapter 1: Introduction

In order to lay the basis for the research presented in this thesis I will begin with an overview of existing research. In **Section 1.1** I will introduce the Atlantic meridional overturning circulation (AMOC) in general terms and present some of the research on the AMOCs past from paleoclimate studies using a combination of models and ice/sediment core analysis. I will also explore some of the projections of how anthropogenic climate change may impact the strength of the AMOC, and the serious repercussions this may have for weather and climate patterns. I will then consider thermohaline forcing in **Section 1.2**, which can control AMOC strength via changes in buoyancy. On longer, millennial, timescales the AMOC is controlled by mechanical energy sources that will be described in **Section 1.3**. Following this I will take a more focused look at the literature that helped to define my experimental design in **Section 1.4**, before giving an outline of the original research in the remainder of this thesis in **Section 1.5**.

1.1 The Atlantic meridional overturning circulation

The AMOC is an oceanic flow that may be described as a system of currents carrying warm buoyant waters to high northern latitudes, balanced by cool deep return flows. More mathematically it can be defined as the ocean velocity field across the Atlantic basin, integrated zonally (Huisman et al. 2010). Surface waters are most strongly warmed by insolation at low latitudes. As waters travel northward in the Atlantic they are both freshened by precipitation and cooled by contact with an increasingly cold overlying air mass. Of these two influences temperature wins out over salinity and the water becomes sufficiently dense to sink down through the water column. However, were the surface waters of the North Atlantic to become freshened by increases in ice melt, precipitation, and river runoff, the increasing buoyancy of the waters would reduce downwelling. Buoyancy plays an important role due to its impact on the meridional Atlantic density gradient, where the more dense the North Atlantic is compared to the South Atlantic, the stronger the overturning (Cimatoribus et al. 2014).

This complex 3 dimensional system of currents can be simplified by considering the basin-wide zonal mean transport, which gives the meridional overturning cell **Figure 1.1a**. The AMOC transports waters between the Southern Ocean and the highest northern latitudes **Figure 1.1b**, with some weak transport through the Bering Strait into the Pacific Ocean. Ganachaud and Wunsch (2000) were able to estimate the strength of the transports across the ocean basins at multiple latitudes using a combination of hydrographic sections, transports of boundary currents, and Ekman transports estimated from satellite wind observations, **Figure 1.1b**. Their technique identified a transport of 16±2 Sv across the Atlantic at 24˚N. Lumpkin and Speer (2003, 2007) furthered this technique with the inclusion of air-sea flux estimates in order to constrain deep-water formation rates. This gave transports of 17.2±1.8 Sv across the Atlantic at 24˚N **Figure 1.1a**. Throughout the meridional extent of the Atlantic, the AMOC net transports warmth northwards and coolness southwards. It is the primary cause of inter-hemispheric asymmetries in climate, exporting 0.5 PW of heat across the equator, warming the northern hemisphere relative to the southern hemisphere (Buckley and Marshall 2016).

Observations of the AMOC were until recently both temporally and spatially sparse (Bryden et al. 2005). The strength and vertical structure of the AMOC has now been tracked by a series of moorings across the Atlantic basin at 26˚N by the joint UK RAPID-US Meridional Overturning Circulation and Heatflux Array (MOCHA) project. These have been providing a continuous time series since 2004, highlighting the high frequency variability of transports and enabling research into the connection between ocean transports, sea surface temperatures and seasonal-scale climate events. They have shown mean AMOC strengths of 17.2 Sv (with intra-annual variability of ~30 Sv (Srokosz and Bryden 2015)) and mean heat transport of 1.25 PW over the years 2004–2012 (McCarthy et al. 2015). Further moorings and gliders are deployed across the sub-polar North Atlantic in order to monitor the AMOC at higher latitudes (Hand 2016) and in the South Atlantic (Ansorge et al. 2014). The overturning in the sub-polar North Atlantic program (OSNAP) is intended to provide measures of heat and freshwater flux, determine overflow pathways, and to describe the relationship between deep-water formation and AMOC variability. While still being in the early years, and so not able to determine longer-scale variability, OSNAP has shown stronger than expected variations in transports and suggests that the dense water formation in

the Irminger and Iceland basins may be more strongly related to AMOC variability than are changes in the Labrador Sea (Lozier et al. 2019). Given time to develop longer time series, these arrays will enable greater insight into the extent of the meridional coherence of the AMOC.

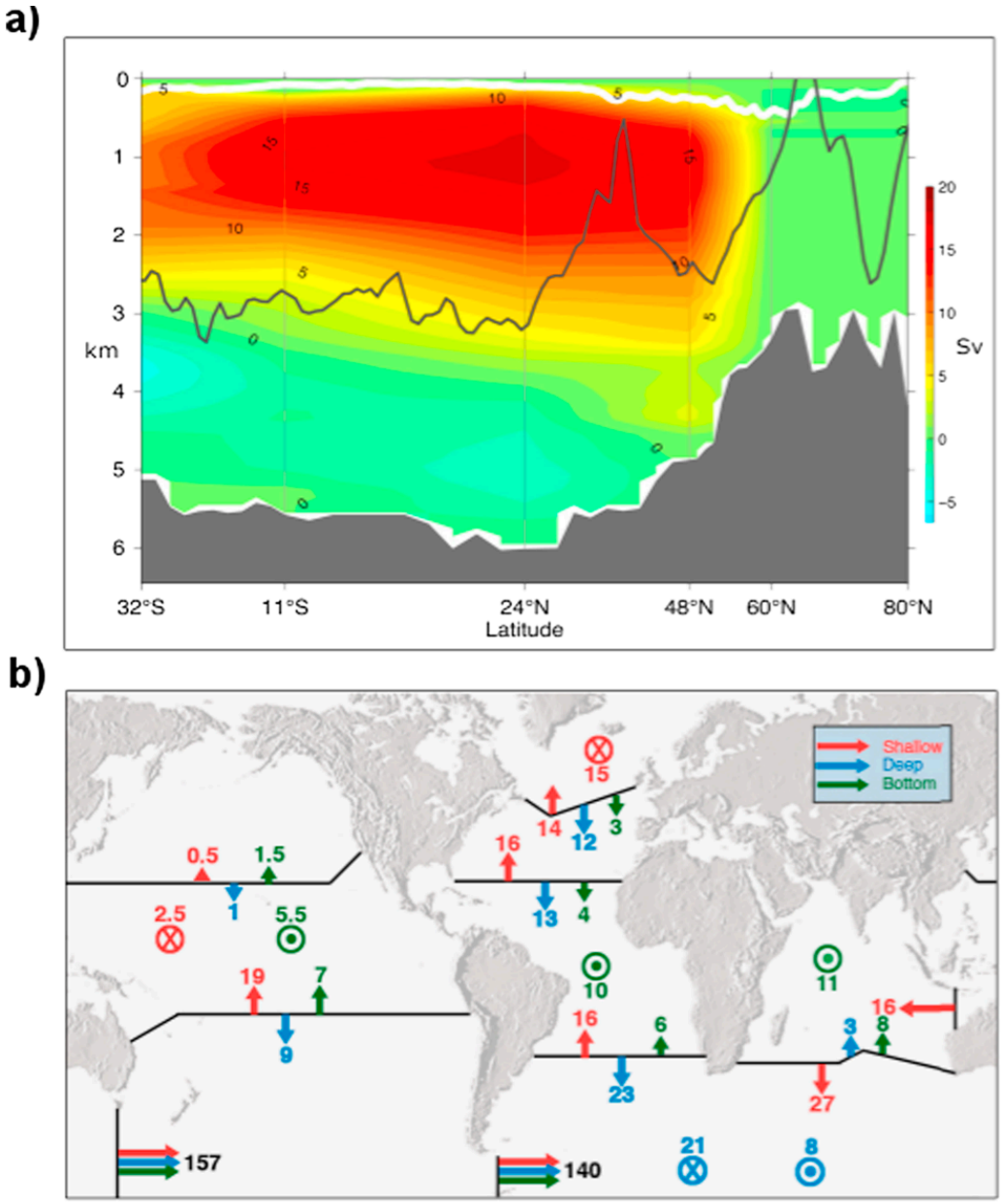

Fig. 1.1 a: Mean Atlantic meridional overturning stream function from tracer inversion. Grey shading: maximum depth in the Atlantic at each latitude, black line: crest of the Mid-Atlantic Ridge. White line near the surface: the deepest (climatological) mixed layer depth. **b**: Estimated global ocean circulation patterns based on the box model inversion of Ganachaud and Wunsch (2000). **Arrows** indicate volume transports in Sverdrup (where 1 Sv = 10^6 m^3 s^{-1}). **Red**: shallow (<2 km), **blue**: deep (2–4 km), **green**: bottom (>4 km). **Open circles** indicate regions of vertical transport (dot for upwelling and cross for downwelling). Taken from Buckley and Marshall (2016), see references within

1.1.1 Evidence of AMOC variability in the paleo-record

Due to the significant role that the AMOC plays in the global climate system, it is extremely important to try to understand the potential for large-scale AMOC variability. While the observational record for the AMOC is starting to give us greater understanding of the intra- to inter-annual variability in the current climate, the use of isotopic analysis and ice and sediment cores gives an indication of the role of the AMOC in past abrupt climate change events. The use of climate models alongside isotopic and sediment analysis helps to identify broader spatial patterns, and mechanisms, and to suggest locations for further sampling to best investigate phenomenon of interest. Isotopic analysis can focus on any time within the core record, with a recent study exploring AMOC decline over the previous century (Thibodeau et al. 2018). Paleoclimate research on glacial-interglacial periods has taken a strong interest in deep-sea circulation, due to the deep-ocean containing the majority of mass, thermal inertia and carbon in the ocean-atmosphere system (Adkins 2013). Due to this profound oceanic carbon reservoir, past variations of atmospheric CO_2 cannot be fully explored without an understanding of the deep ocean carbon reservoir and its ventilation. Exploring paleo-oceanographic dynamics enables us to explore the degree of change possible with different forcings, and understand how these changes may have interacted with the surrounding climate.

The sedimentary record shows evidence of large-scale ice rafting events known as Heinrich events (Heinrich 1988) associated with changes in atmospheric CO_2 levels (Ahn and Brook 2014), where glacial instability leads to armadas of icebergs breaking away and drifting southwards in the Atlantic, distributing debris as they melt. The melting icebergs cause surface freshening and cooling, and are associated with AMOC decline. Brown and Galbraith (2016) found that by forcing the AMOC with freshwater they were able to recreate climate impacts consistent with Heinrich Stadials. However, the full Heinrich event climate likely results from a combination of concurrent changes including altered atmospheric circulation patterns induced by melting ice sheets reducing topographic height (Roberts et al. 2014). The response of atmospheric CO_2 levels to changes in the AMOC may act as an internal negative feedback. During Heinrich Stadial cold events, the AMOC is weak and CO_2 levels slowly increase – which triggers a transition to warm conditions, with strong AMOC and gradually reducing CO_2 levels, which eventually result in abrupt cooling (Zhang et al. 2017).

The isotope record of atmospheric temperature developed from Greenland ice cores has been used to identify abrupt climate changes within the last glacial period (Dansgaard et al. 1993). This was done by analysing the deviation of the ratio of 2 oxygen isotopes (δ18O/16O) in the ice cores, which is used as an indicator of the temperatures when the ice formed. Dansgaard–Oeschger (D-O) events consist of rapid warming of the northern hemisphere (10 ˚C within decades) followed by a slower period of cooling (centennial scale), which may be 'kick started' by Heinrich events **Figure 2** (Peltier and Vettoretti 2014). While the cause of D-O events is controversial (Timmermann et al. 2003), core analysis has been used to demonstrate that the Greenland temperature changes follow Antarctic climate changes by a couple of centuries (Dima et al. 2018). It has been suggested that the cooling of North Atlantic air temperature may be driven by AMOC weakening resultant from North Atlantic freshening by ice melt (Zhang et al. 2014). By contrasting the Greenland ice cores with Antarctic ice cores the D-O events have been found to show inter-hemispheric coupling, with a bi-polar seesaw (Crowley 1992), with the northern hemisphere warming when the AMOC is strong, and cooling when it is weak (Peltier and Vettoretti 2014).

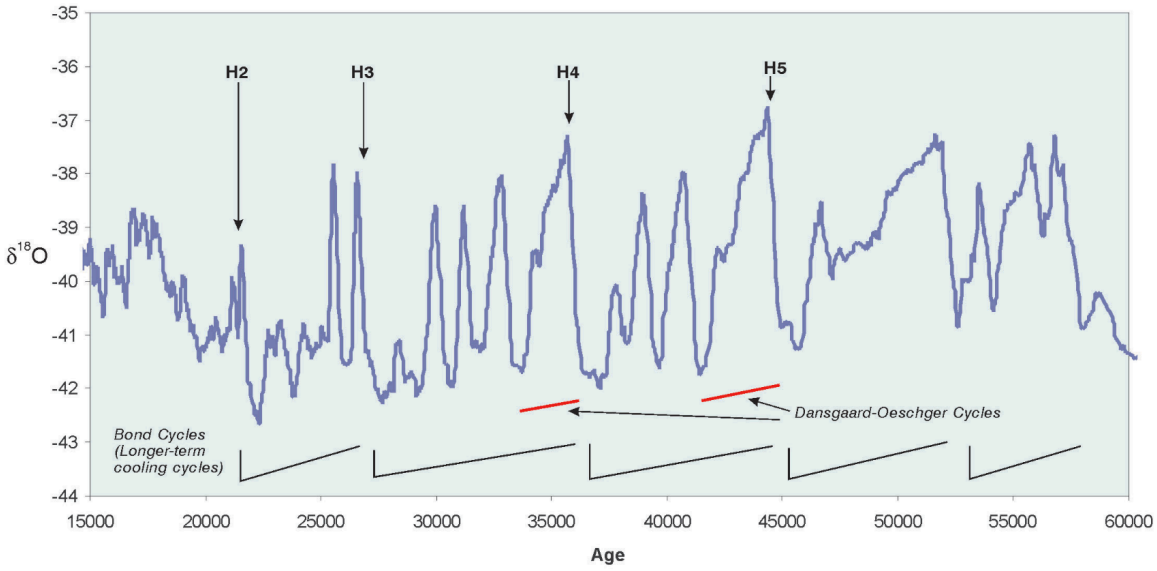

Fig. 1.2 Oxygen isotope record for the Last Glacial Maximum from Greenland Ice Core Project ice core, showing Dansgaard–Oeschger cooling cycles, with Heinrich (H) rapid warming events marked. Figure taken from Delaney (2003)

The underlying physics of the D-O events may be related to changes in the meridional salt gradient between the low and high latitude North Atlantic (Peltier and Vettoretti 2014). When the AMOC is weak, high latitude salinity decreases and low latitude salinity increases. This meridional gradient increases until a threshold is reached, and a high salinity flux travels northwards. When these high-density waters reach the convective region they reinvigorate the AMOC, leading to warm interstadial conditions. A coupled climate model simulation (Vettoretti and Peltier 2016) found that during the cold phase, thermal convective instability due to subsurface warming was inhibited by a stabilising vertical salinity gradient. However, when high salinity waters are transported into the region from low latitudes, this enables convective instability to occur below the sea ice, leading to the formation of a winter polynya in the North Atlantic and the rapid retreat of sea ice. The formation of this glacial North Atlantic super-polynya was then considered to characterise the transition to a warmer state during a D-O event. Wary et al. (2017) have suggested that the subsurface warming might have caused ice melt, leading to enhanced iceberg releases from the bordering ice sheets, giving a positive feedback on freshwater release.

The ratio of stable isotopes Carbon-13 and Carbon-12 (δ13C) in the sediment record, found in microfossil shells of both epibenthic (sea floor dwelling) and planktonic (free drifting) foraminifera, can be used to indicate the location and extension of water masses and ocean transport strengths (Henry et al. 2016). Water ventilated in the North Atlantic is seen to have a more positive isotopic signature than does water ventilated in the South Atlantic enabling the meridional reach of water masses through the basin to be tracked in the sediments. For example, Hudson Strait (freshwater release) events are associated with a lower δ13C on the Bermuda Rise, which suggests that the AMOC was weak relative to the AABW (Henry et al. 2016). Comparison of the δ13C age difference between paired planktonic and benthic foraminifera can give an indication of ocean circulation strength. Skinner and Elderfield (2007) used benthic foraminiferal magnesium to calcium (Mg/Ca) ratios to understand changes in deep ocean temperature. As calcite takes up more magnesium at warmer temperatures, the greater the Mg/Ca ratio, the warmer the conditions in which the crystal grew. Their study showed that sudden temperature changes over Greenland (using δ18O/16O) and in the deep North Atlantic (using Mg/Ca) were coupled, via

perturbations in AMOC strength (using epibenthic δ13C for the deep water ventilation timescale).

The ratio of uranium decay products Protactinium-231 (Pa) and Thorium-230 (Th) in sediments is used as a kinematic proxy for the AMOC (McManus et al. 2004; Henry et al. 2016). Uranium dissolves in the ocean and becomes well mixed, due to its long residence time. Pa and Th are both absorbed onto the surfaces of suspended particles, which become deposited on the ocean floor and thereby enter the sedimentary record. Th is more efficiently scavenged from the water column than is Pa, which gives the latter a greater ocean residence time. Pa is therefore more likely to be redistributed laterally, with its deposition pattern reflecting changes in basin scale circulation (Henry et al. 2016). McManus et al. (2004) found that the AMOC was significantly reduced during the coldest deglacial interval in the North Atlantic region, beginning with a catastrophic iceberg discharge Heinrich event, 17,500 yr ago, and declined sharply but briefly into the Younger Dryas cold event, about 12,700 yr ago. Following these cold events, the 231Pa/230Th record indicates that rapid accelerations of the AMOC were concurrent with the two strongest regional warming events during deglaciation (McManus et al. 2004). Some studies link this with the AMOC not just recovering, but temporarily exceeding its initial strength (Henry et al. 2016).

Wan et al. (2010) found basin wide sea surface salinity increase in the tropical North Atlantic during periods of weak AMOC, in line with reconstructed paleo-salinity. In their model, this was primarily controlled by the atmospheric response (changes in the wind fields) to North Atlantic cooling. Wan et al. (2010) finds that AMOC weakening reduces North Atlantic heat content, impacting the overlying atmosphere via changes to the surface fluxes. This then feeds back into the ocean, via changes in wind forcing, impacting gyre transport and therefore ocean advective salinity transports.

The North Pacific does not currently exhibit overturning due to strong density gradients primarily resultant from geographical factors (Rahmstorf et al. 1996), as the fresh surface waters and strong stratification prevent deep-water formation occurring. Some freshwater forcing simulations have shown AMOC weakening to

be in part compensated for by the development of meridional overturning in the Pacific (Saenko et al. 2004; Hu et al. 2012a). In these models the Bering Strait tends to be closed to advective transport, cutting off transfers of heat and salinity (Hu et al. 2012a). Global sea level is believed to have been ~50 m lower during the time of the Heinrich Events (Lambeck and Chappell 2001), effectively closing the shallow Bering Strait (Hu et al. 2010) and enabling a Pacific-Atlantic see-saw in meridional overturning (Hu et al. 2012a). It has also been suggested that during the weak AMOC of the Younger-Dryas event, the Pacific thermohaline was weaker than in modern times (Marotzke 2000). As the modern ocean has an open Bering Strait, Pacific overturning would not be expected to occur due to a modern AMOC collapse.

1.1.2 Projected impacts of anthropogenic climate change

Climate projections suggest that the AMOC will weaken over the next 100 years due to anthropogenic climate change, though models forced with likely anthropogenic forcing generally do not show AMOC collapse (Jungclaus et al. 2006; Stouffer et al. 2006; Driesschaert et al. 2007; Collins et al. 2013). The AR3 IPCC report showed an average reduction of 25-30% for the A1B scenario running up to 2100 (Schmittner et al. 2005; Jungclaus et al. 2006). The AR5 IPCC report gave a range of AMOC weakening during the 21st century of 11% for RCP2.6 to 34% for RCP8.5 (Collins et al. 2013). However, these model scenarios generally do not include North Atlantic freshening from Greenland ice sheet melt. Projected increases in Greenhouse gas concentration may warm the Greenland annual average temperature by 3 ˚C by 2100 (Gregory et al. 2004). A temperature increase of as little as 1.6 ˚C may be sufficient to gradually eliminate the Greenland ice sheet (Robinson et al. 2012). Such ice melt would release profound quantities of freshwater into the North Atlantic, reducing local density and potentially rising global sea level by ~7 m over a millennium (Gregory et al. 2004). Even if global average temperatures were later brought back down to pre-industrial levels the ice sheets would return, if at all, over a longer timescale. This means that the input freshwater would remain in the oceans, and the anomaly would be dissipated and redistributed by ocean circulation. The warm fresh summers associated with increased North Atlantic sea surface temperatures can also delay wintertime convection. This leads to a reduction in convective

freshwater export, allowing for anomalous freshwater to remain in the Irminger Sea region, allowing the freshening to build year on year (Oltmanns et al. 2018).

Models using radiative forcing with dynamic ice sheets have found the initial AMOC weakening due to atmospheric warming to be later reinforced by freshening from melt water (Levermann et al. 2005; Gierz et al. 2015). When freshwater input from Greenland ice melt (Jungclaus et al. 2006) is included in the IPCC simulations (Schmittner et al. 2005) the AMOC reduces by 35% and 42%, for conservative and high melting estimates respectively. Bakker et al. (2016) used radiative forcing with Greenland ice melt in longer simulations, and found an 11% chance of AMOC collapse with 6 K of warming, and 30% chance for 8 K warming. While the impact of the ice melt on the AMOC can be relatively weak, the scale of the AMOC response to forcing may vary with the initial ocean state (Mikolajewicz et al. 2007).

Large reductions in the size of the Greenland ice sheet have been found to correspond to temporary reductions in the strength of the AMOC (Driesschaert et al. 2007). A sustained freshening of 0.1 Sv from ice melt gave an AMOC reduction of approximately 1 Sv (also seen in Jungclaus et al. 2006 and Swingedouw et al. 2015), while in other models this level of forcing has been sufficient to eventually reduce the AMOC to < 4 Sv (Jackson and Wood 2018a). Stouffer et al. (2006) used an ensemble of climate models forced with 0.1 Sv and showed that the response was highly model dependent, with the AMOC in 14 models weakening by 1-10 Sv over 100 years. Ice melt from radiative forcing of RCP4.5 and RCP6 can both give a reduction of roughly 2 Sv, reducing surface temperatures across the North Atlantic and neighbouring land masses by 1-2 ˚C (Gierz et al. 2015). Driesschaert et al. (2007) found that at the end of a 1000-year simulation radiative forcings of 4 Wm^{-2} and 7 Wm^{-2} gave additional freshwater fluxes into the ocean of approximately 0.01 Sv and 0.05 Sv, respectively. This non-linear response to forcing occurs largely due to the length of the melting season, and extent of ice melt, increasing in warmer climates giving a second-order dependence of total melt on the temperature rise (Driesschaert et al. 2007).

An AMOC collapse would have global climate impacts, with particularly severe consequences for landmasses bordering the North Atlantic. This could include the northern hemisphere cooling by 1.7 ˚C in the first decade, with regional anomalies in North-Western Europe of up to 8 ˚C (Vellinga and Wood 2008). This could be balanced by warming in the southern hemisphere, as the mechanisms that balance the global heat budget readjust. In the northern hemisphere cooling leads to a weakening of the hydrological cycle, with cooled surface temperatures leading to reduced evaporation and therefore less atmospheric moisture available for precipitation (Jackson et al. 2015 and references within). Changes in European summer precipitation patterns (decreased in the North and increased in the South) were associated with a negative summer North Atlantic Oscillation signal (Jackson et al. 2015). Jackson et al. (2015) also found in support of AMOC weakening leading to a strengthening of the North Atlantic storm tracks and a southward shift of the Intertropical Convergence Zone (ITCZ), caused by changes in Atlantic sea surface temperature gradients, which alters low-latitude precipitation patterns. A regional climate simulation study explored the North American climate impact of collapsing the AMOC by raising the atmospheric CO_2 concentration (Pu et al. 2012). They found that it lead to a decrease in precipitation over the Western and Central United States of up to 40%, and by up to 50% over Eastern Mexico.

Changes in ocean circulation could also impact region sea level, with a model study suggesting 5 cm of sea level rise inshore of the Gulf Stream projected for every 1 Sv of THC weakening (Levermann et al. 2005). A cessation of North Atlantic deep water (NADW) formation was found to lead to between 0.5 m and 1 m of sea level rise along the North Atlantic coast, with some regions experiencing sea level rise of 20-25 mm yr-1 (Levermann et al. 2005).

Liu and Fedorov (2019) considered the different timescales of response to reduced albedo of snow/sea ice at high northern latitudes, including fast atmospheric readjustment and slower ocean response including AMOC weakening. The atmospheric response dominated the first 2 decades giving northern hemisphere warming and southern hemisphere cooling, with a northward shift of the ITCZ. On multi-decadal to centennial timescales the ocean response dominated, as the AMOC weakened, the southern hemisphere warms,

and ITCZ becomes southwardly displaced, and a North Atlantic warming hole develops. Liu and Fedorov (2019) highlight that this interplay between fast and slow consequences of Arctic ice melt is important for prediction of climate change on human timescales, and is often overlooked.

1.1.3 Early warning indicators

The AMOC observational record is too short to provide a baseline from which to statistically distinguish long-term trends from the background and decadal variability. The RAPID array mooring has shown an apparent AMOC weakening over the ~10 years of data so far gathered, however this is likely to be part of a decadal variability as opposed to indicating a long term trend (Jackson et al. 2016). It is likely that such an array would only be able to identify changes to ocean circulation when the AMOC reached ~30% of its mean value. However, other indicators such as specific regional changes in sea level may enable earlier detection (Levermann et al. 2005).

As the ocean system gets closer to transitioning from a strong AMOC state to a weak AMOC state, its recovery rate from small perturbations has been shown to decrease (Boulton et al. 2014). This is phenomenon, known as 'critical slowdown', is observed in a range of low-order dynamical systems capable of hysteresis, with tipping points between multiple stable states. Models of various levels of complexity have exhibited critical slowdown as the AMOC approaches collapse. A study using FAMOUS, a fully coupled atmosphere-ocean global climate model (GCM), (Boulton et al. 2014) was able to detect early indicators of AMOC collapse 250 years before the occurrence by identifying critical slowdown, however this required a baseline established from ~550 years of monitoring. This suggests that critical slowdown would be an impractical tool in predicting anthropogenically forced AMOC collapse. However, Held and Kleinen (2004) suggested that it may be possible to examine the reducing decay rates associated with previous AMOC collapses in the paleo-record, and use this to interpret the modern ocean's proximity to a bifurcation point.

A study using complex network theory on data from FAMOUS (Feng et al. 2014) found that analysing spatial coherence of the AMOC during a freshwater forcing simulation gave a better indicator of collapse than looking for critical slowdown did. They suggest that collapse could be indicated 100 years before the event, however, there is again a lack of observational data to enable the use of this method with the real ocean.

1.2 Thermohaline forcing

The density changes that drive change in the strength of the AMOC result from changes in temperature and salinity. In a warming world higher air temperatures would result in reduced heat loss from the high-latitude ocean (Gregory and Tailleux 2011). The resulting decrease in the density flux into the ocean in the high North Atlantic would be further enhanced by increased freshwater input from ice melt and precipitation changes. Comparing the impact from these forcings, changes in temperature tend to dominate over salinity changes (Gregory and Tailleux 2011). However this view is complicated by the timescales and feedbacks. A model study exploring anthropogenic climate change scenarios (Korper et al. 2009) found that the initial response to greenhouse gas forcing was for thermal effects to increase the meridional density gradient, strengthening the AMOC, while the saline contribution acted in opposition. These 2 contributions had similar scales, and so no net response was seen in ocean circulation over the first century. Later in the simulations the halosteric impact became dominant leading to AMOC weakening. This altered meridional density gradient continued to drive AMOC weakening after the greenhouse gas concentrations had stabilised.

In order to understand the meridional density forcing on AMOC strength it is therefore helpful to break the thermohaline forcing down between influences of temperature and salinity. We will start in **Section 1.2.1** with mechanisms and feedbacks associated with changes in salinity. In **Section 1.2.2** we will consider specifically temperature driven aspects of circulation, before considering the resulting interactions of temperature and salinity in **Sections 1.2.3**.

1.2.1 Salinity Driven

1.2.1.1 Hysteresis

The AMOC has been found to demonstrate hysteresis (Hawkins et al. 2011; Hu et al. 2012b; Boulton et al. 2014; Jackson and Wood 2018b), meaning that the behaviour of the system at any time is dependent on its past condition, see **Figure 3**. When the system is in either the stable 'on' or 'off' state the strength of the AMOC will return to that state after perturbations. However if the AMOC is in a bistable regime, a sufficiently large perturbation can led to a transition between the 2 states available under the same forcing (Huisman et al. 2010).

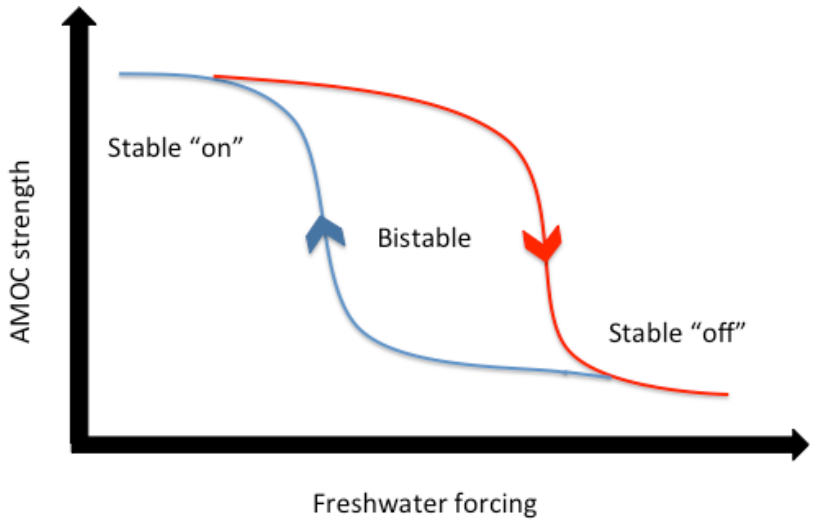

Fig. 1.3 Hysteresis diagram showing the 'on' and 'off' states of the AMOC with a central bistable regime. The pathway of AMOC collapse is shown in red and pathway of AMOC recovery is in blue

The parabolic form of the curves shown in **Figure 3** indicates the non-linearity of the system (Rahmstorf 2000), which may be described quadratically. Originating from an 'on' condition, the AMOC requires strongly increased freshwater forcing to induce a collapse, while for a transition from the 'off' to the 'on' condition the freshwater forcing must become much weaker. The accumulation of advected salinity has been suggested to explain the nonlinearity behaviour (Bouttes et al. 2015). Salinity advective feedbacks were found to give the system a longer memory. This suggests that using different initial states, or observational data,

may not give reliable predictions due to the sensitivity of behaviour on the preceding conditions (Bouttes et al. 2015).

The presence of clear bistability in hysteresis behaviour may be model dependent – with some recent models showing greatly reduced regions of bistability (See **Section 1.4.2**). However, it has been suggested that even if the hysteresis associated with the salt advective feedback is no longer present that multiple equilibrium in the ocean circulation can still be present (Huisman et al. 2009). Gregory et al. (2003) found that in the both the 'on' and 'off' states the freshwater content of the Atlantic remained relatively constant, despite varying forcing levels. Their research suggested that the 'off' state actively suppressed the AMOC, and that removal of forcing in the real climate system may not lead to a recovery of the AMOC.

1.2.1.2 Freshwater transports

Changes in the freshwater content of the Atlantic have been suggested to play an important role in the slowdown and recovery of the AMOC, due to its impact on sub-polar densities (Jackson 2013). Changes in Atlantic salinity can be tracked using the freshwater flux into the Atlantic basin at ~30°S by the AMOC, F_{ov}, (described in full in **Chapter 2 Introduction** and **Methods**). F_{ov} has been used as a stability indicator for the AMOC. When the AMOC is net exporting salinity with positive F_{ov}, a weakening of the AMOC net increases basin salinity, increasing the density and thereby reinvigorating the AMOC. This acts as a negative feedback on AMOC perturbations, keeping the AMOC stably 'on' or 'off'. When F_{ov} is negative the AMOC is importing salinity; weakening the AMOC reduces Atlantic salinity, reducing density. This in turn further reduces the strength of the AMOC, giving a positive feedback on the perturbation (Rahmstorf 1996). Simulations modelling AMOC collapse have shown a negative value for F_{ov} during the collapse, with positive values on either side where the AMOC is in a stable regime (Hawkins et al. 2011). Observations and reanalysis suggest that the Atlantic is currently a net exporter of freshwater at 30°S, indicating that the AMOC may currently be in a bistable state (Hawkins et al 2011; Bryden et al. 2011; Garzoli et al. 2013). The observed values indicate a positive salinity advective feedback, meaning that freshwater perturbations may be amplified and that a sufficiently large freshwater perturbation could induce AMOC collapse (Garzoli et al. 2013).

Various models find F_{ov} at the southern limit of the Atlantic basin to be an adequate indicator of multiple equilibrium states, when assuming that changes in the diffusive upwelling and southern gyre transport to be negligible (Cimatoribus et al. 2014). Other studies suggest that it is important to consider the salinity flux from the northern basin limit as well as at the southern limit (Liu and Liu 2013). Improved understanding of the impact of transports on Atlantic salinity can be achieved by looking at freshwater convergence over the entire Atlantic basin. Here net convergence suggests a monostable regime, whereas net divergence would be suggestive of a bistable regime (Liu and Liu 2013). A stability indicator based on convergence, Σ, has been developed for this purpose (Dijkstra 2007), and has since been explored in model studies (Huisman et al. 2010; Liu and Liu 2013). Observational studies have found the net freshwater convergence over the Atlantic basin to be negative, again indicating that we are currently in a bistable regime (Bryden et al. 2011; Liu and Liu 2013).

The mechanism behind the importance of the high latitude salinity transport for Σ can be examined by comparing models and observations with an open Bering Strait against models where the Bering Strait is closed to volume transports. The North Pacific near surface water has low salinity, at about 32.5 PSU (Bryden et al. 2011), which enters the Arctic and Atlantic via the Bering Strait. A positive freshwater transport of 0.10 ± 0.05 Sv has been estimated to be coming out of the Arctic (cumulative from Greenland to Norway), with a potential additional transport of approximately 0.05 Sv on the Greenland shelf (Oliver and Heywood 2003). When the Bering Strait is closed in model studies low salinity water cannot be imported from the North Pacific, modulating the Artic freshwater budget. This reduces the northern freshwater transport, contributing to a freshwater divergence over the Atlantic basin. This destabilises the AMOC and shifts it towards bistability (Weijer et al. 2001; Liu and Liu 2013). When the Bering Strait is open, as in the modern ocean, the AMOC is less vulnerable to sudden collapse and the Pacific has a weaker response to AMOC collapse (Hu et al. 2012a, 2012b). When the salinity flux from the North Atlantic is reversed by strong hosing regimes in model experiments, an open Bering Strait allows the passage of freshwater from the North Atlantic and Arctic into the North Pacific, reinforcing the halocline (Jackson et al. 2016). However, Jackson and Wood (2018b) did find AMOC collapse and hysteresis with a 1/4˚ resolution GCM with an open Bering

Strait. While questions remain, these impacts demonstrate the importance of taking high latitude dynamics into account.

Another important contribution comes from the salinity flux by gyre transport, F_{az}, (Jackson 2013) (see **Chapter 2 Introduction** and **Methods**). The freshwater transport by the wind driven gyre will scale with zonal salinity gradients (Cimatoribus et al. 2014). Changes in F_{az} are compensated for by changes in F_{ov} as a result of changes in the intermediate depth ocean stratification (Cimatoribus et al. 2012). However, F_{ov} success at identifying multiple equilibrium regimes indicates that there is a balance between vertical diffusion and horizontal advection in some models (Cimatoribus et al. 2014).

1.2.2 Temperature driven

As atmospheric temperatures increase with anthropogenic climate change the North Atlantic is expected to lose less heat to the overlying atmosphere at high latitudes. This weakening of the heat flux will cause the surface waters to remain more buoyant as they enter the deep convection regions. The warmed climate will also globally warm the surface ocean more strongly, leading to further increased buoyancy and thermal expansion. While studies of salinity forcing generally apply freshwater hosing, studies wanting to explore the role of increased temperatures tend to use radiative forcing. Increased radiative forcing leads to ice melt and changes in the hydrological cycle, and so can have the impacts of freshwater forcing as a by-product. This can make it hard to study the impact of temperature in isolation.

When the AMOC is enhanced by internal low-frequency variability, it leads to increased ocean heat transport into the sub-polar gyre (Zhang 2015). It therefore seems reasonable to expect AMOC weakening to lead to reduced warming by ocean transport. Studies using a range of historical and future climate scenarios have found an ‘Atlantic Warming Hole’, where weakening the AMOC results in North Atlantic sea surface temperatures either reducing or falling behind surrounding anthropogenic warming (Drijfhout et al. 2012; Rugenstein et al. 2012). However, some models show anthropogenic AMOC weakening to lead to

subsurface warming of the sub-polar gyre (Jungclaus et al. 2014; Koenigk and Brodeau 2014). Oldenburg et al. (2018) have explained this by splitting ocean heat transport changes into contributions from dynamic circulation changes and thermodynamic temperature advection. This revealed that when the AMOC is weakened with greenhouse gas forcing, sub-polar gyre heat convergence is reduced as expected. However, thermodynamic advection by time mean overturning and dynamic heat redistribution by enhanced gyre circulation increase Arctic ocean heat transport – as they are advecting in anomalously warm surface waters.

Anthropogenic forcing can result in an accumulation of warming into the deep ocean, extending the duration of ocean mean temperature anomalies and thermal expansion based sea level rise for decades after forcing is reduced (Nakashiki et al. 2006). Nakashiki et al. (2006) found that different emissions scenarios leading to the same total greenhouse gas concentrations could result in different long-term behaviour and recovery mechanisms, due to the interplay of the timescales of temperature response at the surface and within the ocean interior.

Were greenhouse gas concentrations to become stabilised, the globe would continue to warm on the centennial scale, exporting warmth to the deep oceans and continuing to contribute to thermal expansion, AMOC weakening, and driving sea level rise (Meehl et al. 2005). Others have argued that if geoengineering were used to combat climate change and reduce thermal expansion, that regional sea levels would remain altered as the ocean penetration of anomalous heat would be different during warming and cooling (Bouttes et al. 2013). This redistribution of heat in the global oceans would change the distribution of density, impacting overturning. Some studies suggest that the Southern Ocean would experience significant deep warming (Gillett et al. 2011), while the shallow land-locked Arctic may be slightly cooled by the influence of the surrounding landmasses. The impact on the meridional density gradient from these thermal influences would be expected to enhance the AMOC. However, heat may leave the oceans more quickly than it is taken up by the ocean, due to a combination of the vertical profile of ocean temperature change and the dependence of vertical heat transports on temperature gradients (Bouttes et al. 2013).

Oka et al. (2012) examined the role of temperature in AMOC collapse in glacial and interglacial climates. They found a thermal threshold for AMOC collapse present in glacial climates, where moderate North Atlantic surface cooling enhanced the AMOC and further cooling led to increased ice extent, effectively suppressing deep convection. The thermal threshold resulted from the nonlinear response of North Atlantic deep convection and sea ice to surface cooling. However, greater warmth during interglacial climates prevented the thermal threshold from being crossed, indicating that abrupt climate change by this mechanism is unlikely in an interglacial climate.

1.2.3 Interaction of temperature and salinity

Total density change results from the sum of changes in temperature and salinity, with cooling enhancing the AMOC by increasing density, while freshening weakens the AMOC by reducing density. Temperature and salinity anomalies can modulate each other's otherwise more dramatic impacts of AMOC strength, with lesser net density changes resulting from cool fresh anomalies or warm saline anomalies. Otterå et al. (2003) found that the residence time within regional climates determined the accumulated effect of heat and freshwater fluxes, with slower velocities meaning that the water was impacted by a regional climate for longer. A water parcel in the North Atlantic subtropical gyre will experience strong insolation and evaporation – making it warm and saline. Further north, it will experience more precipitation and cooling.

As the AMOC weakens in response to increased radiative forcing, surface density in the North Atlantic decreases as surface temperature and high latitude freshwater both increase (Cao et al. 2016). A study using increased radiative forcing in eleven climate models (Gregory et al. 2005) found that AMOC weakening is caused more by changes in surface heat flux than by changes in surface freshwater flux. Reduced northward transport rates in Otterå et al. (2003) amounted to an additional 8 months of travel time to traverse 4700 km of the South America coast. This resulted in positive salinity and temperature anomalies of up to 0.2 PSU and 0.8 ˚C, over the upper 600 m of the western tropical North Atlantic.

While in models forced by increasing radiative forcing the AMOC is generally primarily weakened by North Atlantic warming, controls on density in the recovery phase can be more model dependent (Sgubin et al. 2015). Smith and Gregory (2009) found that the AMOC started to recover soon after freshwater hosing ended, with similar rates of recovery seen for runs where the AMOC had been weakened to different extents with different hosing rates. Studies have found a weak AMOC to lead to a build up of salinity in the subtropical gyre, which can reinvigorate the AMOC when it is advected to high latitudes (Otterå et al. 2003; Wu et al. 2011; Jackson et al 2014) as it increases the density of the deep-water formation regions. Sgubin et al. (2015) found that the recovery process for a range of radiatively forced experiments was largely determined by the model dependent changes in salinity transport by the sub-tropical gyre.

In simulation studies that continue for a substantial amount of time after a forced AMOC collapse, the AMOC is often seen to recover, sometimes with an overshoot (Hawkins et al. 2011; Cao et al. 2016). Northward transport of low latitude high density waters have been reported to give an initial overshoot as the AMOC returns to the 'on' condition (Bouttes et al. 2015). An overshoot may be due to the gradual warming of subsurface waters at low- and middle-latitudes (Manabe and Stouffer 1994; Stouffer and Manabe 1999) along with increased northward salinity advection (Thorpe et al. 2001; Bitz et al. 2007). Alternatively, Smith and Gregory (2009) attributed AMOC overshoot to 'double-up' resulting from the model responding to surface forcing reducing deep-water formation in the Labrador Sea region by initiating a 'compensating' deep-water formation in the Nordic Seas. As the original down welling recovered on the removal of hosing, this new additional source of deep-water continued for some time, with the 2 down welling sites temporarily giving a net increase on control values (Smith and Gregory 2009).

1.2.4 Reverse cell

Stommel's original box model had 2 equilibrium solutions, the first being a basic description of the modern AMOC, the other consisting of a much slower reversed haline-driven circulation with sinking of warm saline waters in the tropical box (Stommel 1961). A reverse thermohaline circulation (RTHC) cell between the high

latitude North and South Atlantic has been observed in numerous model studies (Gregory et al. 2003; Yin and Stouffer 2007; Hawkins et al. 2011; Cimatoribus et al. 2012). There are also paleo-oceanographic studies that indicate that during that Last Glacial Maximum the basin scale abyssal circulation of the Atlantic Ocean may have been reversed (Negre et al. 2010).

The formation of a RTHC gives the AMOC 'off' state greater stability (Yin and Stouffer 2007). In a numerical model, increased Atlantic salinity values have been shown to reduce the strength of the reverse cell, reducing the Atlantic salt flux into the Southern Ocean. At the same time, the strengthened South Atlantic vertical salinity gradient can increase the salt flux (Sijp et al. 2012a). These processes combine to give non-linear behaviour to salt forcing in the Atlantic, held to be critical in maintaining the AMOC in the 'off' state. Contrasts between RTHC and non-RTHC forming simulations can include differences in the southward propagation of the salinity and temperature anomalies away from the freshwater hosing region, and the related impact on the meridional density gradient (Yin and Stouffer 2007).

1.3 Mechanical forcing

Energy is input into the ocean in the form of kinetic energy from wind and tides, which is converted into potential and kinetic energy through the generation of the large-scale circulation (Wunsch and Ferrari 2004). There is also some impact on deep circulation from the input of geothermal energy (Emile-Geay and Madec 2008; Hofmann and Maqueda 2009). Various studies have found that for the AMOC to be maintained there needs to be a continuous input of mechanical energy to the ocean and generation of available potential energy (APE) by tides and Southern Ocean wind forcing (Munk and Wunsch 1998; Toggweiler and Samuels 1998; Wunsch and Ferrari 2004; Johnson et al. 2007). Simulations examining energetics have suggested that the AMOC is driven by available potential energy (APE) being release as kinetic energy (KE), primarily in the deep western boundary currents (Sijp et al. 2012b). Reductions in potential energy in the ocean interior due to the processes of overturning and eddy-generation need to be balanced by small-scale mixing processes (Wunsch and Ferrari 2004).

1.3.1 Role of mechanical forcing and pycnoclines

Simple box model studies have been used to explore the relationship between mechanical drivers and thermohaline forcing in controlling the AMOC and its multiple equilibria. The role of these relatively simple tools is to aid the development of conceptual frameworks that help to formulate questions to be furthered using more complex models and observations (Johnson et al. 2007). Some studies have found overturning induced by surface buoyancy leads to shallow overturning with a fairly static, cold, deep ocean. This lead to suggestions that deep overturning required mechanical energy, from wind and tidal forcing (Wunsch 2005). A study looking at 2 GCMs found that wind stress contributed the major part of the mechanical energy required to balance convection in the buoyancy budget (Gnanadesikan et al. 2005). Gnanadesikan (1999) explored the role of Southern Ocean wind strength and interior mixing on the behaviour of overturning. They considered the balance between the Southern Ocean processes of wind stress, which steepens isopycnals leading to a deepened thermocline, with baroclinic eddies which flatten isopycnals by mixing across the boundaries. The depth of the thermocline was determined by this balance, combined with influences from Northern Hemisphere convective sinking and diapycnal upwelling in the interior. While this gave a reasonable solution, it did not show the multiple equilibria demonstrated in models forced by buoyancy. This idea was extended in a box model study that incorporated heat and salt budgets (Johnson et al. 2007), resulting in a mechanically driven overturning system exhibiting multiple equilibria. The additional equilibrium had no northern deep convection, but a significantly deeper thermocline with northward surface Ekman transport balanced by volume transport via eddies below in the Southern Ocean. This resulted in a small ocean circulation, with water sinking in the Southern Ocean and being upwelled in the ocean interior.

The dependence of ocean overturning on buoyancy forcing at equilibrium has been found to become weaker with weak mixing in a box model study (Oliver et al. 2005). Diapycnal mixing modifies pressure gradients within the ocean interior, impacting AMOC strength. Diapycnal mixing may have a stabilising impact on overturning via a negative feedback to changes in buoyancy forcing. Weakened overturning was seen to lead to increased buoyancy in the low-latitude

subsurface ocean as the dense inflow was unable to balance the buoyancy input due to mixing. On short timescales Oliver et al. (2005) found the expected positive feedback between high latitude salinity and AMOC strength, however on longer timescales they found AMOC strength to be controlled by the advective-diffusive balance between diapycnal mixing and overturning.

1.3.2 Available Potential Energy (APE) and kinetic energy (KE) during AMOC weakening/recovery

The relationship between the AMOC strength and meridional density gradient relies on essentially geostrophic large-scale ocean circulation, where currents and pressure gradients are orthogonal. In order to exclude the dominant geostrophic balance, analysis can be focused on the KE budget instead of momentum (Gregory and Tailleux 2011). Ocean KE is input by the surface windstress and is dissipated by a combination of internal friction/viscosity and boundary friction (Sijp et al. 2012b). The potential energy produced by buoyancy forcing is converted into KE via the pressure-gradient force, which can be either a source or sink of KE. The KE balance tells us about the strength of circulation, and can help to identify drivers and brakes. Different climate models represent sources and sinks of KE differently, potentially in part accounting for their differences in AMOC behaviour (Gregory and Tailleux 2011).

In FAMOUS KE is supplied to the ocean by the wind and is then dissipated by viscous forces in the global mean of the steady-state control climate. The circulation acts to reduce the pressure-gradient force, particularly in the Southern Ocean (Gregory and Tailleux 2011). In the Atlantic Ocean the pressure-gradient force does work on the circulation, especially in the high-latitude regions of deep-water formation. In CO_2-forced simulations exploring climate change scenarios (Gregory and Tailleux 2011) a strong temporal correlation has been found between the AMOC strength and the rate of KE generation by the Atlantic pressure-gradient force between 50˚N and 70˚N. Exploring this with experiments where atmospheric CO_2 increased by 1% $year^{-1}$, the largest change in the KE balance of the Atlantic in HadCM3 and FAMOUS was found to be associated with a decrease in KE production by the pressure-gradient forces in the North Atlantic, a strong reduction in AMOC strength, and a decrease in dissipation of KE.

In an idealized climate change simulation (Saenko 2013) this research was taken further to explore available potential energy (APE) during both weakening and recovery of the AMOC. They found APE to accumulate in the Southern Ocean emphasising the regions potential significance in controlling longer-term changes in the strength of the AMOC. This suggests the importance of understanding mesoscale eddies in order to understand the APE (Saenko 2013). They also found that the Atlantic pycnocline depth was closely linked to the Southern Ocean APE, indicating a mechanical contribution to AMOC recovery.

Hogg et al. (2012) explored the role of mechanical forcing, taken as the sum of KE and APE, in a freshwater forcing study. They found that changes to the meridional salinity gradient altered the thermal wind, and therefore the Southern Ocean circumpolar transport. This resulted in increased wind power input and KE, consistent with the findings of Saenz et al. (2012). Hogg et al. (2012) found global energetics to be a poor indicator of AMOC strength, as they found the global energy budget to increase as overturning reduced. The surface APE density was a better indicator of AMOC strength, and was able to explain the asymmetry between weakening (decades) and recovery (centuries). As the APE input and local density anomalies were coupled, the AMOC did not recover until the density distribution had recovered.

A disadvantage of working with mechanical energy is that it is difficult to relate results from simulations to observational studies. This is due to the dependence of the KE balance on the ageostrophic circulation (Gregory and Tailleux 2011), in itself a very small fraction of the total velocity, while observations of large-scale circulation are usually inferred by using an assumption of geostrophy in the ocean interior (McCarthy et al. 2015).

1.4 Open questions

Research into the impact of climate change on the AMOC has tended to focus on the weakening of the AMOC and whether or not the AMOC can be said to

'collapse'. In this thesis I want to focus on the mechanical processes that determine the strength of the AMOC and the implications of changes to the ocean state on AMOC resilience to forcing. While there has been significant research into the weakening of the AMOC, there has been less focus on the response of the AMOC to the removal of hosing. Some studies have looked at hysteresis and non-recovery, however a full AMOC collapse is currently considered unlikely. This highlights the importance of understanding the consequences of intermediate AMOC weakening, and the recovery process that may follow sufficient climate change mitigation. In particular, understanding the mechanical process of recovery following a temporary weakening.

As the AMOC weakens due to freshwater forcing the distribution of temperature and salinity in the Atlantic Basin will be altered. Some previous freshwater forcing studies have focused on the changes in North Atlantic salinity, and related changes in the strength of the AMOC to changes in the mean salinity of a broad volume in the ocean. However, volume mean salinity may give an incomplete explanation of changes in North Atlantic density. Freshwater forcing studies have found high latitude subsurface temperature to increase during freshwater forcing (Mignot et al. 2007; Krebs and Timmermann 2007). While this feature is suggested to be highly model dependent (Kleinen et al. 2009) it has been supported by some paleoclimate studies (Hernández-Almeida 2015). The development of subsurface warming suggests not only that temperature changes may be significant in driving perturbations in AMOC strength, but additionally that the vertical structure, lost in volume mean salinity studies, may be materially important for understanding the response of the AMOC to forcing.

In this thesis I aim to explore these gaps in and questions raised by the existing literature by addressing the following questions:

- How does the AMOC recovery process differ from the AMOC weakening process? Can it be considered an 'undoing' of the weakening process?
- Are changes in North Atlantic temperature significant in freshwater forcing studies?
- Is the vertical structure of density anomalies important in understanding changes in AMOC strength and resilience?

1.5 Methodology

This thesis is primarily concerned with decadal to centennial timescales, on which we expect the relative density in the north and south of the Atlantic to be the primary driver. To explore the underlying mechanics of change this can be split further between density changes occurring at different heights within the ocean and density changes resultant from changes in salinity and temperature. In order to have a depth-dependent interrogation of the roles of changes in salinity and temperature in driving change in the strength of Atlantic overturning we adopt the methodology presented in Butler et al. (2016), described in full below.

This is a method intended to reconstruct the vertical profile of AMOC strength at 30˚N based on a scaling relationship with the meridional density gradient between 50˚N and the southern limit of the Atlantic basin. We begin by taking the assumption of geostrophic balance:

$$fv = \frac{1}{\rho}\frac{\partial P}{\partial x}$$

where the Coriolis parameter, f, multiplied by the meridional velocity, v, is equal to the reciprocal of density, ρ, multiplied by the rate of change of pressure, P, with longitudinal distance, x. This tells us that for a given latitude the meridional velocity is proportional to the zonal pressure gradient.

Taking the vertical derivative of this balance, and multiplying through by density, gives:

$$\frac{\partial}{\partial z}(\rho f v) = \frac{\partial}{\partial x}\left(\frac{\partial P}{\partial z}\right)$$

The hydrostatic approximation tells us that $\frac{\partial P}{\partial z} = -\rho g$. This can then be substituted into the equation above to give:

$$\frac{\partial}{\partial z}(\rho f v) = \frac{\partial}{\partial x}(-\rho g)$$

which can be rearranged to find the vertical derivative of meridional velocity:

$$\frac{\partial v}{\partial z} = \frac{-g}{\rho f}\frac{\partial \rho}{\partial x}$$

This gives the general form of the meridional component of the thermal wind equation. Here, we will use this relationship on the basin-scale, and so rewrite the equation as the scaled form of the thermal wind equation where the vertical derivative of the basin-scale zonally averaged meridional velocity, $< V >$, is:

$$\frac{\partial < V >}{\partial z} = \left(\frac{-g}{f_0 \rho_0}\right) \cdot \left(\frac{\Delta \rho_x(z)}{L_x}\right)$$

where g is the gravitation constant, f_0 and ρ_0 are reference values for the Coriolis parameter and density, respectively, $\Delta \rho_x(z)$ is the zonal density gradient on each depth level, and L_x gives the zonal length scale.

The next step is to link $\Delta \rho_x$ to the basin-scale meridional density gradient, $\Delta \rho_y$ (all meridional gradients are calculated as the northern value minus the southern value). In order to achieve this an assumption of proportionality is made between zonal and meridional velocities (Robinson 1960). This approach was reasoned by Marotzke (1997) as changes in the meridional pressure gradient induce changes in zonal flow, impacting zonal pressure gradients, resulting in changes to meridional flow. The zonal and meridional density gradients can then be related using a proportionality factor, n, where $\Delta \rho_x \sim n \, \Delta \rho_y$. Grouping the constants in the velocity equation above together with n as a scaling factor, c_ρ, then gives the approximation $< V > \sim c_\rho \, \Delta \rho_y H$, where H is the depth scale. Others have attempted to mathematically define a scaling factor between the zonal and meridional density gradients (see discussion in Sijp et al. (2012)). Approaches that take the mean of the density profile may neglect potentially significant features in the profile structure, becoming distorted by strong anomalies in the surface region. Using the mean of the density profile can yield the qualitatively wrong AMOC response in circumstances where using the depth dependent pressure gradient gives the qualitatively correct response (de Boer et al. 2010). As we are here interested in the physical mechanisms of AMOC weakening, we need to use a method that retains depth dependence in order to be sensitive to processes directly impacting deep pressure gradients.

We take c_ρ as a dimensionless constant of proportionality between the basin-scale meridional and zonal pressure gradients, where $\frac{\Delta\rho_x}{L_x} = c_\rho \frac{\Delta\rho_y}{L_y}$. This is then substituted into the equation for the vertical derivative of the basin-scale zonally averaged meridional velocity, to give:

$$\frac{\partial < V >}{\partial z} = \left(\frac{-c_\rho g}{f_0 \rho_0 L_y}\right) \cdot \left(\Delta\rho_y(z)\right)$$

The value of c_ρ is model dependent, taking values of 0.65 and 0.33 in the models FAMOUS and HadGEM3-GC2 used in this thesis, respectively. These values were chosen empirically for each model, in order to match the reconstructed control run AMOC strengths to those calculated from the model velocity field at 30˚N.

In order to retain the depth dependence of $\Delta\rho_y$ Butler et al. (2016) derived an expression for the basin-scale meridional velocity from the previous equation, by integrating up the water column (constrained by an assumption of zero net flow through the Bering Strait):

$$< V(z) > = \frac{-c_\rho g}{f_0 \rho_0 L_y} \left(\frac{1}{h} \int_{-h}^{0} \left(\int_{z'}^{0} \Delta\rho_y(z'')dz''\right) dz' - \int_{z}^{0} \Delta\rho_y(z')dz'\right)$$

where h is the bottom depth. The Atlantic meridional overturning stream function, Ψ, using the vertically integrated meridional velocity in terms of the depth dependent meridional density gradient, is then given as:

$$\Psi(z) = L_x \int_{z}^{0} < V(z') > \, dz'.$$

1.6 Research directing experiment design

We have so far considered the AMOC in broad terms and on a range of timescales. This section will focus on the aspects most pertinent to the research undertaken in this thesis. The research presented in **Chapters 2**, **3**, and **4** will consider the impacts of freshwater forcing in GCMs on the centennial scale. In

particular, how freshening leads to changes in the density of the North Atlantic, the impact on AMOC strength, and long-term consequences for the ocean state.

1.6.1 Models

Within this project 2 models have been used, FAMOUS in **Chapters 2** and **3**, and HadGEM3-GC2 in **Chapters 3** and **4**, and are described in some detail in those chapters. The HadGEM3-GC2 runs have been used in previous studies, and so further extensive discussion on them can be found elsewhere (Jackson and Wood 2018a, 2018b). The FAMOUS runs were produced specifically for this research, and so will be described in a little more detail below.

The Fast Met Office/U.K. Universities Simulator project (FAMOUS) is a low-resolution ocean-atmosphere general circulation model. The XDBUA version of FAMOUS (Smith and Gregory 2009) was run on the NOCS computer 'Mobilis' which has 72 nodes of 2 x 8-core Intel Xeon E5-2650 v2 'Ivy Bridge-EP' processors. FAMOUS ran most efficiently split as 4x4 over the 16 cores of 1 node. FAMOUS is comparatively computational cheap, and so was able to produce approximately 450 simulation years per wall clock day, per node.

In FAMOUS, Iceland has been removed to improve northward ocean heat transport, the bathymetry does not include deep overflow channels (which were used in HadCM3 for better representation of the NADW), and while HadCM3 used the global salinity reference value to simulate surface freshwater fluxes, FAMOUS XDBUA instead uses local surface salinity (Smith and Gregory 2009). Climate sensitivity and regions of North Atlantic deep-water formation are similar between FAMOUS and HadCM3. NADW is formed south of Greenland and in the Greenland, Iceland, and Norwegian seas. Freshwater accumulation on land in the form of snow on land-ice grid boxes is balanced by ocean freshening in the form of an ice calving variable. This is a surface freshwater flux with greatest values near Greenland and Antarctica (Smith and Gregory 2009). Freshwater hosing was achieved in our experiments by adding additional regions of freshening to the ice calving variable.

1.6.2 Compensation of freshwater forcing

Varying the method with which forcing is applied in model studies can cause the ocean state to respond differently to the same total quantity of forcing applied (Jackson et al. 2017). One reason for this in the FAMOUS model is the choice between using surface or volume compensation. In FAMOUS the total volume of water cannot be altered, so the freshwater hosing over the North Atlantic needs to be balanced with compensating salt increases elsewhere to conserve total density. This can either be done throughout the surface waters or in each grid cell throughout the entire volume of the global ocean. The former increases surface density relative to deep density, impacting stratification, accelerating AMOC collapse once the tipping point is reached. It has also been found to induce an overturning seesaw between the Atlantic and the Pacific, though this appears to only occur when the Bering Strait is closed (Hu et al. 2012a). Surface compensation contributes to this as it erodes the North Pacific halocline inducing deep convection and overturning. Surface compensation also stabilises the “off” state, relative to volume compensation (Jackson et al. 2017). Jackson et al. (2017) found this to result in volume compensated experiments showing significantly reduced regions of bistability compared to surface compensated experiments **Figure 1.4**.

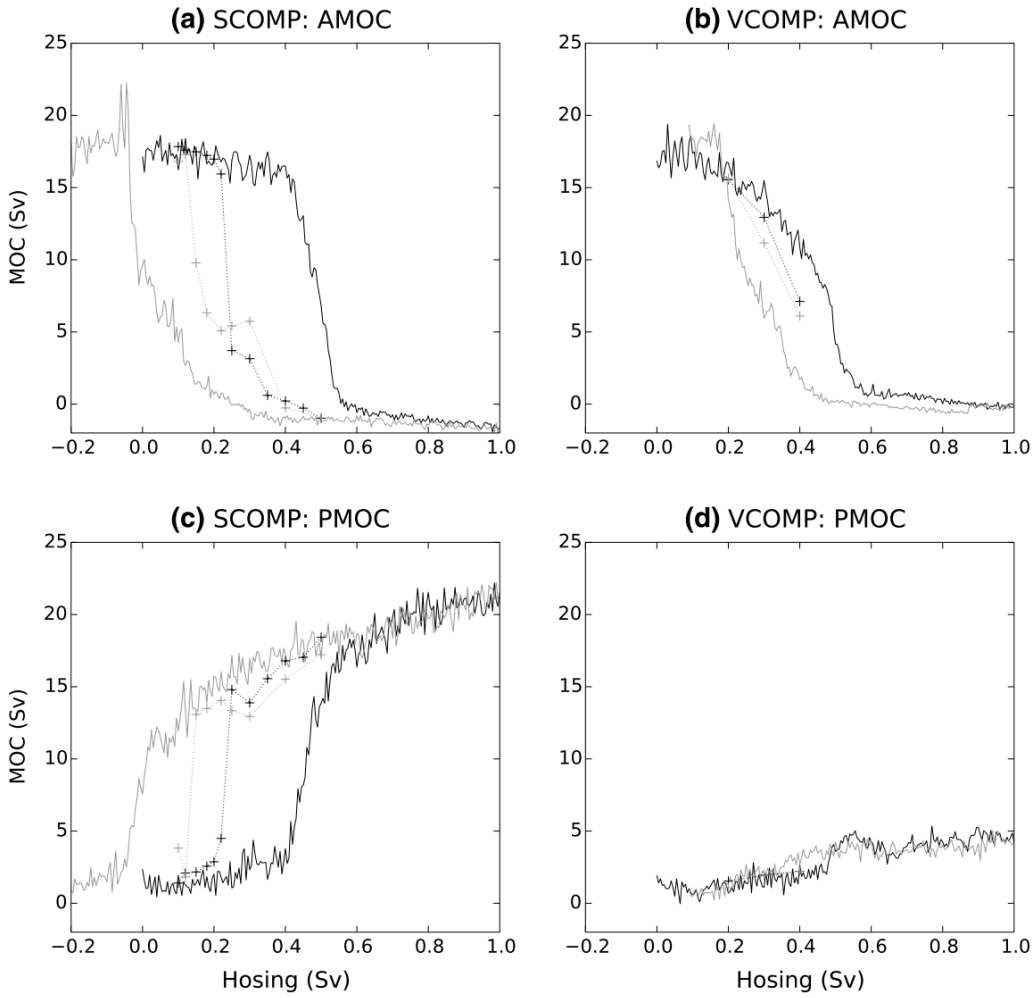

Fig. 1.4 AMOC (**a**, **b**) and Pacific meridional overturning circulation (**c**, **d**) strength against freshwater forcing rate for surface (**a**, **c**) and volume (**b**, **d**) compensated experiments. **Dark lines**: freshwater hosing is ramped up from 0 to 1.0 Sv over 2000 years, **Light lines**: freshwater hosing ramped back down to 0 Sv over 2000 years. **Dotted lines with crosses**: final states of constant hosing experiments. Figure taken from Jackson et al. (2017), who used the model FAMOUS

1.6.3 Impact of selected hosing region

Various studies have found that the AMOC responds differently to freshwater forcing depending on the choice of hosing region (Rahmstorf 1996; Manabe and Stouffer 1997; Smith and Gregory 2009; Yu et al. 2016). A conceptual model (Rahmstorf 1996) used 4 freshwater hosing regions throughout the Atlantic basin. The study found that the further north in the Atlantic that was hosed, the greater was its efficiency at impacting NADW formation. This concept was reinforced by a model study (Manabe and Stouffer 1997) that found that hosing

the sub-tropical Atlantic had a 4-5 times weaker impact on AMOC strength than did hosing the northern North Atlantic.

A study using FAMOUS to explore the relative impact of a 0.5 Sv hosing in different regions of the North Atlantic (Smith and Gregory 2009) found that the AMOC was most sensitive to hosing around 50-60˚N. They also found a 4 Sv greater reduction in the strength of the AMOC due to hosing on the eastern than western side of the Atlantic basin between 40˚N and 60˚N, while other latitudes were not similarly affected. This suggested that extent of AMOC weakening depends on the extent of freshening in deep-water formation regions. Running these regional hosing simulations with 1 Sv of hosing did not show the same sensitivity to location within the North Atlantic region. This is likely due to so much freshwater being added that the amount dispersed or circulated away from deep-water formation areas was insubstantial compared to the total added. In a different GCM of similar resolution Yu et al. (2016) found that releasing freshwater on the eastern Greenland coast had a greater impact on the AMOC than releasing a similar amount of freshwater on the western coast, or evenly over the entire coast, as it gave a stronger reduction in Irminger Sea convective mixing.

Reductions in deep-water formation around 50-60˚N may be partially compensated for by increased mixed layer depth (MLD) in the Nordic seas (Stouffer et al. 2006; Smith and Gregory 2009). As the MLD and convection reduce, warm sub-surface waters are unable to release their heat as they travel northwards. This can lead to destabilisation of the water column at higher latitudes (Smith and Gregory 2009). The simulations that gave the greatest reduction in AMOC strength simultaneously prevented deep-water formation both south of Greenland and in the Nordic seas, preventing compensation from occurring (Smith and Gregory 2009).

While reduced AMOC generally leads to cooled temperatures, some models do show warming to the north of the hosing region (Stouffer et al. 2006; Smith and Gregory 2009; Kleinen et al. 2009). Saenko et al. (2007) found warming over the Labrador Sea when hosing the continental boundaries of Labrador and Greenland.

This was attributed to changes in the wind stress curl and the retreat of sub-polar sea ice. A study into the climate sensitivity to freshwater hosing region (Kleinen et al. 2009) found little difference in AMOC impact between 4 experiments hosing different areas of the North Atlantic and Artic Oceans. They also found that adding the freshwater to the East and West Greenland currents or to the Caribbean area (decreasing the salinity of the Gulf Stream) had a similar qualitative impact on the AMOC, but was quantitatively weaker, due to some of the freshwater being recirculated in the sub-tropical gyre.

In HadCM3 the climate response is robust with different freshwater hosing regimes (Kleinen et al. 2009). They found an ~25% decrease in the AMOC lead to a 4 ˚C warming over the Nordic and Barent Seas and extending on into Scandinavia. Areas with the greatest warming were found to have increased MLD and salinity. Northward advection of warm and comparatively saline waters from lower latitudes was prevented from progressing up into the Nordic Seas by a surface layer of cold fresh water. The surface freshwater leads to a strong reduction in the strength of the sub-polar gyre, increasing sub-surface heat transport to the Nordic Seas. This leads to instability in the water column between 70˚N and 75˚N, strongly warming the sea surface.

1.7 Thesis outline

I am presenting my thesis as a set of three manuscripts, which are published (**Chapter 2**) submitted for publication (**Chapters 3**) and in preparation for submission (**Chapter 4**) in the international peer-reviewed journal 'Climate Dynamics'. On each of these manuscripts, I was the lead author with the co-authors consisting of my PhD supervisory team: Kevin Oliver, Laura Jackson, Richard Wood, and Sybren Drijfhout.

Chapter 2: Explaining asymmetry between weakening and recovery of the AMOC in a coupled climate model

I performed temporary freshwater forcing experiments with FAMOUS to explore the roles of salinity and temperature in AMOC weakening and recovery. The

behaviour of the AMOC was well reconstructed by applying 'rotated geostrophy' to the meridional gradient in density profiles at 50°N and 30°S, following the Butler et al. (2016) method. This made it possible to determine the roles of overturning, gyre, and surface fluxes in the North and South Atlantic. This paper was published online in Climate Dynamics in December 2018 (Haskins et al. 2018).

Chapter 3: Temperature domination of AMOC weakening due to freshwater hosing in two GCMs

I then explored the mechanisms controlling AMOC weakening in response to constant hosing. I used the same approach as in **Chapter 2**, but split the reconstruction of the AMOC between impacts from changes in temperature and salinity as well as from changes in the North and South Atlantic. Mechanisms were described for similar experiments run in FAMOUS and HadGEM3-GC2. The AMOC was also reconstructed for HadGEM3-GC2 using volume mean densities in the North and South of the Atlantic, and the theoretical and physical basis of the 2 approaches were discussed. Climate Dynamics published this paper online in October 2019 (Haskins et al. 2019).

Chapter 4: Mechanistic investigation of AMOC recovery and non-recovery in response to the removal of freshwater forcing

I used existing temporary freshwater forcing experiments with HadGEM3-GC2 to investigate the changes in the ocean state required for AMOC non-recovery. When hosing was removed simulations weakened directly by the freshwater input generally recovered, while those weakened by the subsequent subsurface warm anomaly identified in **Chapter 3** did not. I used salinity and temperature budget analysis to understand the role of surface and ocean feedbacks in the recovering and non-recovering ocean states. These were initially taken over the region 30°N in the Atlantic to the Bering Strait, and were then divided into smaller regions to explore more regional density exchanges and feedbacks. This Chapter is currently being prepared for submission for publication.

Chapter 5 consists of some general discussion and closing remarks on the presented findings, and some suggestions for future work.

Chapter 2: Explaining asymmetry between weakening and recovery of the AMOC in a coupled climate model

Abstract

The Atlantic meridional overturning circulation (AMOC) is projected to weaken in the coming century due to anthropogenic climate change. Various studies have considered AMOC weakening and collapse, with less research focusing on the processes and timescales of the recovery phase. This study uses a coupled climate model to explore the roles of salinity and temperature in AMOC recovery after a weakening. The North Atlantic and Arctic region was hosed with freshwater for 200 years. The mean Atlantic salinity increased strongly during recovery, and remained elevated for ~600 years post hosing. The behaviour of the AMOC was well reconstructed by applying "rotated geostrophy" to meridional density gradient profiles between 50°N and 30°S. This makes it possible to determine the role of overturning, gyre, and surface fluxes in the North and South Atlantic. Changes at 50°N dominate the weakening and early recovery. The magnitude of the overshoot to high AMOC transports in the recovery phase was related to density changes in the South Atlantic.

2.1 Introduction

2.1.1 The AMOC and its stability

The Atlantic meridional overturning circulation (AMOC) is an oceanic system of currents carrying warm buoyant waters to high northern latitudes, balanced by a cool deep return flow. Climate projections suggest that the AMOC strength will decline due to anthropogenic climate change. The IPCC report stated best estimate reductions of 11% and 34% for the RCP2.6 and RCP8.5 scenarios, respectively, running up to 2100 (Collins et al. 2013). However the degree of resilience to short term forcing remains unclear. A potential driver of AMOC weakening is the melting of the Greenland ice sheet. By 2100 annual average

temperatures over Greenland could increase by 3 ˚C due to greenhouse gas increases – sufficient to give a gradual effective elimination of the sheet ice (Gregory et al. 2004). It has been suggested that a temperature increase of 1.6 ˚C may be sufficient (Robinson et al. 2012). Should the entire ice sheet melt, it would release profound quantities of freshwater into the North Atlantic Ocean, impacting regional buoyancy over a period of 1000 years or more (Gregory et al. 2004). A model study (Jungclaus et al. 2006) which reassessed previous IPCC simulations (Schmittner et al. 2005) with the addition of a freshwater source from Greenland ice melt found AMOC reductions of 35% and 42%, for conservative and high melting estimates respectively, compared to 30% without Greenland melting. Further freshwater may be supplied by the melting of Arctic sea ice (Sevellec et al. 2017). The focus of this study is the mechanistic nature of AMOC weakening and recovery, and how these two processes differ from one another.

Freshwater hosing experiments seek to explore the impact of the North Atlantic being freshened by ice melt. Kleinen et al. (2009) found that the ocean responded dynamically to the input of freshwater (hosing) in the HadCM3 climate model. Hosing weakens the AMOC, reducing the northward advection of heat and salt. However, a fresh buoyant cap forms at the air-sea boundary, beneath which the subsurface waters become isolated from surface fluxes and so remain warm and salty as they travel north. This leads to density anomalies that can cause instability in the water column.

In hosing simulations that continue for a substantial time with no additional hosing after the AMOC has weakened, the AMOC often recovers and sometimes with an overshoot (Vellinga et al. 2002; Stouffer et al. 2006; Cao et al. 2016). This may be due to the gradual warming of subsurface waters at low- and middle-latitudes (Stouffer and Manabe 1999) along with increased northward salinity advection (Thorpe et al. 2001; Bitz et al. 2007). In low-resolution (FAMOUS) simulations, the AMOC has been shown to begin recovery soon after hosing ends (Smith and Gregory 2009), with similar rates of recovery seen in simulations where the AMOC had weakened to different extents. Smith and Gregory (2009) found no evidence of irreversible weakening in the AMOC. Two of their simulations ended with AMOC strengths greater than that of the control run, as had been previously reported (Stouffer et al. 2006). This was attributed to double-

up – where the model responded to surface forcing reducing deep-water formation in the Labrador Sea region by initiating a 'compensating' deep-water formation in the Nordic Seas. As the original down welling recovered on the removal of hosing, this new additional source of deep-water continued for some time, with the 2 down welling sites temporarily giving a net increase on control values (Smith and Gregory 2009).

2.1.2 Changing salinity of the Atlantic Ocean

It has been suggested that the principle diagnostic for controlling AMOC strength is the mean Atlantic salinity. Changes in Atlantic salinity have been found to play an important role in weakening and recovery of the AMOC due to its impact on water density (Jackson 2013). It has also been shown that the strength of overturning scales with the meridional density gradient (Stommel 1961; Cimatoribus et al. 2014) and that it may be possible to estimate the Atlantic stream function by a comparison of density profiles in the North and South of the Atlantic (Sijp et al. 2012a; Butler et al. 2016). Changes to the North-South Atlantic density gradient have been found to be able to collapse the overturning (Cimatoribus et al. 2014).

To understand the role of salinity in the Atlantic, we need to consider the freshwater transports at the southern limit of the basin. When the northward freshwater transport by overturning, F_{ov}, at 30˚S is positive the AMOC is net exporting salinity. Under this condition, if the strength of the AMOC is reduced it leads to a build up of salinity. This increases Atlantic density, which in turn drives an increase in the AMOC. Positive F_{ov} therefore results in a negative feedback to a perturbation in the strength of the AMOC. However, when the F_{ov} is negative the AMOC is importing salinity. A reduction in the strength of the AMOC results in a decrease in the salinity of the Atlantic, reducing Atlantic density. This in turn further reduces the strength of the AMOC, giving a positive feedback (Rahmstorf 1996). Simulations modelling AMOC collapse (Hawkins et al. 2011) have found a negative value for F_{ov} during the collapse, with positive values on either side. It has been suggested that negative F_{ov} indicates the presence of a bistable regime (de Vries and Weber 2005; Hawkins et al. 2011), though this is inconclusive with other studies suggesting a need to find the freshwater divergence over the basin

(Dijkstra 2007; Huisman et al. 2010; Liu and Liu 2013, 2014). The use of F_{ov} as an indicator of freshwater transport into the basin may be undermined if there are large changes in the salinity transport by either gyre activity (Jackson 2013) or the Antarctic bottom water (AABW), as each of these can lead to a mismatch between the overturning transport and the salinity feedback.

While F_{ov} originates in bistability studies, as a diagnostic it is underpinned by the idea that the dominant feedback on AMOC transport is captured by the basin scale transport of freshwater at 30˚S. We therefore intend to explore whether this diagnostic can be used to understand the weakening and recovery pathways in the essentially mono-stable simulations presented here.

Observations and reanalysis suggest that the Atlantic currently has negative F_{ov} at 30˚S (Weijer et al. 1999; Hawkins et al. 2011; Bryden et al. 2011; Garzoli et al. 2013). The observed values indicate a positive salt advective feedback, meaning that freshwater perturbations may be amplified potentially enhancing any weakening (Garzoli et al. 2013). However, F_{ov} cannot always be assumed to scale with the total freshwater transport, as a significant contribution can also be made by the freshwater transport by gyre activity, F_{az}. F_{ov} has been found to reduce and become negative with increasing F_{az}, (de Vries and Weber 2005; Huisman et al. 2010; Cimatoribus et al. 2012; Jackson 2013; Cimatoribus et al. 2014). Changes in F_{ov} can also be compensated for by changes in F_{az}, reducing the impact on the total freshwater transport (Jackson 2013).

2.1.3 Aims

While previous studies have identified processes related to AMOC weakening, recovery and overshoot, questions remain concerning the extent of mechanical symmetry between weakening and recovery phases, and how well these processes can be defined using the frameworks described in **Section 2.1.2**. In this study, we use both approaches to examine the decline and recovery phases. We use an ensemble of freshwater hosing simulations in a low-resolution coupled climate model to robustly distinguish between driving mechanisms and chaotic variability, and to determine the ability of the 2 frameworks to capture the driving

mechanisms. We find that meridional density gradients explain the detailed temporal structure of the AMOC during both phases (**Section 2.4**), and that we are therefore able to reduce the problem to a density analysis of the North and South Atlantic (**Section 2.5**).

2.2 Methods

2.2.1 Model description

We used the Fast Met Office/U.K. Universities Simulator (FAMOUS), (Smith et al. 2008; Smith 2012). FAMOUS is a low-resolution ocean-atmosphere general circulation model. It is a computationally cheaper version of the higher resolution HadCM3, (Gordon et al. 2000), using mostly the same code, which has been tuned to produce similar climate results. FAMOUS has an ocean resolution of 3.75˚ longitude by 2.5˚ latitude, with 20 vertical levels. The horizontal atmospheric resolution is 7.5˚ longitude by 5˚ latitude, with 11 vertical levels. The atmosphere and ocean were coupled once per simulated day, consisting of 24 atmospheric time steps and 2 ocean time steps. Higher resolution models may have significant feedbacks that are absent from FAMOUS, such as altered net advection through the Bering Strait where a reduction of the freshwater flux may impact the response of the AMOC to freshwater forcing (de Boer and Nof 2004; Hu et al. 2012b; Liu et al. 2013, 2017). However the relationship between Atlantic meridional density gradient and AMOC strength has been shown to be robust in an eddy-permitting model (Butler et al. 2016) indicating that our analysis approach is applicable to such models.

FAMOUS representation of the AMOC compares well with a variety of higher resolution fully coupled climate models (Boulton et al. 2014). Comparison with observational data is difficult due to the short observational record. However, the mean transports at 26˚N in the Atlantic given by FAMOUS and those estimated by the RAPID/MOCHA/WBTS array over the years 2004–2012 (McCarthy et al. 2015) both give ~17.5 Sv. In the control runs, which used a pre-industrial climate with constant forcings, FAMOUS was found to have interannual variability of ~2 Sv. FAMOUS has broadly realistic sea surface salinity and temperature values **Figure 2.1**. The surface salinity values vary more strongly, with a wider range of values, in FAMOUS than in observations**.** In the northern hemisphere FAMOUS has a high latitude cold bias in

winter, making it 5 ˚C cooler than observations (Smith and Gregory 2009; Smith 2012, see **Figure 2** for errors in seasonal surface temperature with respect to the NCEP reanalysis). This leads to excessive North Atlantic sea ice and likely contributes to the strength of the AMOC. The control decadal mean stream function and zonal mean salinity are given in the top panels of **Figure 2.2**.

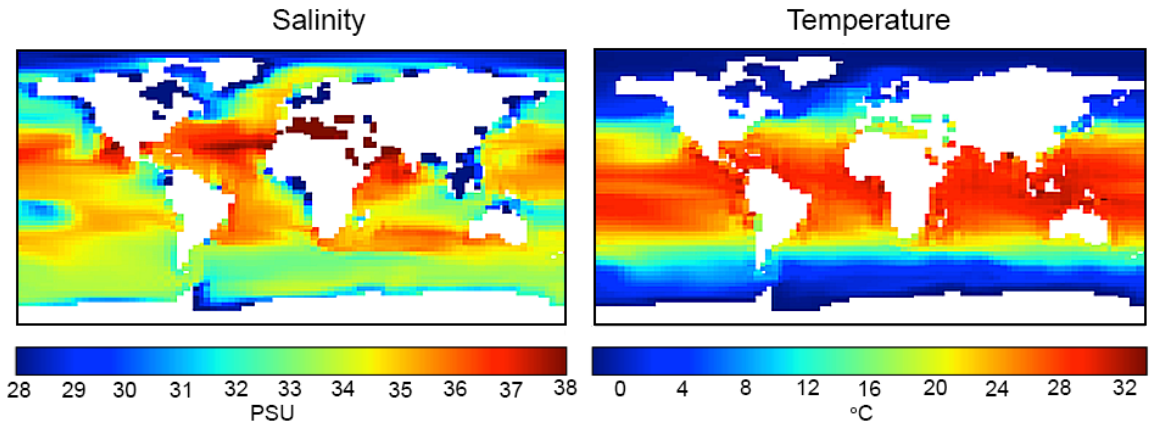

Fig. 2.1 Decadal mean surface salinity, PSU, and temperature, ˚C, from the last 10 years of the control simulation

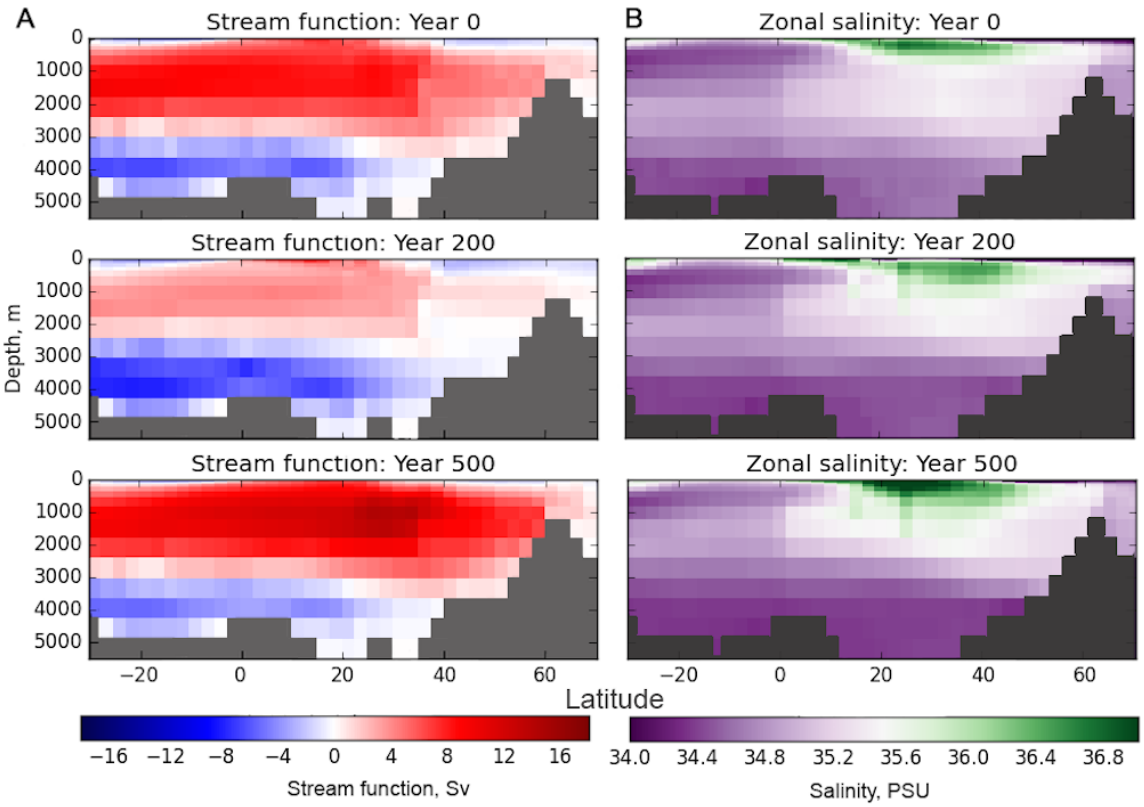

Fig. 2.2 Zonal mean Atlantic plots for the 0.5 Sv ensemble group for **A**: the stream function, in Sv, and **B**: the salinity, in PSU. Given as decadal means, showing the initial, end of hosing, and post-overshoot states

2.2.2 Freshwater hosing scenarios

The freshwater forcing, F, was achieved by applying an additional freshwater flux to the ice calving parameter, in units of kg m^{-2} s^{-1}. This was calculated as:

$$F = \frac{H\ 10^6\ \rho_{fw}}{A}$$

where H is the hosing rate in Sv, ρ_{fw} is a constant for the density of freshwater, here taken to be 1000 kg m^{-3}, and A is the hosing area in m^2.

Simulations were hosed with 0.2 or 0.5 Sv of freshwater. This was applied evenly over the surface from 50°N in the Atlantic to the Bering Strait. The freshwater input was balanced by volume compensation, throughout the entire ocean, effectively subtracting salt out of the surface of the hosing region and adding it back in equally over all ocean boxes to conserve the global reservoir. This was chosen in preference to surface compensation, where the freshwater input is balanced by returning the salinity to the surface boxes only. Surface compensation impacts global density stratification and has been shown to result in a bistable AMOC in FAMOUS, while the volume compensation used here results in an essentially mono-stable AMOC (Jackson et al. 2017).

'Top hat' experiments were used, where the full hosing value was imposed from the first time step. Hosing was applied constantly for 200 years, and then stopped. The simulations were then run on for a further 400 years to observe the recovery process. Ten simulations were run with each of 0, 0.2 and 0.5 Sv of freshwater forcing, each of the 10 runs being initialised from a different point along an equilibrium state simulation. Unless otherwise specified, the results presented will be the ensemble mean for each hosing rate.

2.2.3 Salinity budget and transports

As there is no advection through the Bering Strait in FAMOUS, we take the Atlantic basin as having 2 open boundaries, at 30°S and at the air-sea surface. The salinity budget of the Atlantic is the change in salinity (S, in PSU), over time (t, in s), throughout a volume (V, in m^3):

$$V\frac{dS}{dt} = F_S + Surf + Res$$

where F_s is the northward salinity flux at 30˚S which can be described using the freshwater transports F_{ov}, F_{az}, and a small term for the diffusion, F_d. Surf is the net salinity input due to precipitation, evaporation, river runoff, ice melt, and hosing. Additionally there is a residual component, Res, which includes small terms such as the Mediterranean outflow, Gent-McWilliams scheme, and the Robert-Asselin filter (Smith et al. 2008).

The freshwater flux into the Atlantic basin by overturning, F_{ov}, at ~30˚S is calculated using the mean zonal salinity and velocity through a zonal section. F_{ov} may be calculated using the equation:

$$F_{ov} = -\frac{1}{S_o}\int_0^H \bar{V}(z)(\langle S(z)\rangle - S_0)\,dz$$

where S_o is a reference salinity, used to remove the barotropic contribution, $\bar{V}(z)$ is the zonally integrated meridional velocity, and $\langle S(z)\rangle$ is the zonally averaged salinity (Jackson 2013).

The F_{az} is related to the strength of the zonal salinity and velocity gradients. This may be expressed as (Cimatoribus et al. 2012):

$$F_{az} = -\frac{1}{S_o}\int v'S'dxdz$$

where $v' = v - \langle v\rangle$, and $S' = S - \langle S\rangle$.

2.3. Ocean response to imposition and removal of freshwater forcing

2.3.1 Asymmetric overturning adjustments during weakening and recovery

The majority of the weakening of the stream function occurred within the first 80 years of hosing **Figure 2.3**. The North Atlantic stream function responded quickly

to the removal of hosing before overshooting the initial value, giving clear asymmetry over the 200 years before and after hosing is removed. After 200 years unhosed the stream functions in all simulations recovered to near control values. The asymmetry either side of year 200 therefore includes both an asymmetry in the rate of change of magnitude, with the rate of recovery being faster than the rate of weakening, and also an asymmetry in magnitude of change, due to the overshoot occurring in the recovery phase.

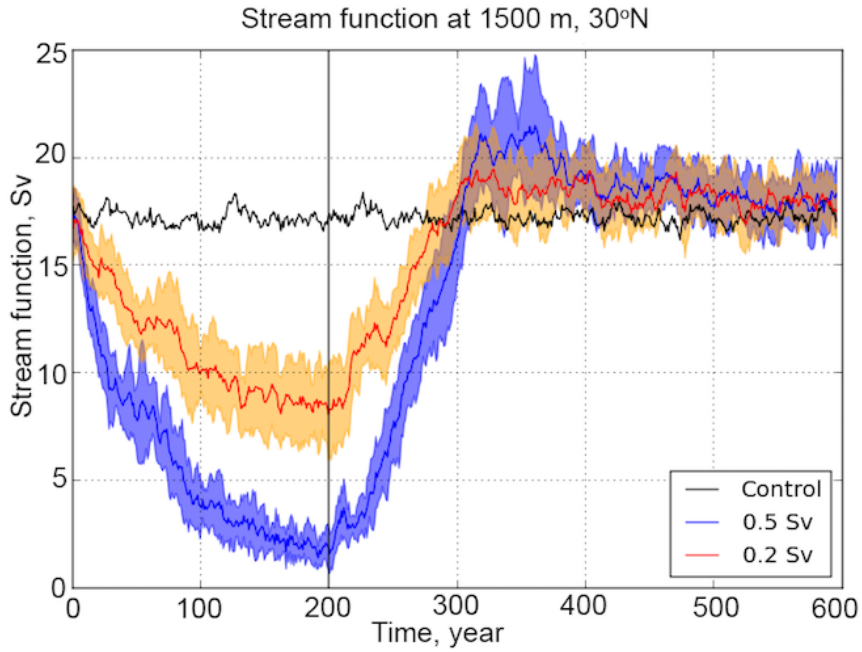

Fig. 2.3 Stream function at 30˚N, 1500 m depth, in the Atlantic. The ensemble means are shown for all 3 experiments, with ±1 standard deviation given by the shaded regions for the hosed simulations. The vertical line marks the end of hosing

These changes indicate wider readjustments between the relative influences of different water masses. The hosing reduces the NADW transport, and a reverse circulation consisting of an enhanced AABW transport develops, **Figure 2.2**. Once hosing is removed the AABW rapidly reduces in latitudinal extent, with the centre of the recovering AMOC between 20˚N and 30˚N, at a depth of <1000 m. As the AMOC gains in strength its centre migrates deeper and northward. Four hundred years after hosing was removed the AMOC has slightly higher maximum values than the initial state, by ~3 Sv, with a greater region showing high values.

2.3.2 Salinity and heat changes in the Atlantic basin

In this section we test the hypothesis that the asymmetry in weakening and recovery phases can be explained in terms of the mean Atlantic salinity and heat. This would be consistent with the idea that AMOC stability is determined by freshwater fluxes at the southern boundary of the Atlantic.

The mean salinity of the region between 30˚S in the Atlantic and the Bering Strait was calculated for all of the hosing simulations. The mean salinity initially decreased due to the hosing. Increasing hosing does not linearly reduce salinity **Figure 2.4A.** This is likely due to a combination of altered salinity transports and feedbacks mechanism both within the ocean (salt advective feedback) and also at the surface, which are explored further in **Section 2.5.2**. In the 0.2 Sv runs these feedbacks lead to the mean salinity returning to initial values during hosing, with partial recovery in the 0.5 Sv ensemble. When the hosing was removed the mean salinity sharply increased, then began to level off after ~50 years. After another ~150 years the salinity reached a peak before returning to control values. This response to hosing is similar for a range of both hosing rates and hosing durations, **Figures 2.4C** and **D**. These panels show a wider range of hosing rates over the same duration **Figure 2.4C**, and a range of post-hosing runs initialised from a longer 0.5 Sv hosing run **Figure 2.4D**, including a 600-year post-hosing run where the mean salinity makes a full recovery. These demonstrate the consistent response of the mean salinity to the removal of hosing, and go some way to demonstrate the independence of the recovery timescale from the forcing applied. They suggest that in all cases the mean salinity takes ~600 years to make a full recovery. This consistency between runs is likely explained by the recovery being controlled by ocean overturning timescales, where the accumulated positive salinity anomaly is exported from the region by the recovered AMOC.

Figure 2.4B demonstrates the absence of a simple relationship between the mean Atlantic salinity and the strength of the Atlantic stream function. Salinity and the stream function are initially well correlated (for the first 80 and 40 years for the 0.2 and 0.5 Sv ensembles, respectively), however the mean Atlantic salinity starts to increase before hosing ends while the AMOC continues to weaken. At the start of the recovery phase there was a quick increase in the value of the mean salinity

before any substantial response in the strength of the stream function. This will partly be the direct impact of the removal of hosing, before the other salinity fluxes have had time to respond. The 0.5 Sv ensemble had maximum mean salinity values during the overshoot, before slowly reducing as the basin readjusts towards the control state.

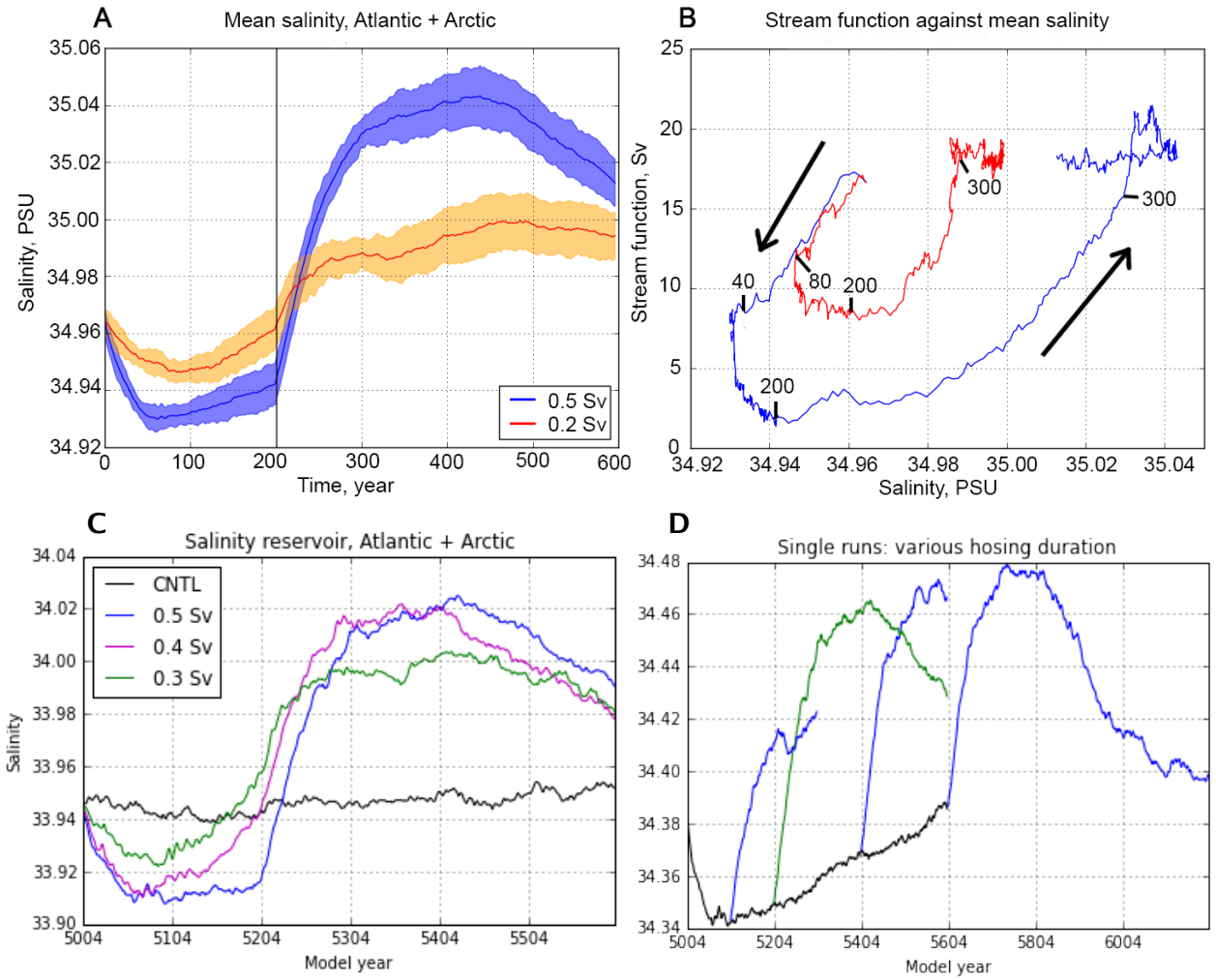

Fig. 2.4 **A**: Ensemble mean salinity from 30˚S to the Bering Strait for 600-year simulations, with 0.2 and 0.5 Sv of freshwater forcing through the first 200 years. **B**: Stream function versus basin mean salinity for the 0.2 and 0.5 Sv ensembles, from 30˚S to the Bering Strait. Reference years marked in black. Legend applies to both plots **A** and **B**. **C**: Mean salinity for single runs with a range of freshwater forcing rates and control run, where the blue line is a run included in the ensemble in **A**. **D**: Black line shows 0.5 Sv constant hosing for 600 years, with a range of post-hosing runs initialled at different times along it. The green line shows post-hosing data for a run included in the ensemble in **A**

The temperature of the basin also varied significantly over the course of the simulation, showing less asymmetry in the response through hosing and recovery. During the hosing phase the mean temperature of the Atlantic and

Arctic region increased **Figure 2.5**. When the hosing was removed, temperature was slower to return to the initial values. The developed temperature anomaly continued to dissipate through the overshoot and later stage of recovery. The impact this had on the densities for the 0.5 Sv ensemble will be explored further in **Section 2.5**.

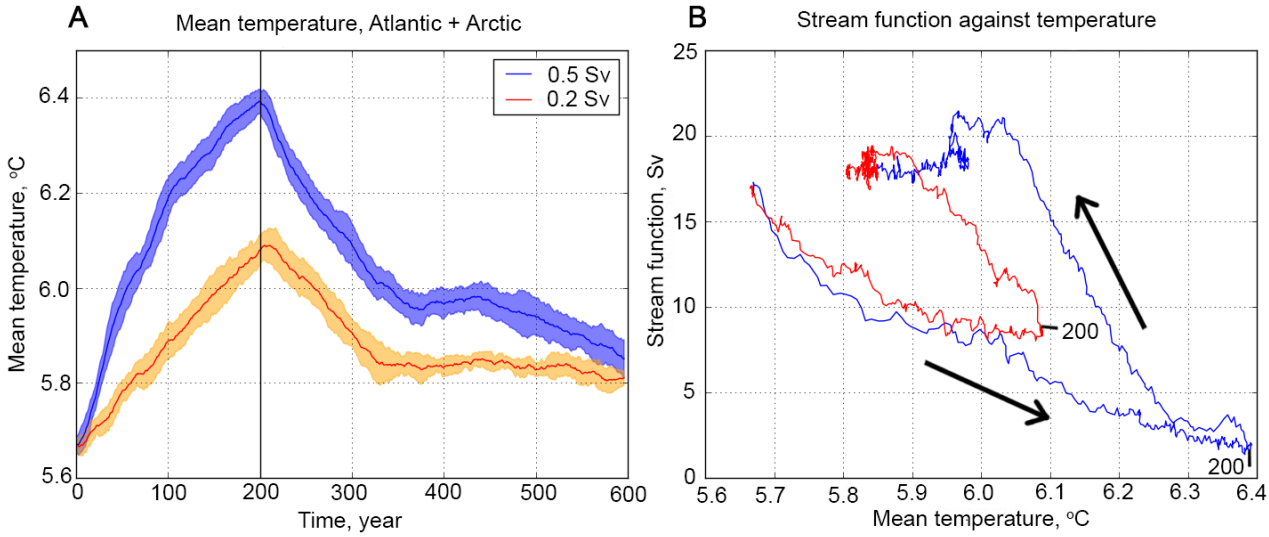

Fig. 2.5 A: Ensemble mean temperature from 30˚S to the Bering Strait for 10 600-year simulations with 0.5 or 0.2 Sv freshwater forcing through the first 200 years. **B**: Stream function versus basin mean temperature for the 0.2 and 0.5 Sv ensemble groups. End of hosing marked in black. Legend applies to both plots

2.4. Understanding AMOC behaviour with meridional density differences

2.4.1 Reconstructing stream function from density profiles

We want to find a mechanistic explanation for the asymmetric response of the AMOC. A promising approach to this problem is to explore the role of salinity and temperature by reconstructing the stream function from meridional density profiles. Butler et al. (2016) used a scaling relationship that links the Atlantic overturning to the twice vertically-integrated meridional density gradient, which they described as geostrophy, rotated by 90˚. We can logically see that meridional pressure gradients can impact meridional overturning, as changes in the meridional pressure gradient will induce changes in zonal flow, impacting zonal

pressure gradients, and thereby driving changes in meridional flow. Butler et al. (2016) obtained the strongest correlations by using density gradients at the western boundary. Here, we will use zonal means because of their connection with meridional heat and salinity transport.

2.4.2 Extent of reconstructive skill in hosing scenarios

The full width of the Atlantic was used to reconstruct the ensemble mean stream function **Figure 2.6**. This gave a good approximation to the form of the stream function profiles calculated from the velocities, both spatially and temporally. We have taken our southern section at 30˚S to describe the densities within the southern limit of the Atlantic Basin. The northern section is at 50˚N, in order to both capture the subpolar densities and retain sufficient depth to include deep ocean processes. The scaling factor applied to the reconstruction was chosen to match the magnitude of the pre-hosing state to the control AMOC, and does not fully capture the magnitude of AMOC weakening.

In order to consider how well the variability was captured we will compare the time series for single simulations as calculated from the velocities and from meridional densities **Figure 2.7**. The reconstructions demonstrate both the features of weakening and recovery and the background decadal variability of the control run. Again, due to the constant scaling factor used, the full extent of weakening in the hosed runs is not seen in the reconstructions.

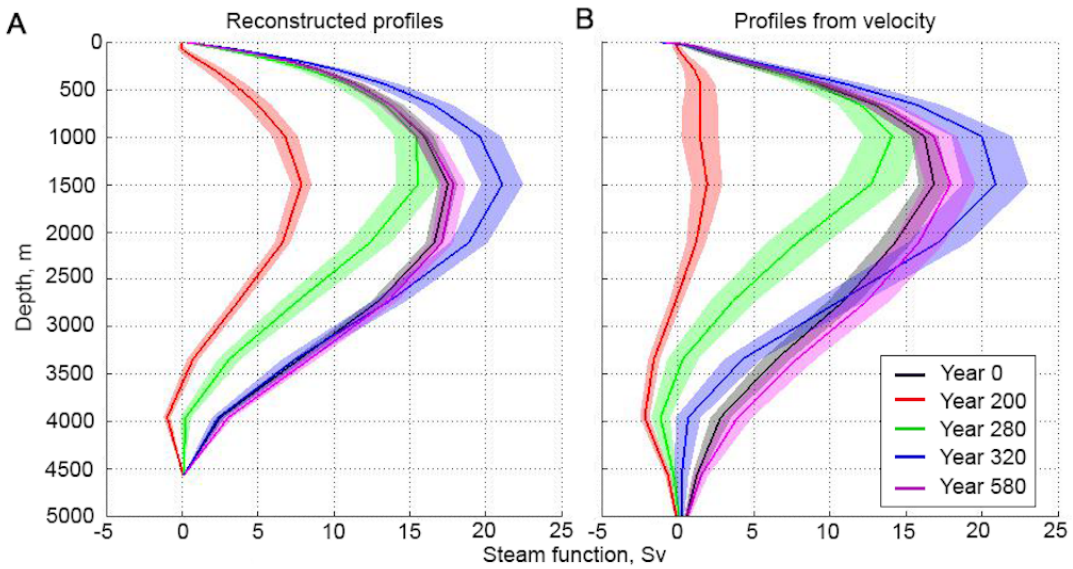

Fig. 2.6 A: Reconstructed stream function profiles for 30˚N, using the full basin width, and **B**: calculated from the velocities. Both panels give the ensemble mean of the 0.5 Sv hosing run, with ±1 standard deviation shaded. The panels share the legend. Note that **B** is deeper than **A** due to the maximum depth in the reconstructed AMOC at 30˚N being limited to the maximum depth of data at 50˚N used in the calculations

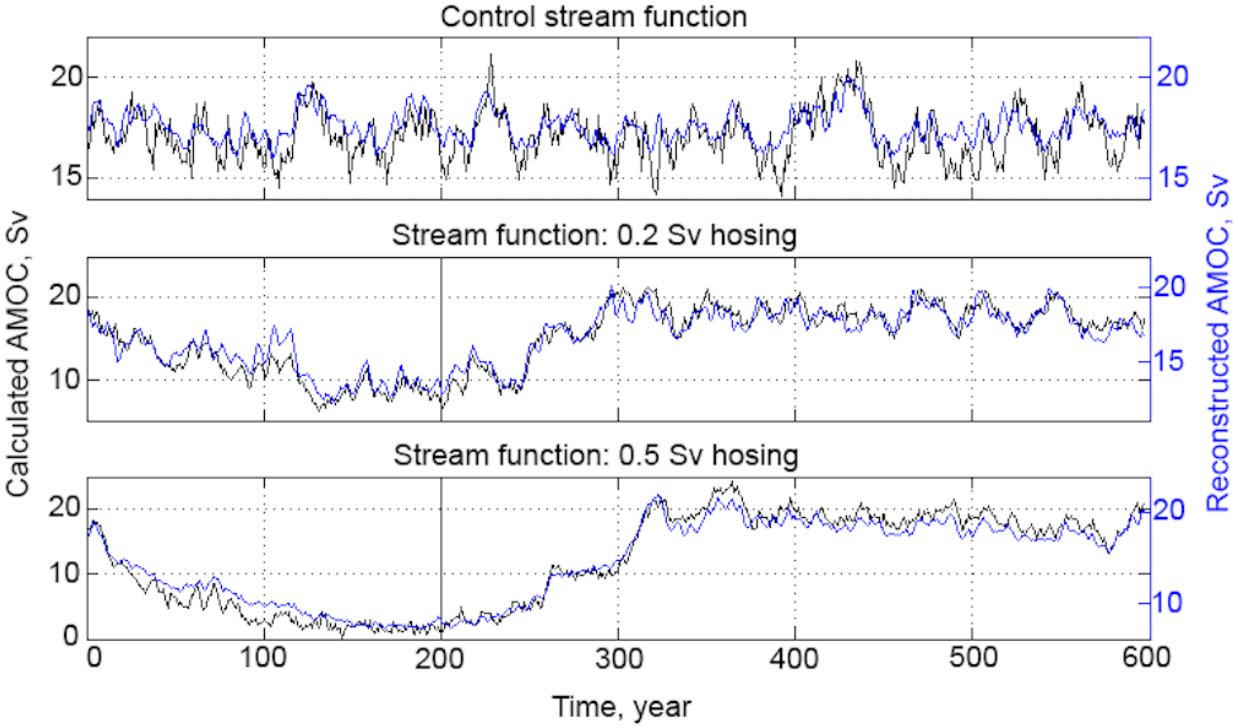

Fig 2.7 Comparison of reconstructed stream functions for 30˚N, and that calculated from the velocities for control, 0.2, and 0.5 Sv individual runs. Note that different y-axes have been applied to make the comparison of variability and form clearer, while the full extent of weakening is not captured by the reconstruction

2.5. What dominates the density changes?

2.5.1 Relative role of the northern and southern densities

Having seen that the meridional density profiles at 30˚S and 50˚N can be used to reconstruct the strength of the stream function at 30˚N, we now want to understand what induces these density changes. To simplify this question we break the influence down into that led by changes at 50˚N and that due to changes at 30˚S, **Figure 2.8.** This was done by repeating the reconstruction calculation using the 0.2 and 0.5 Sv ensemble means, firstly for the impact from density changes at 50˚N, by holding the density profile at 30˚S constantly equal to its initial state value. Then holding the density at 50˚N constant to find the stream function resulting from changes at 30˚S alone. This showed that the AMOC strength was primarily determined by the changes in the densities in the north. Density changes in the south are well correlated to density changes in the North but smaller in amplitude, acting as a simple moderator of AMOC decline and initial recovery. The 0.2 and 0.5 Sv runs show different magnitudes of impact while responding similarly and on the same timescales. They both show northern values rapidly recover in the first 100 years after hosing, followed by a more gradual adjustment. The 0.5 Sv run has an overshoot that cannot be explained without determining why the densities at 30˚S return to initial values on a longer timescale than densities at 50˚N.

We have concluded that changes in overturning, with the exception of the overshoot, can be explained by changes in density at 50˚N. To explain these density changes we have focused on the 0.5 Sv ensemble and determined the causes of convergence of heat and salinity over the northern and southern regions.

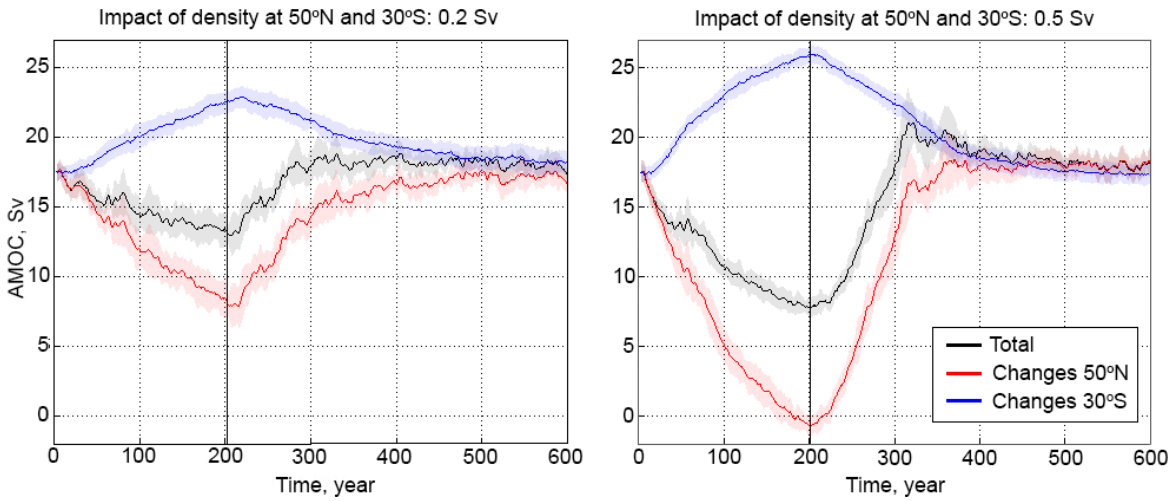

Fig 2.8 Comparison of the reconstructed stream function strength for the 0.2 and 0.5 Sv ensemble means, due to the changes in zonal mean density at 50˚N and 30˚S. The shaded regions give ±1 standard deviation. The black vertical line marks the end of hosing

2.5.2 Understanding density changes with heat and salinity fluxes

The density changes at 50˚N and 30˚S can be understood by considering the changes in ocean transport and air-sea fluxes of heat and salinity. To do this we consider the ocean convergences (including overturning, gyre, and diffusion components) and surface fluxes over the boxes 45˚N - 55˚N, and 32˚S - 22˚S, **Figure 2.9**. We chose these broader regions to avoid impacts from localised variability. The northern box was chosen to centre on 50˚N, and the southern box was chosen as the southernmost 10˚ where the domain would be zonally contained within lateral continental boundaries. The residual term was taken as the rate of change of the variable minus the sum of the ocean convergences and the surface fluxes, calculated using decadal mean values. The heat residual term is small, however the salinity residual is non-negligible, due in part to the sub-grid scale eddy transports as represented by the Gent-McWilliams scheme (Gent and McWilliams 1990). In both the northern and southern boxes, there is some salinity reduction that cannot be attributed since it appears in the residual term.

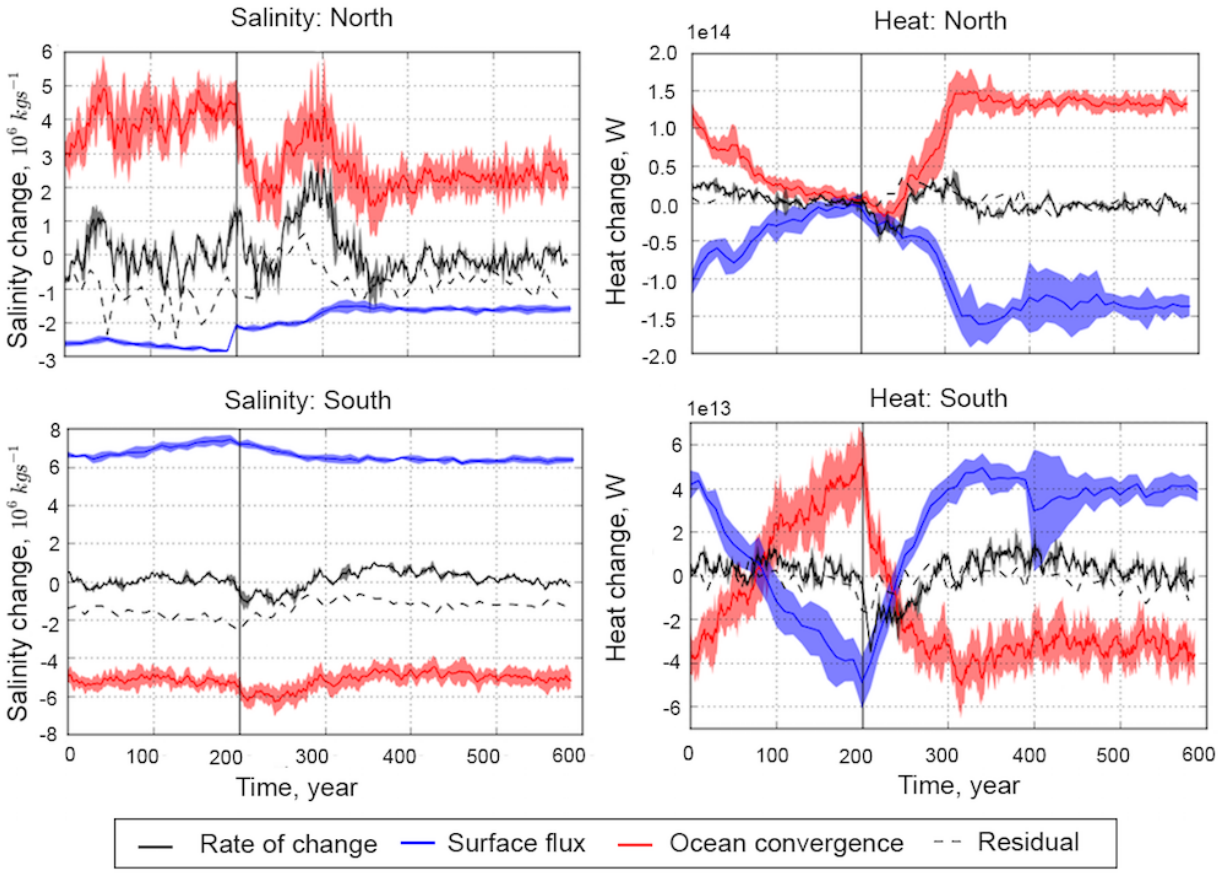

Fig. 2.9 Change in salinity and heat over boxes in the north (45˚N - 55˚N) and south (32˚S - 22˚S) of the Atlantic. **Red**: ocean convergence including overturning, gyre activity and diffusion, given as 10-year rolling means. **Blue**: surface flux including hosing input, using decadal mean data. **Black**: the calculated rate of change of variable in box, given as 10-year rolling mean. **Dashed**: the residual term calculated from the decadal data for the rate of change minus the sum of surface fluxes and ocean convergence. The shaded region gives ±1 standard deviation and the black vertical line marks the end of hosing

At the start of hosing we see an initial freshening in the northern box, due to half of the box being within the hosing region. Then there is a strong increase in salinity convergence over the northern box, due to high salinity, reduced velocity, northward transports into the region. This acts to increase the density of the local water mass. The ocean heat convergence reduces during hosing, in line with the weakening of the AMOC. However, the heat content of this box increases significantly in the hosing phase. The region typically has a large heat flux to the atmosphere, as it imports warm lower latitude waters that release heat as they travel northward. The imposed freshwater forcing acts as a cap over the surface of the region, trapping warm saline waters underneath, greatly reducing the surface heat loss. In this model, the AMOC weakening is driven by the reduced

density of the northern upper ocean resulting from freshening at the surface and warming from 200-2000 m, **Figures 2.10**.

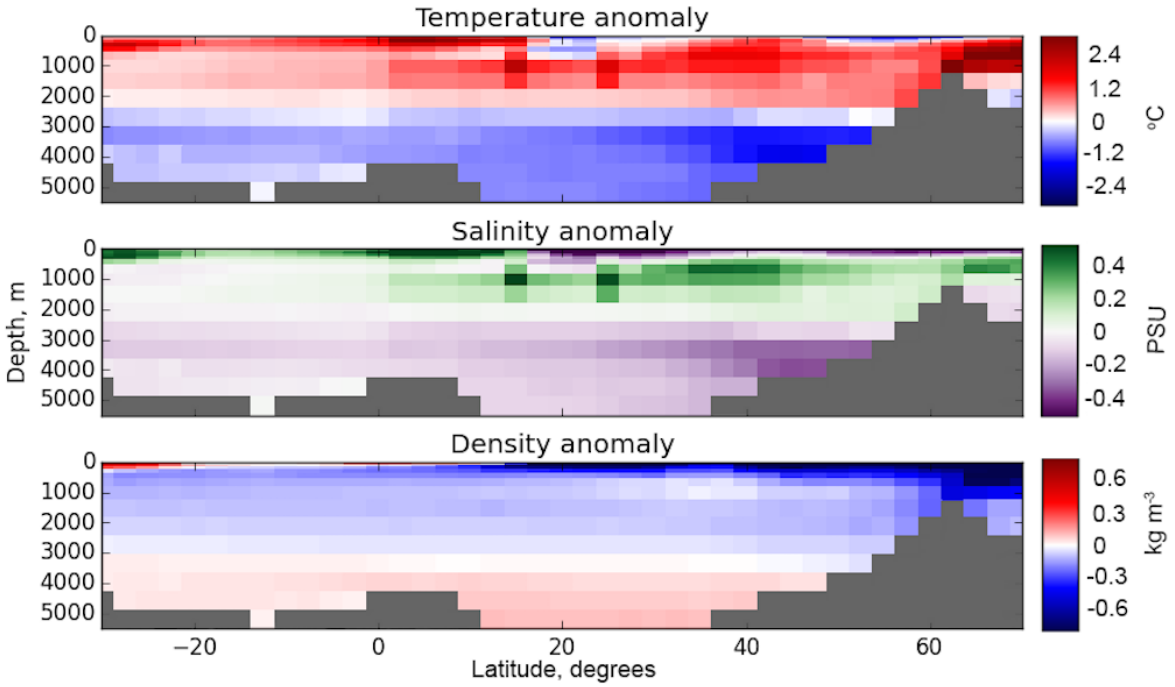

Fig. 2.10 Atlantic mean zonal anomaly plots for temperature, salinity, and density, using the mean for the final decade of hosing (years 189-199)

When hosing is switched off (year 200) the northern surface freshwater input decreases, **Figure 2.9**. The ocean salinity convergence responds quickly (20 years), with reduced northward transport of salinity into the northern region. This represents the shutting down of the high salinity subsurface transport that was seen in **Figure 2.2**. The recovering AMOC brings in high salinity anomalies that contribute to the overshoot. These anomalies developed at low latitude due to changes in atmospheric circulation patterns, notably the southward shift of the ITCZ, during weak AMOC (not shown), as has been previously reported (Wu et al. 2011; Jackson 2013; Bouttes et al. 2015). The heat of the northern box decreases over the first 50 years after hosing ends. During this time, the surface cap dissipates allowing for the surface flux to start to recover, as the strengthening AMOC exports some of the heat anomaly. The heat convergence then undergoes a fast transition, as the recovering AMOC again brings in waters warmed at lower latitudes. The high frequency structure of the overshoot is lead by these density fluctuations being transported into the down welling region.

The process of accumulation and release of subsurface warmth in the North Atlantic contributes to the asymmetry (in rate of change of overturning strength) seen between the weakening and recovery phases. When the ocean is forced with freshwater at the surface, the ocean is capped and the subsurface temperatures gradually build. This slow accumulation contributes to the gradual weakening of the AMOC. When the freshwater forcing is removed (in one time step) the surface heat flux is quickly enhanced. The accumulated subsurface heat can be released to the atmosphere at a greater rate than it was accumulated in the subsurface by ocean transports. The removal of freshwater forcing therefore gives a shock to the system, giving a much faster initial recovery.

The southern box shows smaller amplitude net change during hosing. As the AMOC weakens, the South Atlantic changes from transporting heat northwards to bringing it southwards, in a more hemispherically symmetric manner. This means that instead of being a region of cool waters taking up atmospheric heat, the surface waters are able to warm the overlying atmosphere. On the removal of hosing, the ocean heat convergence responds significantly faster than the surface flux, leading to a cooling of the local ocean.

2.5.3 Role of overturning and gyre feedbacks

In order to identify the ocean mechanisms related to changes in the convergence of density we break the transports down into components of overturning, gyre activity, and diffusion. The distinction between these components at 50°N is less clear, due to the horizontal elements of the overturning transport in the sub-polar region, however we can still learn something from the apparent components. The northward salinity transports at 50°N, **Figure 2.11A**, increased over the first 30 years of hosing, after which gyre transport began to weaken, while the overturning transport strengthened – due to high salinity values, **Figure 2.2**. The two components therefore compensated for each other, suggesting a shift in the circulation structure and giving a steady total transport for much of the hosing phase. The overturning quickly recovered its initial values on the removal of forcing, while the gyre took longer, first exceeding initial values. This shows the low latitude high salinity anomalies being transported to the downwelling region by the gyre. This enhances the stream function recovery, with the gyre transports

returning to near initial values during the stream function overshoot. A similar behaviour can be seen in the thermoclines at 50˚N, which show a 'double dip' during recovery at around 1500 m deep, **Figure 2.12B**. After a relatively fast initial recovery there seems to be a fluctuation during the overshoot, due to the downwelling of patches of warm water transported north from the sub-tropics by gyre activity, **Figure 2.11A**.

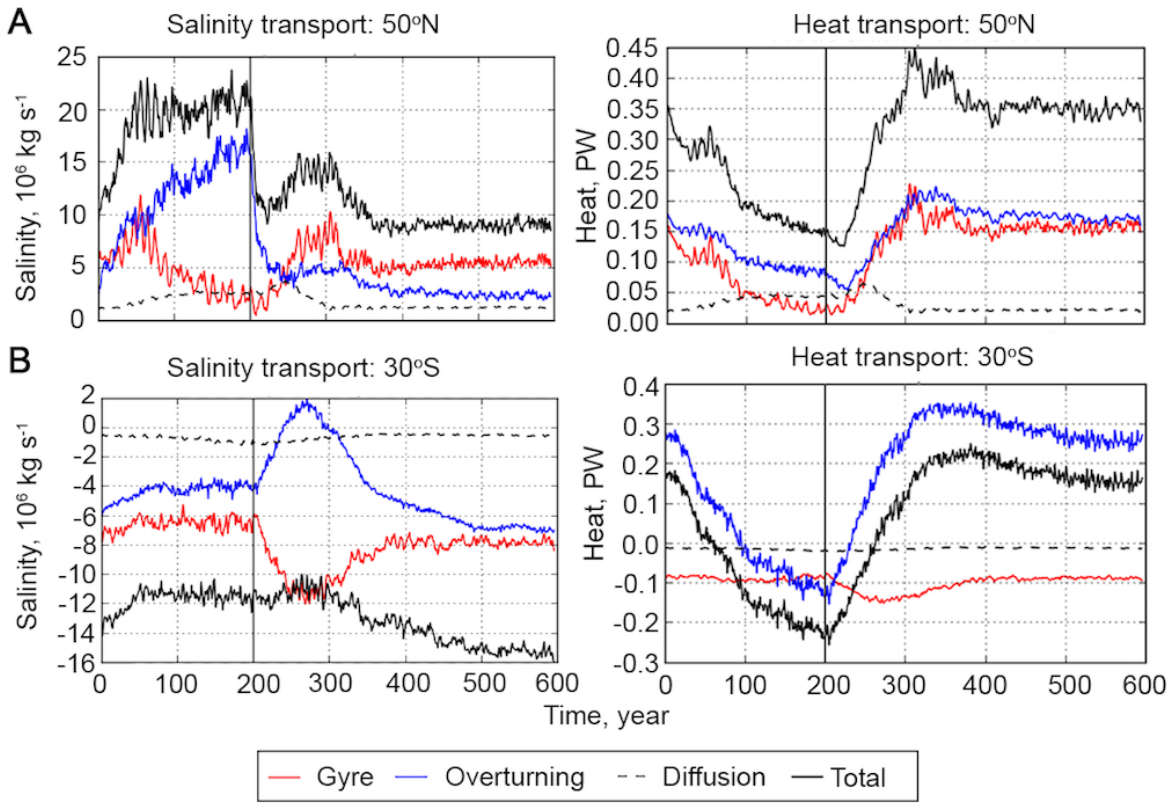

Fig. 2.11 Salinity and heat transports at 50˚N (**A**) and 30˚S (**B**). The key applies to all panels. Ensemble mean of 600-year hosing simulations, with 0.5 Sv hosing for the first 200 years. Standard deviations are excluded for clarity

Changes to the total salinity transport at 30˚S were less pronounced, and yet as the boundary to the Atlantic basin, may still be significant to the basin state. The value of F_{ov} at 30˚S was positive in the control state (0.17 Sv, which is equivalent to a -6×10^{6} kg s^{-1} salinity transport) and it remained so throughout hosing, having a minimum value of 0.1 Sv, **Figure 2.11B**. This suggests that the AMOC control state may have been more stable in these simulations than in observation and reanalysis. The overturning did begin to import salinity into the basin at 30˚S during the recovery phase, however this was compensated for by changes in gyre activity (increase in F_{az}) – and so did not indicate change in the total salinity imported into the Atlantic basin. The use of F_{ov} as an indicator requires that the

changes in other contributions to freshwater transport, such as F_{az}, are smaller at 30˚S (Jackson 2013) which was not the case here. Weak AMOC coincided with times of reduced total northward freshwater transport at 30˚S.

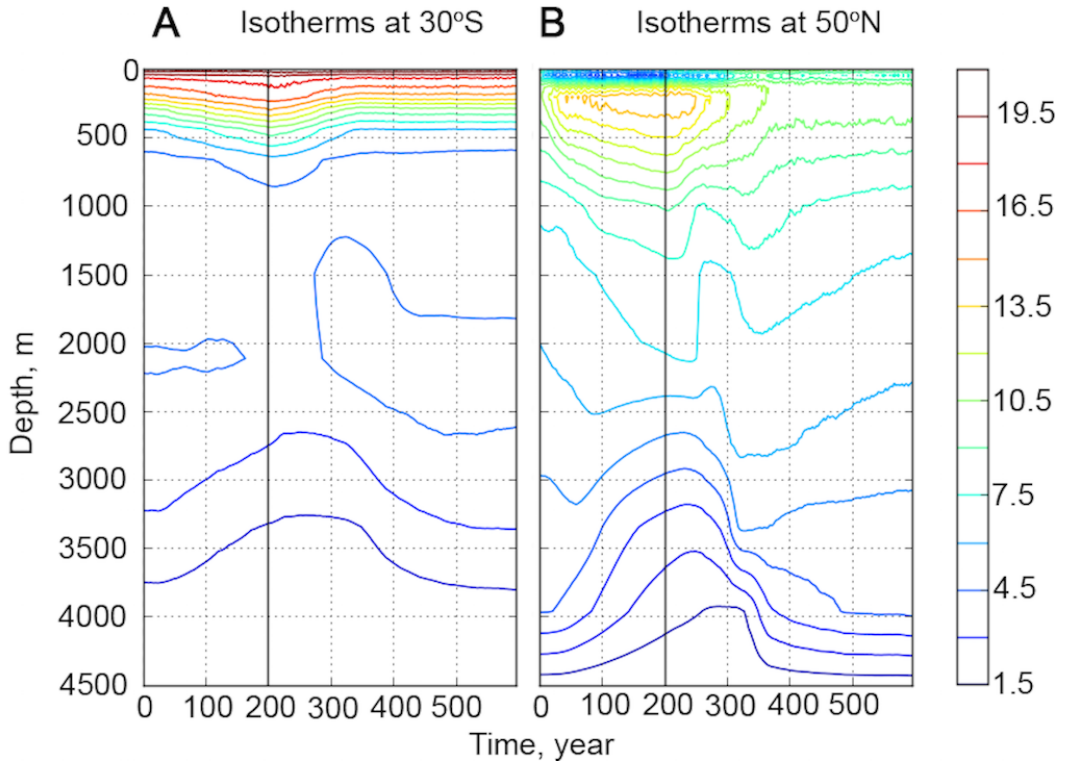

Fig. 2.12 Hovmoller plots of the ensemble Atlantic zonal mean temperatures at **A**: 30˚S and **B:** 50˚N, through the duration of the 600-year simulation, hosed with 0.5 Sv. Temperatures given in ˚C

2.5.4 Influence of 30˚S in AMOC overshoot

The changes in the southern density profile enhanced the strength of overturning. This was due to the warming caused by ocean heat convergence exceeding the atmospheric cooling, **Figure 2.9**, net reducing local densities. The thermocline at 30˚S deepens during hosing, **Figure 2.12A**, due to reduced North Atlantic overturning leading to the Atlantic exporting less dense water. The thermocline later shoals as it drains. This occurs on a multi-centennial timescale, with some lag to changes in freshwater forcing. As the response time is longer further from the site of hosing, the density profile at 30˚S still contributes to an enhanced AMOC once the northern signal showed a near return to control values, **Figure 2.8**.

To understand the broader extent of change in the South Atlantic region we can look at changes in atmospheric fields that occur during the hosing phase. **Figure 2.13** shows the global barotropic stream function and surface winds at the start of the 0.5 Sv hosed run and the anomaly in the fields by the end of the hosing phase. This shows particularly strong changes in these atmospheric fields over the South Atlantic, which suggests strongly changed atmospheric forcing on the ocean, including the South Atlantic gyre. By the end of hosing, the strong positive values of the stream function over Antarctica are enhanced, and extend further equatorward towards the South Atlantic. The eastward circumpolar winds become weaker near the Antarctic coast and are strengthed over 30˚S. These are not direct consequences of the freshwater forcing, but develop as a consequence of a chain of causality during the hosing phase. When forcing is removed these anomalies will not be instantanteously resolved, and so nor will the altered surface forcing on the ocean at 30˚S which they drive. The process of recovery of the atmospheric forcing in the South Atlantic will likely contribute to the extended timescale of the ocean recovery process.

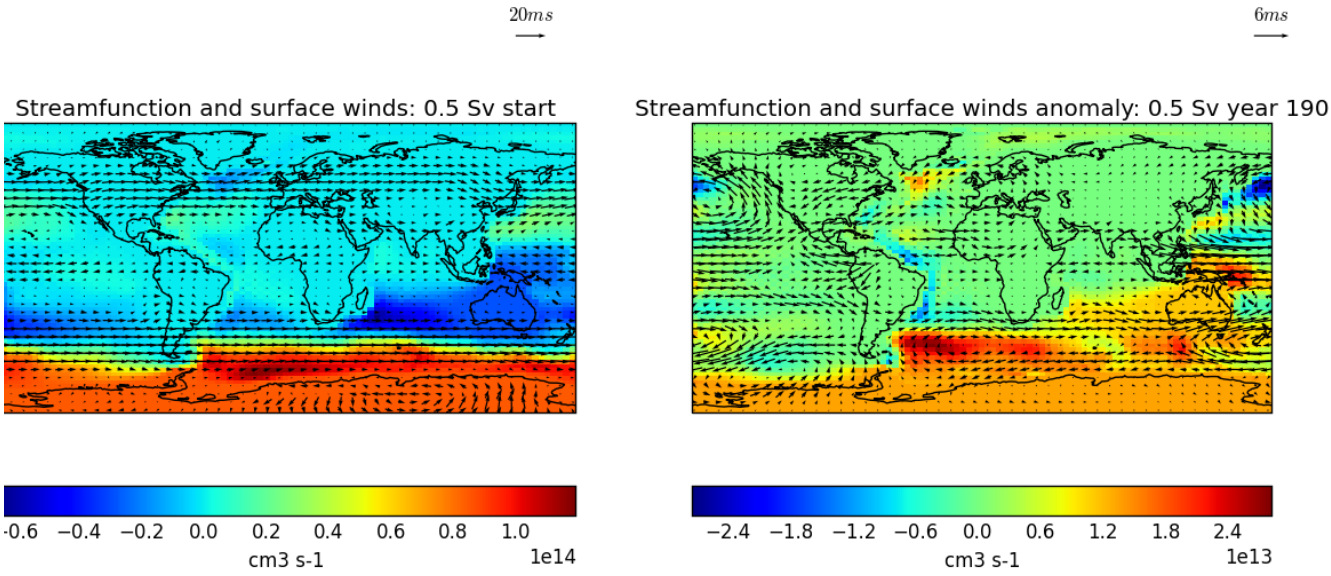

Fig. 2.13 Atmospheric barotropic stream function and surface wind fields (arrows) at the beginning of the 0.5 Sv run and the anomaly at the end of hosing (each as 30-year means)

This means that the densities of the South Atlantic provide a low frequency signal that gives the magnitude of the overshoot, with the higher frequency variability coming from the North Atlantic. This is in contrast with previous model studies' explanation for overshoot behaviour. It has been reported that as the AMOC begins to recover, the salinity anomaly built up in the subtropical gyre is

advected to higher latitudes (Wu et al. 2011; Jackson 2013, using CO_2 and freshwater forcing, respectively) leading to higher density waters in the down welling regions – briefly enhancing the AMOC (Bouttes et al. 2015).

2.6. Discussion

All hosed runs displayed asymmetry between weakening and recovery. The stream function at 30°N, 1500 meters deep, weakened quite smoothly over the 200 years of hosing. In the following 200 years it recovered, overshot and returned to near control values. The ensemble mean stream function strength for the 0.5 Sv simulations increased by 20 Sv over the course of 120 years. Multiple studies have explored the climate impacts of an abrupt AMOC weakening (Vellinga and Wood 2002; Jackson et al. 2015) however less research has been done on the climate impact of abrupt recovery and overshoot. The findings of this study suggest that this could be an important topic for future research.

The meridional density gradient was a better indicator of the stream function than the mean basin salinity. This indicates that the distribution of heat and salinity within the Atlantic, rather than the mean value, was the primary control. High latitude subsurface heat increase, resulting from suppression of ventilation, has been reported in previous freshwater forcing studies, (Mignot et al. 2007; Krebs and Timmermann 2007). This has been suggested to destabilise the water column and contribute to an abrupt AMOC recovery, once the forcing is removed allowing the isopycnal slopes to readjust, and heat to be released to the atmosphere. In this study the heat changes played a strong, destabilising, role throughout. A high salinity anomaly in the sub-tropical North Atlantic, accumulated during weak AMOC, being transported northwards as the AMOC recovers has been previously observed in models. The high-density water mass reaching down welling regions has been used to explain strong recovery and overshoot, (Wu et al. 2011; Jackson 2013; Bouttes et al. 2015). The way in which models disperse this density anomaly defines the recovery process within each model (Sgubin et al. 2015). Our results indicate that the progress of the high-density water mass through the North Atlantic plays a crucial role in the recovery,

and gives the high-frequency variability within the overshoot. However, the overshoot itself was caused by the longer timescale behaviour governing pycnocline depth in the South Atlantic.

In summary, the results of this study suggest a recovery process of the AMOC that is mechanistically different from the weakening process, influenced by the deepening of the South Atlantic thermocline. The initial stream function recovery in FAMOUS was related to the removal of hosing input, allowing North Atlantic surface heat and freshwater fluxes to recover. For the full recovery, the density needed to increase in the northern latitudes. The overshoot took its high frequency structure from the north Atlantic density transports, and its magnitude from density changes at 30°S.

Chapter 3: Temperature domination of AMOC weakening due to freshwater hosing in two GCMs

Abstract:

Anthropogenic climate change is projected to lead to a weakening of the Atlantic meridional overturning circulation (AMOC). One of the mechanisms contributing to this is ice melt leading to a freshening of the North Atlantic Ocean. We use two global climate models to investigate the role of temperature and salinity in the weakening of the AMOC resulting from freshwater forcing. This study finds that freshwater hosing reduces the strength of the AMOC, but in some situations it is not through reduced density from freshening, but a reduction in density from subsurface warming. When the freshwater is mixed down it directly reduces the density of the North Atlantic, weakening the strength of the AMOC. As the AMOC weakens, the mixed layer depth reduces and surface properties are less effectively mixed down. A buoyant surface cap forms, blocking atmospheric fluxes. This leads to the development of a warm anomaly beneath the surface cap, which becomes the primary driver of AMOC weakening. We found that the mean North Atlantic salinity anomaly can be used as a proxy for AMOC weakening because it describes the extent of this surface cap.

3.1 Introduction

Climate change projections suggest that global warming will cause ice melt and freshening of the North Atlantic Ocean. Paleoclimate research suggests that inputs of large quantities of freshwater have in the past greatly weakened the strength of the Atlantic meridional overturning circulation (AMOC), resulting in far reaching climatic impacts (McManus et al. 2004; Henry et al. 2016). Various simulation studies have shown that forcing the North Atlantic with freshwater reduces the strength of the AMOC (Stouffer et al. 2006; Hawkins et al. 2011). Though freshening is considered to be of secondary importance to radiative forcing in AMOC weakening associated with anthropogenic climate change, the inclusion of ice melt in climate scenarios has been shown to significantly enhance

the AMOC weakening response (Swingedouw and Braconnot 2007; Bakker et al. 2016).

Freshwater forcing studies have been used to investigate the relationship between Atlantic salinity and AMOC weakening. The more freshwater that is added to the North Atlantic, the more buoyant it becomes in comparison to the South Atlantic, reducing overturning by altering the Atlantic meridional density gradient (Cimatoribus et al. 2014; Jackson et al. 2017; Jackson and Wood 2018). The theoretical arguments that underlay AMOC theory (e.g. Bryan 1987; Butler et al. 2016; Sévellec and Huck 2016) indicate that density changes that are confined to the surface have a negligible effect on the AMOC, because thermohaline-led changes to the large-scale circulation require perturbations to horizontal pressure gradients over a substantial depth range (Oliver et al. 2005). Therefore it is necessary for the buoyant anomaly to propagate downwards through the water column; which is assumed to occur through the mixing down of freshwater. Questions therefore arise concerning whether the freshwater forcing is increasing buoyancy over a sufficient depth of the North Atlantic in order to directly reduce the strength of overturning, or whether there are intermediate mechanisms involved.

In this study we explore the driving mechanisms of AMOC weakening in response to freshwater forcing. We use two general circulation models (GCMs) to understand the timescales and forcing rates at which different ocean mechanisms become the primary driver of AMOC weakening.

3.2 Methods and Models

3.2.1 Estimating the AMOC from meridional density gradients

The AMOC can be estimated from a scaling relationship with the meridional density gradient, as discussed in Sijp et al. (2012). This is done by firstly finding the meridional component of the thermal wind equation by taking the vertical derivative of the meridional velocity, using geostrophic balance and the

hydrostatic approximation. This gives the basin-scale zonally average meridional velocity, $< V >$, as:

$$\frac{\partial < V >}{\partial z} = \left(\frac{-g}{f_0 \rho_0}\right) \cdot \left(\frac{\Delta \rho_x(z)}{L_x}\right)$$

where g is the gravitation constant, f_0 and ρ_0 are reference values for the Coriolis parameter and density, respectively, $\Delta \rho_x(z)$ is the zonal density difference on each depth level, and L_x gives the zonal length scale.

The next step is to link $\Delta \rho_x$ to the basin-scale meridional density difference, $\Delta \rho_y$. In order to achieve this an assumption of proportionality is made between zonal and meridional velocities (Robinson 1960). This approach was reasoned by Marotzke (1997) as changes in the meridional pressure gradient induce changes in zonal flow, impacting zonal pressure gradients, resulting in changes to meridional flow. The zonal and meridional density difference can then be related using a proportionality factor, n, where $\Delta \rho_x \sim n \, \Delta \rho_y$. Grouping the constants in the velocity equation above together with n as a scaling factor, c_ρ, then gives the approximation $< V > \sim c_\rho \, \Delta \rho_y H$, where H is the depth scale. Others have attempted to mathematically define a scaling factor between the zonal and meridional density gradients (see discussion in Sijp et al. (2012)). Approaches that take the mean of the density profile may neglect potentially significant features in the profile structure, becoming distorted by strong anomalies in the surface region. Using the mean of the density profile can yield the qualitatively wrong AMOC response in circumstances where using the depth dependent pressure gradient gives the qualitatively correct response (de Boer et al. 2010). As we are here interested in the physical mechanisms of AMOC weakening, we need to use a method that retains depth dependence in order to be sensitive to processes directly impacting deep pressure gradients. In order to retain the depth dependence of $\Delta \rho_y$ Butler et al. (2016) (hereafter referred to as B16) derived an expression for V:

$$< V(z) > = \frac{-c_\rho g}{\rho_0 f_0 L_y} \left(\frac{1}{h} \int_{-h}^{0} \left(\int_{z'}^{0} \Delta \rho_y(z'') dz'' \right) dz' - \int_{z}^{0} \Delta \rho_y(z') dz' \right) .$$

where h is the bottom depth. The Atlantic stream function, Ψ, using the vertically integrated meridional velocity in terms of the depth dependent meridional density difference, is then given as:

$$\Psi(z) = L_x \int_z^0 < V(z') > \, dz'.$$

3.2.2 Model simulations

Freshwater (hosing) was applied to the surface of the North Atlantic and Arctic region from 50˚N to the Bering Strait through a uniform additional surface flux (via a virtual salt flux). We used volume compensation to conserve global volume mean salinity by returning the removed salt to the model evenly through all ocean cells. The hosing remained constant throughout the runs, which continued for between 150 and 250 years. The same experimental design was applied to each simulation, with varying forcing strengths. This experimental design has been previously applied in both of the models used in this study (Jackson and Wood 2018; Haskins et al. 2018), and is used to explore the sensitivity of the AMOC to freshening, and not the fate of the freshwater itself. The northern and southern densities are calculated using full sections of temperature and salinity taken at 50˚N and 33˚S in the Atlantic. The southern section was placed to describe the densities at the southern limit of the Atlantic Basin while the northern section both captures the subpolar densities and retains sufficient ocean depth to include deep ocean processes. The calculated model AMOC strength is for 30˚N. All of these time series are given as the maximum of the stream function over a depth of 200–3000 m.

In this study we have used 2 distinct models, with component parts of different provenance, in order to avoid model dependent conclusions. Firstly, the eddy-permitting GCM HadGEM3-GC2 (Williams et al. 2015), that combines the Global Ocean v5 model from NEMO (Megann et al. 2014) with the Global Atmosphere v6 model of the Met Office UM. There are 75 levels in the ocean, with resolution 0.25˚, and 85 levels in the atmosphere with a resolution of ~135 km at mid-latitudes. We used hosing rates of 0.1, 0.2, 0.3 and 0.5 Sv (see Jackson and Wood (2018) for more description of these experiments). The HadGEM3-GC2 control run has a steady AMOC strength of ~14 Sv, with linear drifts in temperature and

salinity in the north and south of the Atlantic. The control run has constant pre-industrial forcing applied and has been spun up for 146 years (after initialisation from a previous present day control run). Although there is little drift in the upper ocean and in the AMOC strength, deep ocean properties have not had time to reach equilibrium. In the control run, the density changes in the south appear to strengthen the AMOC and the north appears to weaken it, both by 1 Sv per 100 years, **Figure 3.1**. This is due to a basin-wide negative drift in deep density, which has little effect on the reconstructed AMOC, but does affect its decompositions into northern and southern components. As the strengths of these drifts are dependent upon the state of the ocean we do not remove linear trends from the experiments, but instead consider the results in the light of these drifts. We would expect the ocean state to change more in the North Atlantic than in the South Atlantic in response to the freshwater hosing, and therefore, for the density drift to be more strongly altered in the north than in the south.

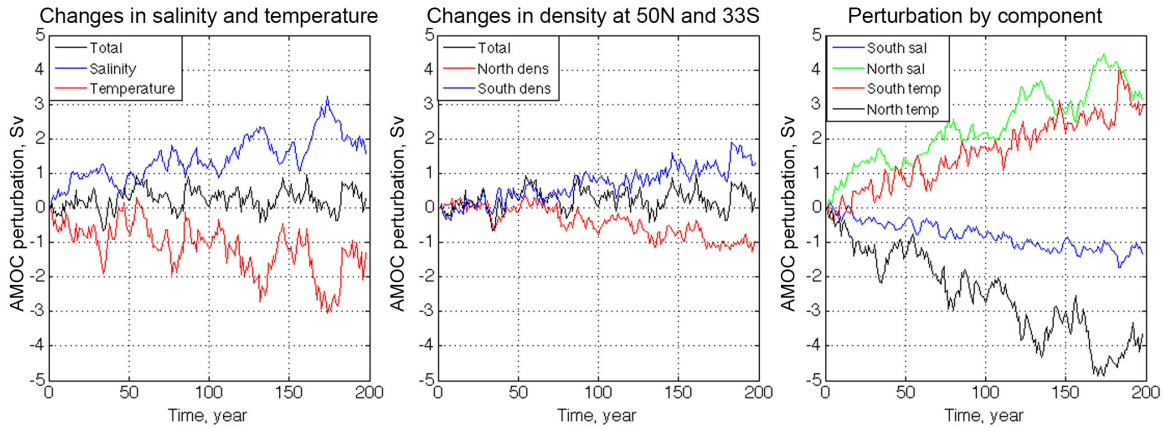

Fig. 3.1 Perturbation in AMOC strength (Sv) due to model drift in northern and southern temperature and salinity, as reconstructed using the *Butler et al.* (2016) method. The panels split the influence on AMOC perturbation between that from **A**: changes in north-south difference in salinity and temperature, **B**: density changes occurring in the north and south of the Atlantic, and **C**: each of these 4 components (southern salinity, northern salinity, southern temperature, northern temperature)

Our second model is the Fast Met Office/UK Universities Simulator 'FAMOUS' (Smith et al. 2008; Smith 2012), which is a computationally cheaper version of HadCM3 (Gordon et al. 2000). FAMOUS comprises the Hadley Ocean model (HadOM3), which is unrelated to the NEMO ocean used in HadGEM, and the Hadley Atmosphere model (HadAM3). The ocean has 20 levels, with resolution 3.75˚ by 2.5˚, and the atmosphere has 11 levels of 7.5˚ by 5˚. The model is not

eddy-permitting and so uses the Gent-McWilliams scheme (Gent and McWilliams 1990). Due to the lower resolution, we are able to use a 1000-year spin-up followed by an ensemble approach with 10 run at each hosing rate. The FAMOUS control run has an AMOC strength of 17.5 Sv, and shows no drift in AMOC, salinity, or temperature. As there is a simple relationship between hosing and model response in FAMOUS, we will only present runs hosed with 0.2 and 0.5 Sv of freshwater. These experiments were previously described in Haskins et al. (2018).

3.3 AMOC behaviour and reconstruction

In both models the freshwater input collects at the surface of the hosing region, with changes in ocean transports unable to dissipate the anomaly at the rate of input. In both models, freshwater hosing leads to a reduction in the strength of the AMOC, **Figure 3.2 (left axis)**. The total extent of AMOC weakening in FAMOUS is larger with greater hosing rates, while all hosing rates in HadGEM3-GC2 ended within a couple of Sverdrup of each other (<4 Sv, see Jackson and Wood (2018)). Unlike HadGEM3-GC2, FAMOUS saw a strengthening of the Antarctic Bottom Water (AABW) cell (not shown). HadGEM3-GC2 shows greater interannual variability than FAMOUS. Due to the differences in control strength between the 2 models, we cannot directly compare their behaviour in terms of magnitude of deviation.

The B16 method is able to reconstruct the primary form of AMOC weakening for all runs **Figure 3.2**. However, as the output is scaled to match the model mean control run strength, the method does not capture the extent of AMOC weakening. For our purposes this is not important, as we are interested in the underlying mechanisms and not the magnitudes of AMOC strength.

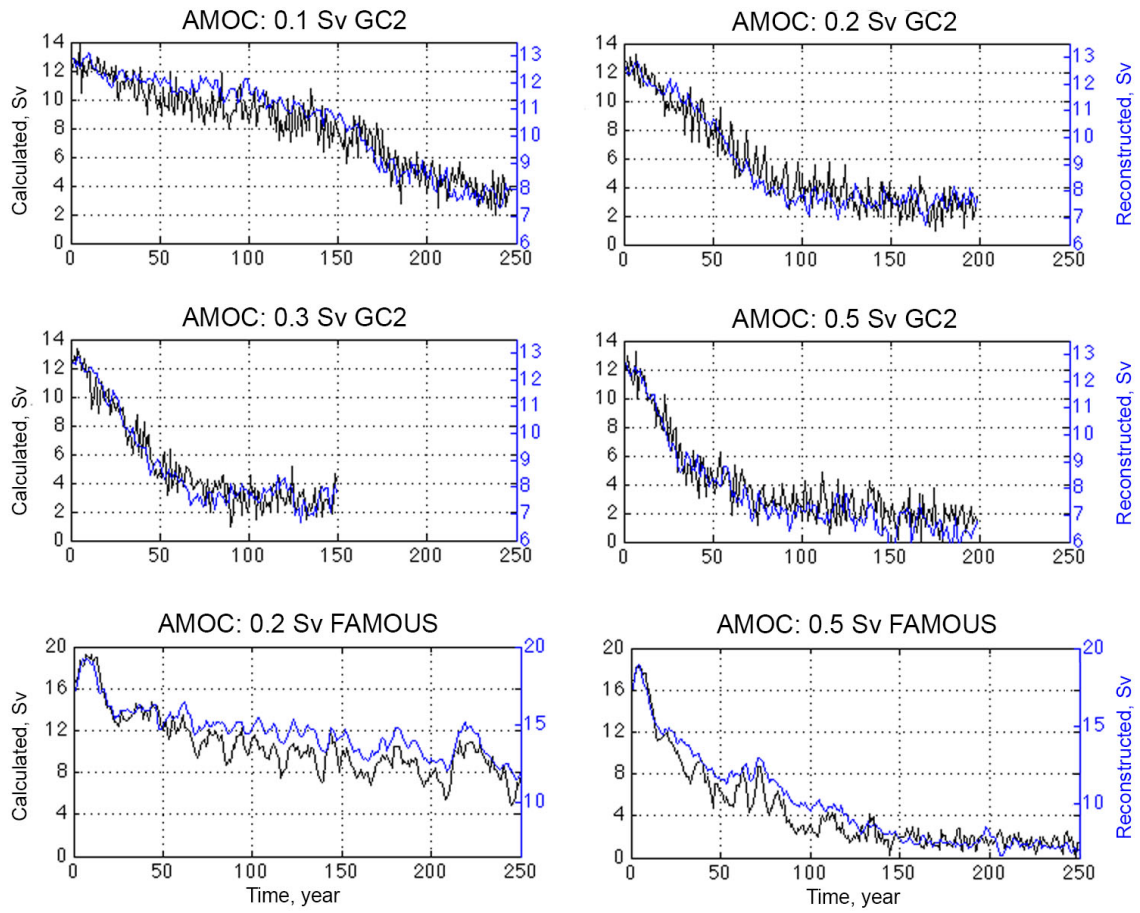

Fig. 3.2 Left y-axis: AMOC as calculated from the model velocities. **Right y-axis:** AMOC as reconstructed using the Butler et al. (2016) method. All panels show annual data for a single run, with the HadGEM3-GC2 (labelled GC2) data having greater variability. The magnitude of weakening is underestimated by the reconstruction. Note that different left and right y-axis scales have been used

3.4 Role of temperature and salinity in AMOC changes

We want to understand the relative influence of temperature and salinity in the north and south of the Atlantic on the weakening of the AMOC. We use the same method to reconstruct the AMOC, while isolating the AMOC perturbation resulting from each component by holding all other profiles constant at the first timestep. This is first split between the AMOC perturbation resulting from density changes at 50˚N and 33˚S, **Figure 3.3A**. In all simulations the AMOC weakens due to changes in density in the north. The density changes in the south modulated the overall weakening. These roles in the north and south were identified in FAMOUS by Haskins et al. (2018), and the present study shows similar behaviour in an eddy-permitting model.

The density in the north and south is then split into the AMOC perturbation driven by changes in temperature and salinity, **Figure 3.3B**. In all runs northern temperature ultimately gives the greatest contribution to weakening the AMOC, even though the weakening is driven by freshwater hosing. In the HadGEM3-GC2 runs, with modest hosing the initial AMOC weakening is driven by changes in northern salinity, but the salinity driven perturbation then diminished and is overcome by the effect of the northern temperature. The greater the hosing rate the sooner temperature dominates the AMOC weakening. The relationship between the AMOC perturbations from temperature and salinity changes shows a progression with increasing hosing rates. The first 200 years of hosing at 0.1 Sv shows a similar pattern to the first 75 years of hosing at 0.2 Sv. In the 0.3 and 0.5 Sv runs weakening from temperature exceeds salinity after the first 30 and 20 years, respectively. If the control run model drifts were removed from these results, the AMOC perturbations from northern temperature and salinity on weakening the AMOC would have been weaker and stronger respectively, reducing the extent of temperature domination.

In FAMOUS, northern temperature changes weaken the AMOC, while the northern salinity changes enhance the AMOC. This dynamic is consistent from the beginning, at both hosing rates. With stronger hosing, the magnitude of AMOC perturbation is greater, and levels off as the AMOC becomes very weak (~3 Sv in **Figure 3.2**).

Density changes in the south strengthened the AMOC in all runs. However, this was achieved by different mechanisms in the 2 models. In all of the HadGEM3-GC2 runs the southern temperature gave a near linearly increasing AMOC enhancement, this is likely significantly contributed to by the South Atlantic warming temperature drift in the model. In FAMOUS, the southern AMOC enhancement was driven by different components for the 2 hosing rates. With stronger hosing rates (0.3 Sv and above) it is driven by reduced salinity.

3.5 Mechanisms of AMOC weakening in the North Atlantic

The AMOC reconstructions by component suggest that to understand the primary mechanisms of AMOC weakening it is sufficient to understand the behaviour of temperature and salinity at 50˚N, and their impacts on density. We will first explore the relatively simple mechanisms in FAMOUS and then examine the more complex response in HadGEM3-GC2.

3.5.1 Mechanisms in FAMOUS

AMOC weakening in response to freshwater hosing in FAMOUS is invariably driven by warming at 50˚N, **Figure 3.3**. In order to understand why this is, we will consider the temporal variations in the profiles of temperature and salinity at 50˚N, **Figure 3.4**. In this description, the first values stated are for the 0.5 Sv 10-member ensemble mean, with the 0.2 Sv ensemble mean value in brackets.

As a result of hosing a 100 m deep fresh cap is established at the surface **Figure 3.4A**, with a final salinity anomaly of -5 PSU (-2.5 PSU). The surface cap shows strong cooling, by -4 ˚C (-3 ˚C). Below the surface cap (200-2000 m) **Figure 3.4B**, the ensembles have warm, saline, anomalies reaching 4.5 ˚C (2.5 ˚C) and 0.8 PSU (0.5 PSU). These warm waters are isolated from the atmosphere by the surface cap, which reduces heat loss to the atmosphere and traps in the heat transported into the region by the ocean (see *Haskins et al*. 2018 for more detail). Below 2000 m a cold fresh anomaly develops more slowly, reaching a maximum magnitude of -2.5 ˚C (in both ensembles) and -0.6 PSU (-0.5 PSU) at greatest depth. This signal results from the intrusion of the strengthened AABW (not shown).

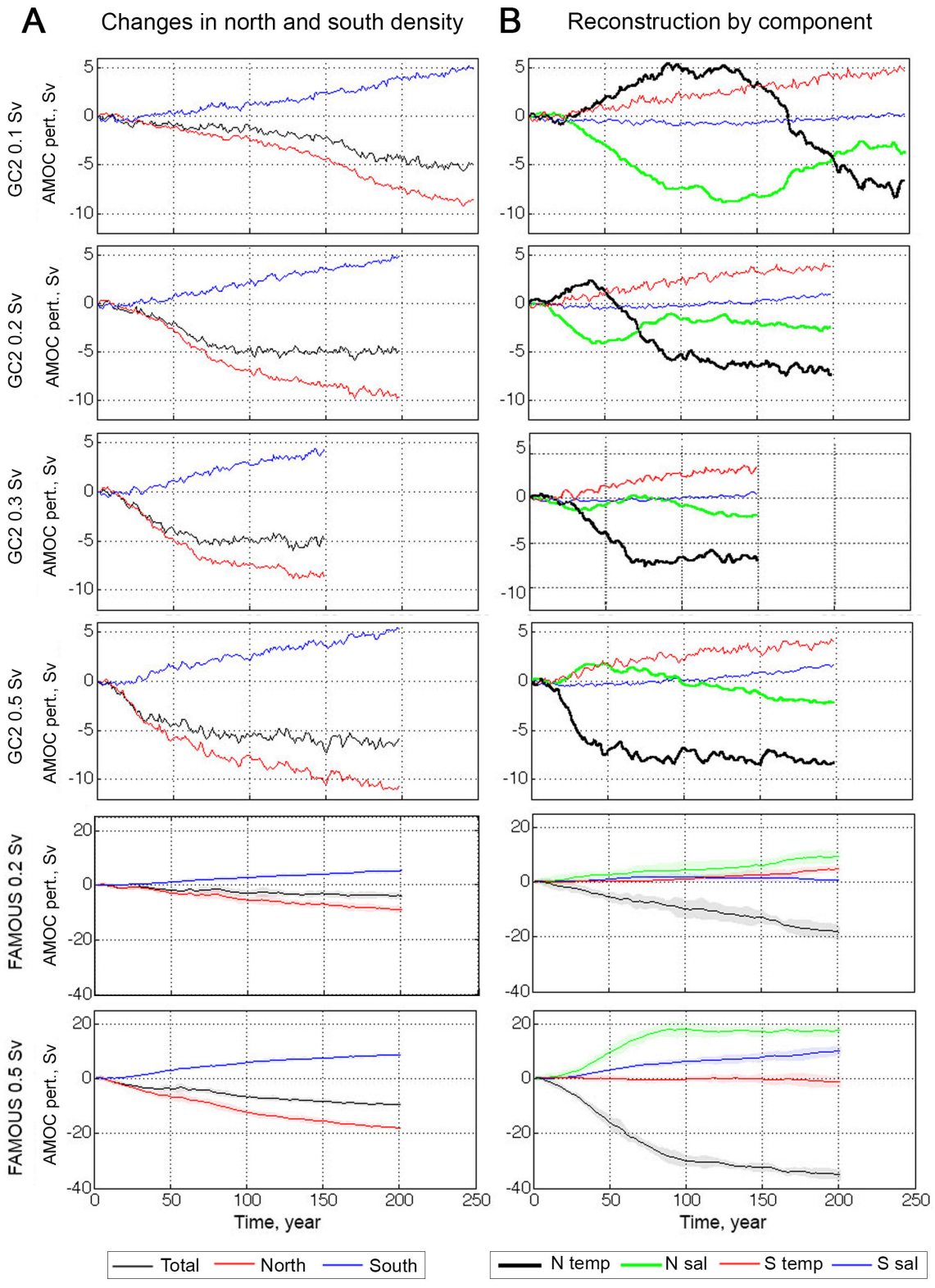

Fig. 3.3A: Reconstruction of AMOC strength, presented in terms of AMOC perturbation resultant from changes in the density profiles at 50˚N (red), 33˚S (blue) and total (black). **B:** Reconstruction of AMOC perturbation from changes in density profiles due to changes in temperature and salinity at 50˚N and 33˚S. The y-axes vary by model. The HadGEM3-GC2 (labelled GC2) results are for single model runs. The FAMOUS panels show the 10-member ensemble mean, with standard deviation shaded

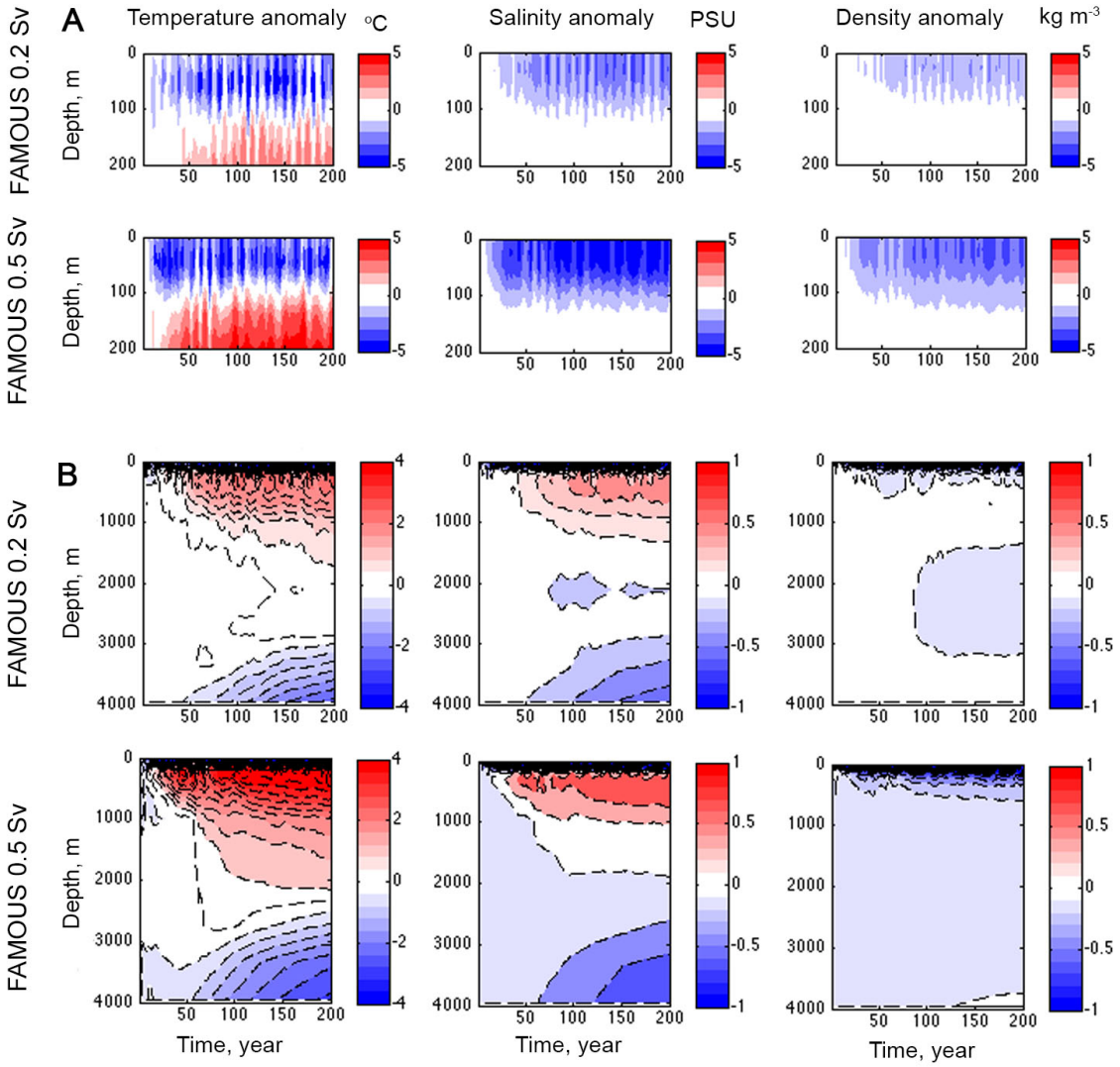

Fig. 3.4 Hovmoller anomaly (from 1st time-step) plots showing the FAMOUS 10-member ensemble mean for temperature (˚C) salinity (PSU) and calculated density (kg m^{-3}) at 50˚N in the Atlantic. **A** shows the formation of the surface cap in the top 200 m, **B** shows the full depth. Note different colour scale in **A** and **B**

To understand the net impact of these changes we look at the resultant changes in density at 50˚N. Both ensemble means develop a low-density cap within the surface 100 m (-3 kg m^{-3} for the 0.5 Sv ensemble), with the impact of freshening outweighing the impact of cooling. However, a more dynamically important change in density comes from subsurface warming. The warming reduces densities through ~2000 m of the water column, giving a particularly strong low-density anomaly to a depth of 500 m. With increasing depth, warm saline anomalies give way to cool fresh anomalies, associated with the extension of the AABW, giving little change to the net density.

In FAMOUS the AMOC is weakened by the high temperature anomaly that develops under the buoyant surface cap, due to the reduction in the surface heat flux. The reconstruction shows that the salinity at 50˚N enhanced the AMOC despite the freshwater hosing. This has been shown to result from an increased ocean salinity convergence in FAMOUS, with an increase in salinity in the waters transported into the region (Haskins et al. 2018). The increased northward salinity transport at 50˚N is caused by changes in the low latitude North Atlantic surface freshwater fluxes (see **Figure 8**). These arise from changes in atmospheric circulation patterns, notably the southward shift of the Intertropical Convergence Zone, during weak AMOC (Wu et al. 2011; Jackson 2013; Bouttes et al. 2015; Haskins et al. 2019). While there is surface freshening, the major influence from salinity is the high salinity anomaly from 200-2000 m, increasing North Atlantic density and thereby enhancing the strength of the AMOC.

3.5.2 Impact of salinity and temperature on density at 50˚N in HadGEM3-GC2

HadGEM3-GC2 had a more complex response to hosing, with initial AMOC weakening dominated by North Atlantic freshening. However, with greater quantities of hosing, temperature eventually dominated AMOC weakening, showing similar behaviour to that seen in FAMOUS. In order to understand the behaviour of HadGEM3-GC2, we will again begin by considering the temporal variations in the profiles of temperature, salinity and calculated density at 50˚N, **Figures 5 and 6**.

The model responds to relatively modest hosing with surface freshening **Figure 3.5**, which extends its vertical distribution with time, and a reduction in subsurface temperatures, consistent with reduced northward heat transport. However, as the quantity of freshwater hosing increases, we again see the development of a fresh surface cap (with a salinity anomaly of -3.5 PSU for the 0.5 Sv run). This anomaly takes longer to establish for lower hosing rates, forming in 30 years in the 0.5 Sv run and 200 years in the 0.1 Sv run. All runs develop a strong cold anomaly within the surface cap, which is stronger for the 0.5 Sv run in HadGEM3-GC2 than it was in FAMOUS (-5 ˚C compared to -4 ˚C).

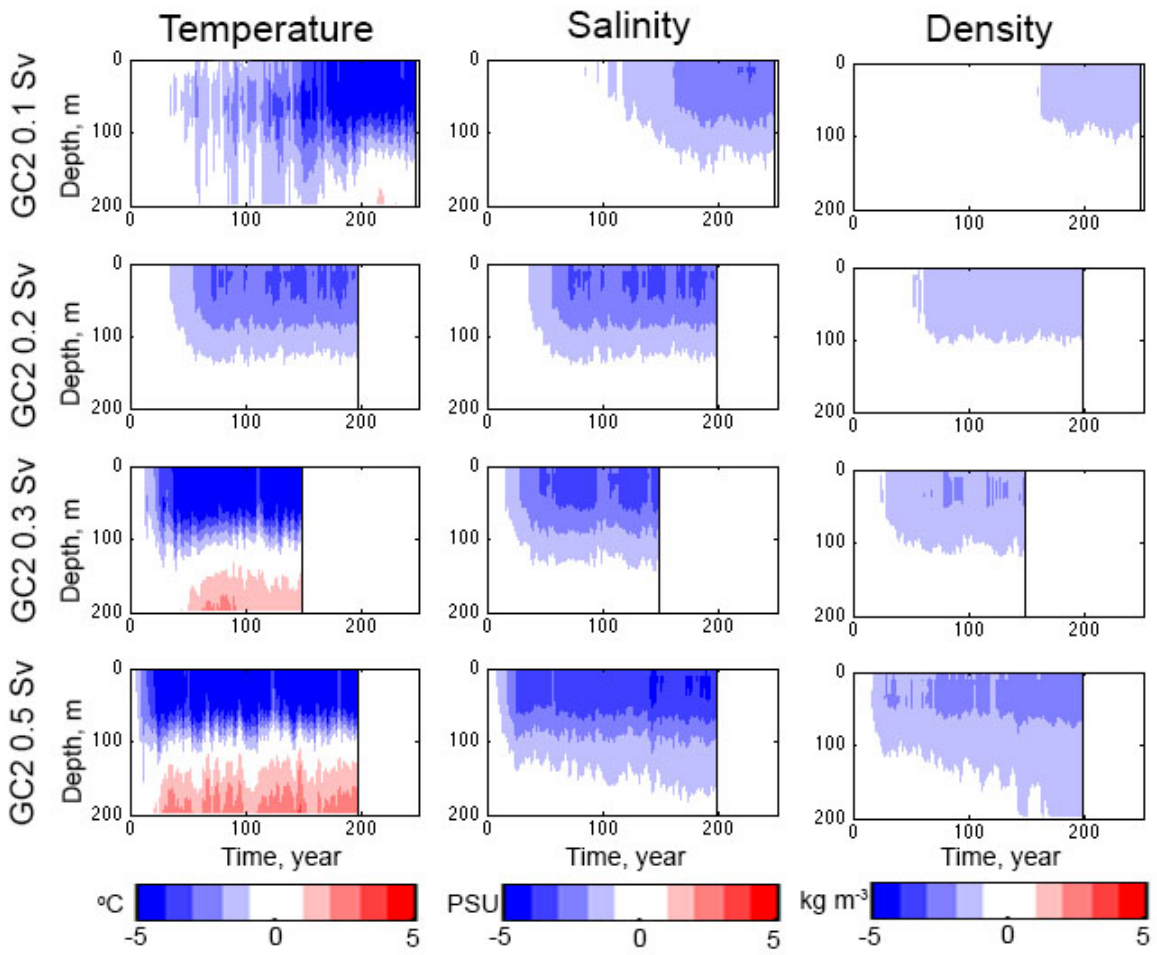

Fig. 3.5 Hovmoller anomaly (from 1st time-step) plots showing the temperature (˚C) salinity (PSU) and calculated density (kg m^{-3}) of the top 200 m at 50˚N in the Atlantic for each hosing rate in HadGEM3-GC2. The same colour bar limits have been applied throughout. Black vertical marks the end of simulation

Below the surface cap we see a warm anomaly develop in all runs **Figure 3.6**, which is weaker (2.5 ˚C for the 0.5 Sv run) in HadGEM3-GC2 than it was in FAMOUS. The temperature anomaly reaches greater depths, and extends downwards faster in HadGEM3-GC2 than in FAMOUS. There is a double-dip in subsurface salinity, where the initial freshening partly recovers, and later again freshens (not seen in the 0.1 Sv experiment, where only one dip is present within the experiment duration). The initial freshening is deeper, and longer lasting, for weaker hosing rates. There is a weak cool anomaly, with some freshening, between 2500-3000 m (-0.7 ˚C for the 0.5 Sv run) consistent with AMOC shoaling.

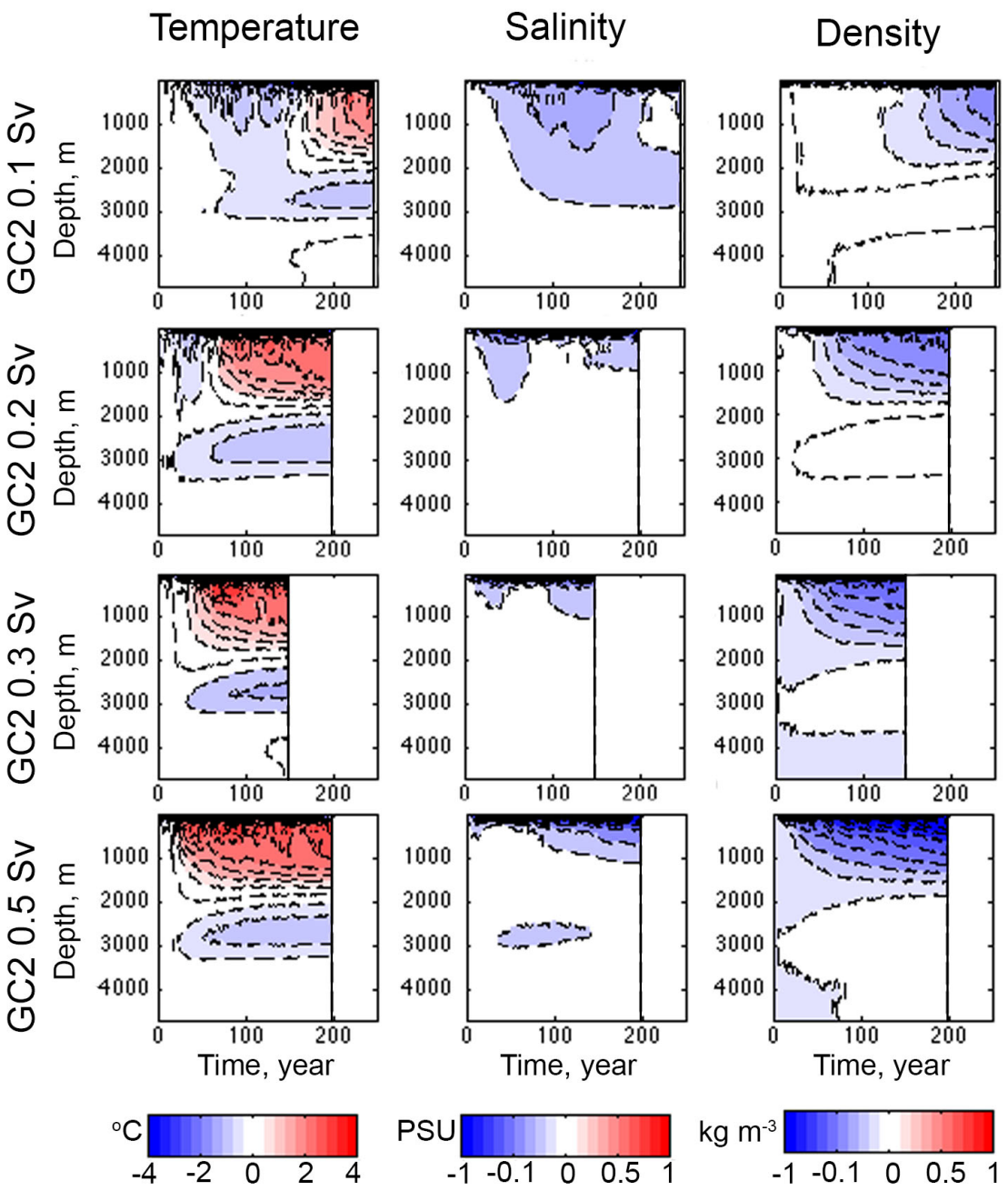

Fig. 3.6 Hovmoller anomaly (from 1st time-step) plots showing the full depth temperature (˚C) salinity (PSU) and calculated density (kg m^{-3}) at 50˚N in the Atlantic for each hosing rate in HadGEM3-GC2. The same colour bar limits have been applied throughout. Black vertical marks the end of simulation

All net density changes at 50˚N are negative, with stronger hosing giving greater reductions in density. While freshening does reduce subsurface North Atlantic density during times of salinity domination in HadGEM3-GC2, the density anomaly is much weaker than that present during times of temperature domination. All runs eventually develop a low-density cap within the surface 100 m, with the

impact of freshening outweighing the impact of cooling **Figure 3.5**. Below this density is reduced by subsurface warming between depths of 200 and 1500 m, developing under the surface cap **Figure 3.6**. The deep (~3000 m) cooling is balanced by freshening, giving no significant change in net density.

3.5.3 Ocean mechanisms and feedbacks on density in HadGEM3-GC2

The time taken for temperature at 50˚N to dominate AMOC weakening is related to the time taken to establish a surface cap, trapping in a heat anomaly. In HadGEM3-GC2, as the AMOC weakens the depth of the March Labrador Sea mixed layer depth (MLD) reduces and becomes steady at ~140 m, reducing convection, **Figure 3.7**. Within the mixed layer there are low-density highly buoyant waters, with the cool fresh anomaly becoming isolated at the surface. The surface fluxes over a 10˚ band centred on 50˚N, **Figure 3.7**, show that the ocean ceases to release net warmth to the atmosphere. The net freshwater surface flux into the same region of the ocean increases during hosing, as reduced northward ocean heat transport leads to surface cooling and reduced evaporation. Therefore, the change in both heat and freshwater surface fluxes act to increase the buoyancy of the surface cap and feed the buoyancy reservoir.

The surface freshwater fluxes over the North Atlantic and Arctic are broadly intensified, **Figure 3.8**. Initially, the region north of the tropics in the Atlantic net received freshwater from the atmosphere, while the Arctic net exported freshwater at the ocean surface - primarily to the formation of high-latitude ice. In the final decade of the 0.5 Sv hosed run both of these fluxes had become stronger. The North Atlantic, into the Greenland, Iceland and Norwegian (GIN) seas, usually gives off heat to the atmosphere. As the AMOC weakens, the surface heat flux is strongly reduced from 30˚N to high latitudes, including a horseshoe shaped reduction in ocean heat loss in the North Atlantic, associated with periods of weak AMOC. Hence the surface flux changes we see at 50˚N in **Figure 3.7** are representative of wider changes to the surface fluxes in the sub-polar region.

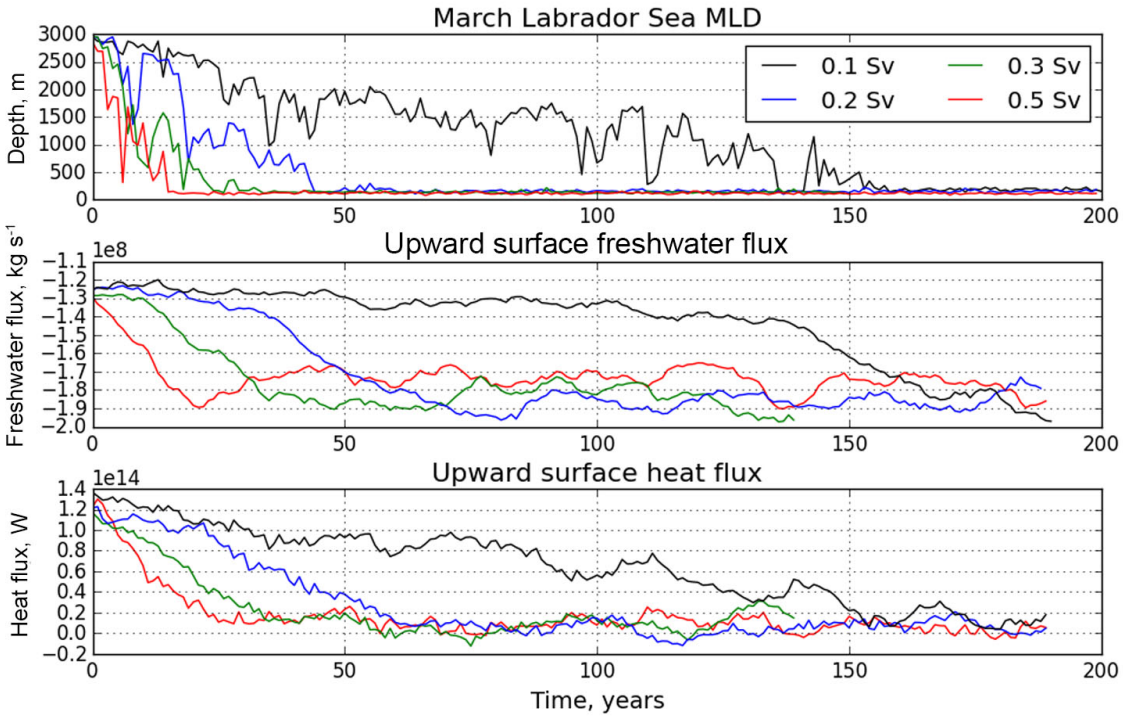

Fig. 3.7 March Labrador Sea MLD (m), upward surface freshwater flux (including net evaporation and sea ice processes) (kg s^{-1}), and the upward surface heat flux (W). Both surface fluxes are 10-year rolling means integrated over a section 45-55°N, over the full width of the North Atlantic. All data is for HadGEM3-GC2. Hosing is not included in the freshwater flux. The legend applies to all panels

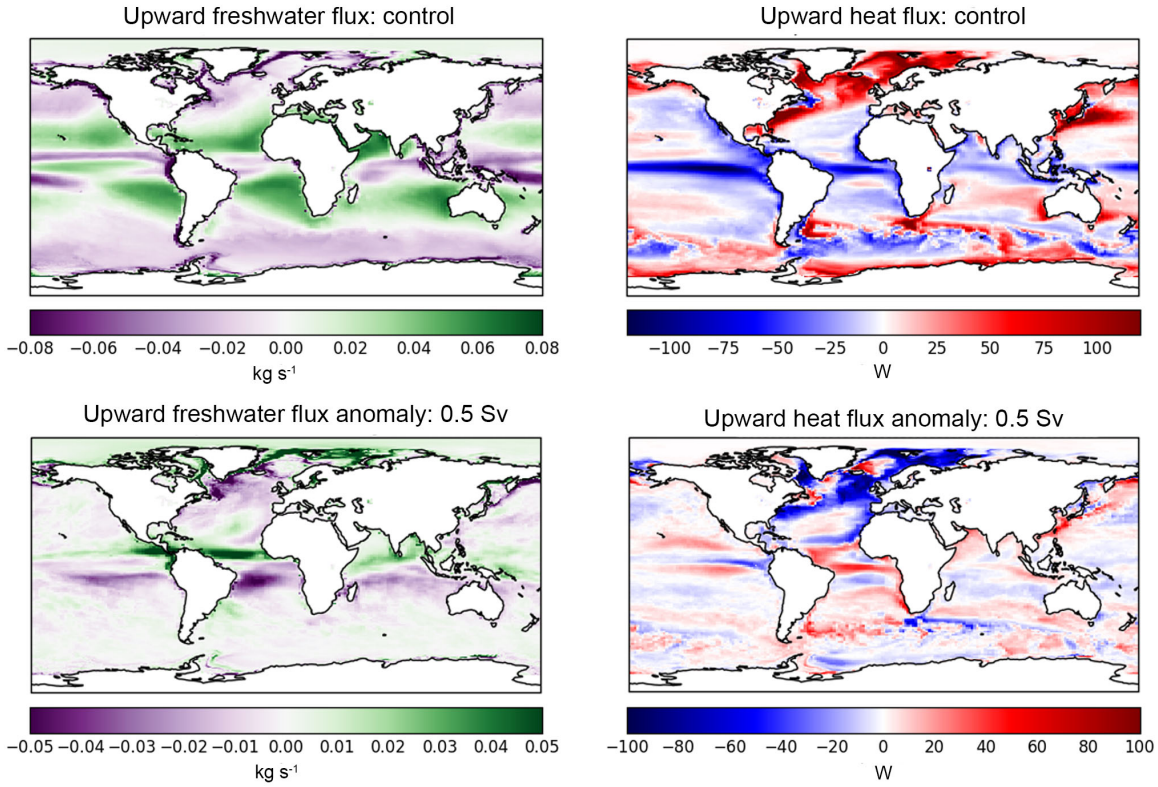

Fig. 3.8 Decadal mean upward surface freshwater flux (including net evaporation and sea ice processes) (kg m^{-2} s^{-1}) and upward surface heat flux (W m^{-2}) for the control run (top) and the anomaly at the end of the 0.5 Sv hosed run (lower)

Changes in northward transport of heat and salinity both act to increase the density at 50˚N, **Figure 3.9**. As the AMOC weakens, salinity convergence from 45-55˚N due to ocean transport is increased, leading to the temporary reduction of subsurface salinity anomalies seen in **Figure 3.6** (years 80-120 and 50-100 in the 0.2 Sv and 0.3 Sv runs, respectively). The heat convergence over the same area reduces as the AMOC weakens. This is lead by reduced northward heat transport at 45˚N (not shown), and is seen in the early cooling **Figure 3.6**. However with further hosing, the warmth previously exported to the atmosphere is trapped below the surface cap, causing subsurface warming. If surface fluxes had remained constant, then changes in ocean heat convergence alone would have given further cooling. Changes in both salt and heat advection therefore act to increase the density and oppose AMOC weakening.

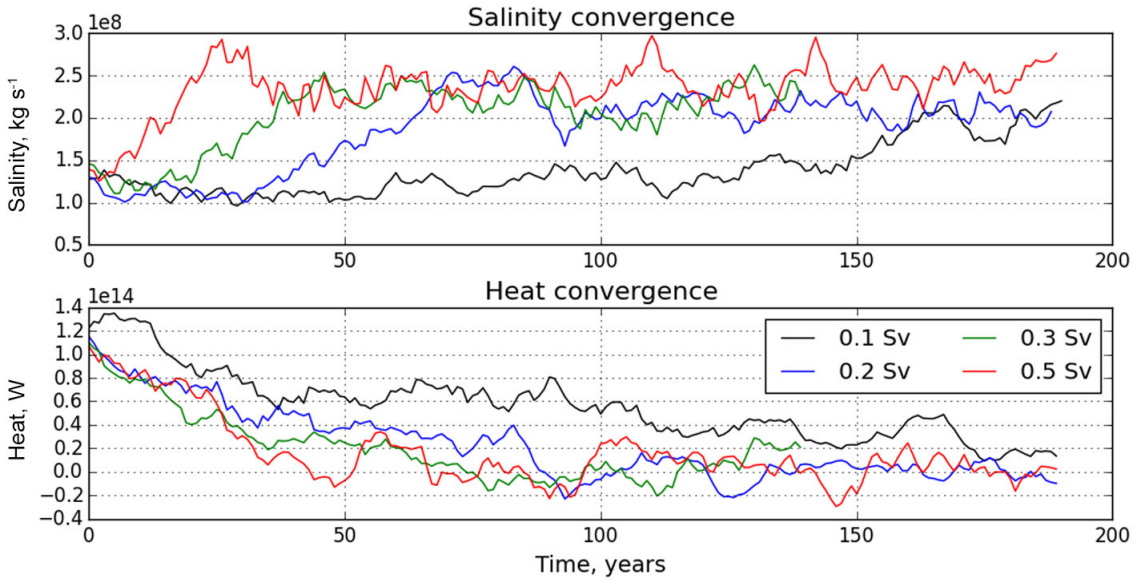

Fig. 3.9 Convergences in northward ocean transports of salinity (kg s^{-1}) and heat (W), for a 10˚ region over 50˚N in the Atlantic in HadGEM3-GC2. A 10-year rolling mean has been applied. Legend applies to both panels

3.5.4 Attributing dominance in HadGEM3-GC2

The pattern in reconstructed AMOC strength due to changes in northern salinity and temperature in HadGEM3-GC2 is simpler when considered in terms of the total freshwater added, **Figure 3.10A and B**. The AMOC changes little during the first 2.5 Sv yrs of hosing (e.g. 25 years at 0.1 Sv or 5 years at 0.5 Sv), but after

this it is weakened by salinity changes. This is due to the early freshwater input being mixed downwards by the continuing overturning, reducing the densities down through the water column. The initial AMOC strengthening by temperature, **Figure 3.10B**, in the HadGEM3-GC2 0.1 and 0.2 Sv runs is due to the reduced northward transport of heat throughout the AMOC depth, which leads to a cooling up to years 150 and 70 respectively, **Figure 3.6**. This is not seen in the heavier hosed runs as they have less time to be impacted by this cooling mechanism before reductions in the surface heat flux cause a more significant warming. The weaker hosing rates have larger anomalies in temperature and salinity, however these largely compensate giving relatively weak net AMOC change.

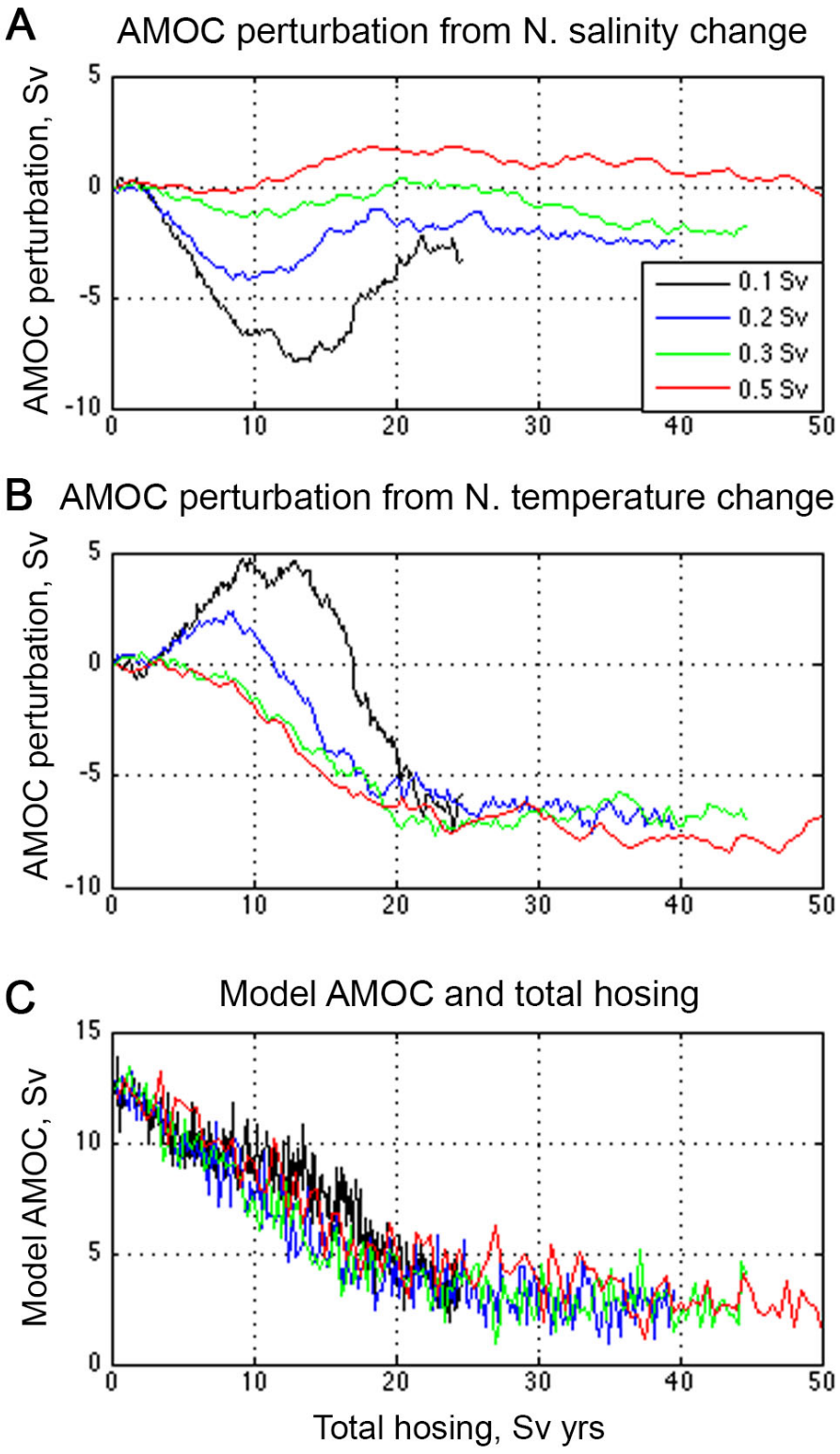

Fig. 3.10A AMOC perturbation (Sv) from changes in salinity at 50˚N (green line on **Fig 3B**) against cumulative freshwater input. **B** AMOC perturbation (Sv) from changes in temperature at 50˚N (black line on **Fig 3B**) against cumulative freshwater input. **C** Model AMOC strength (Sv) against total freshwater hosed (Sv yr). All data is for HadGEM3-GC2, up to a maximum of 50 Sv yrs. Legend applies to all panels

Both the AMOC enhancement by the temperature contribution and AMOC weakening by the salinity contribution start to decline after ~10 Sv yrs of hosing - with the transition occurring earlier for more heavily hosed runs. In the 0.5 Sv run, the AMOC weakening due to subsurface warming is partly moderated by increased salinity. The AMOC enhancement from salinity is caused by the subsurface salinity increasing, in the middle of the freshening double-dip, as the AMOC is strengthened by increased salinity convergence by ocean transports at 50˚N, **Figure 3.9**. Note that changes in the behaviour and influence of temperature and salinity are not apparent in the linear relationship between AMOC strength and total freshwater added **Figure 3.10C** – suggesting that the AMOC is not sensitive to whether the salinity or temperature dominates the weakening.

After 20 Sv yrs, the linear relationship between model AMOC weakening and total freshwater input breaks down, **Figure 3.10C**. The impact of northern temperature change on AMOC strength largely levels off while there is still some weakening from salinity change at 50˚N.

3.6 How does using the volume mean density method compare?

Previous studies (i.e. Jackson and Wood 2018) have estimated AMOC strength using the difference in the volume mean density between the north and south of the Atlantic, and found AMOC weakening to be dominated by the buoyancy impact of the salinity in the North Atlantic. In order to compare the two approaches, we have estimated the AMOC from the difference in the vertical mean of the density profiles at 50˚N and 33˚S for the HadGEM3-GC2 runs, and repeated the above component analysis, **Figure 3.11**. Here the ‘volume’ used is the full depth and width of the basin, taken over 1 latitudinal cell, which we consider representative of densities local to 50˚N and 33˚S, while allowing us to use the same temperature and salinity time series as in the previous method.

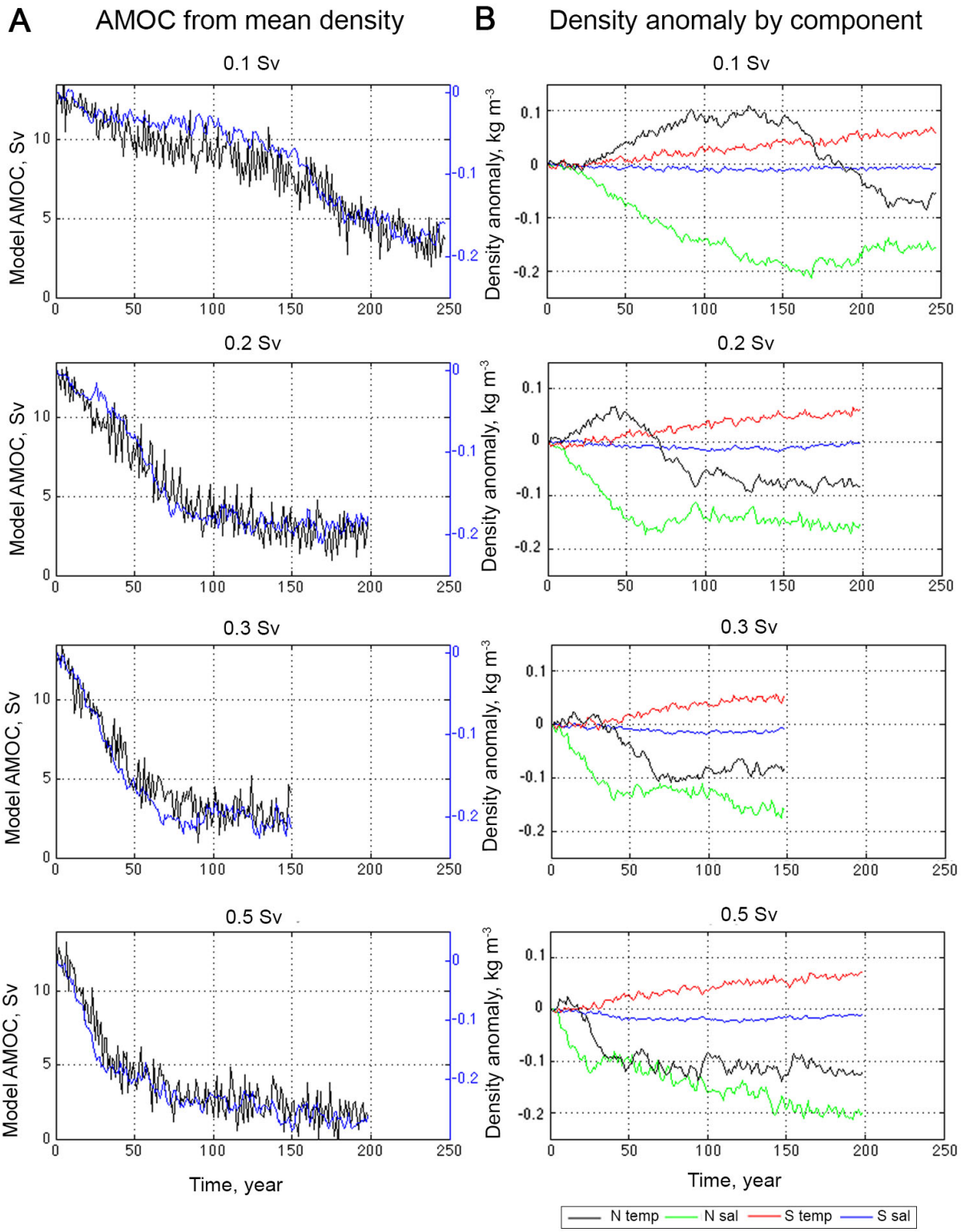

Fig. 3.11A: Comparison of model AMOC strength (Sv) and the estimated form of AMOC change from the anomaly in meridional density difference (kg m^{-3}) calculated from the volume mean density at 50˚N and 33˚S in the Atlantic. Here, the 'volume' is the full depth and width of the basin, taken over 1 latitudinal cell. **B:** Anomaly in meridional density difference (kg m^{-3}) from changes in temperature and salinity at 50˚N and 33˚S

In our experiments, the estimated AMOC from the vertical mean density gives a good approximation to the form of the model AMOC. The breakdown by component suggests domination by northern salinity, with a later contribution by temperature. The higher the hosing rate, the faster and greater the contribution from northern temperature change becomes to AMOC weakening, becoming temporarily comparable with the salinity contribution for the 0.5 Sv experiment through years 40-100. Using the volume mean approach, the northern salinity contribution includes time series features that are qualitatively similar to those seen in the B16 method's analysis. Here the salinity has an additional weakening trend on the AMOC strength due to the volume mean method's greater sensitivity to surface freshening. The AMOC perturbation from the northern temperature has similar form, with a weaker signal, to the results found using the B16 method. The role of density in the South Atlantic is similar between methods.

To understand why the two methods give different results we consider the weighting each gives to different processes in the density profile. The volume mean density approach takes the vertical mean value of the profiles, and so changes may be dominated by the very strong surface salinity anomalies within the surface cap. The B16 method uses a double integration up the water column, and so places greater emphasis on changes at deeper levels within the ocean.

The impact of changes in northern salinity on AMOC strength using the volume mean approach, **Figure 3.11**, appears to primarily represent the development of a fresh surface cap. We can approximately recreate the form of the northern salinity contribution from the mean salinity of the top 60 m at 50°N, **Figure 3.12A**. However, the form of the salinity contributions using the B16 method, **Figure 3.3B**, show a closer correlation to the mean salinity through 180-4700 m, **Figure 3.12B**. This can be understood as the full depth mean salinity being disproportionately impacted by strong surface anomalies, **Figure 3.12C**, which cannot drive large transport anomalies without being propagated to a greater depth.

We are postulating that the mean North Atlantic salinity anomaly acts as a proxy for AMOC weakening because it describes the extent of the surface cap. However,

once the cap is formed the AMOC is not reduced directly by the buoyancy of this freshwater. We find that AMOC weakening is instead driven by increases in subsurface temperature as a consequence of reduced surface heat loss. This is caused by the freshwater cap limiting convection and isolating the subsurface water from the atmosphere.

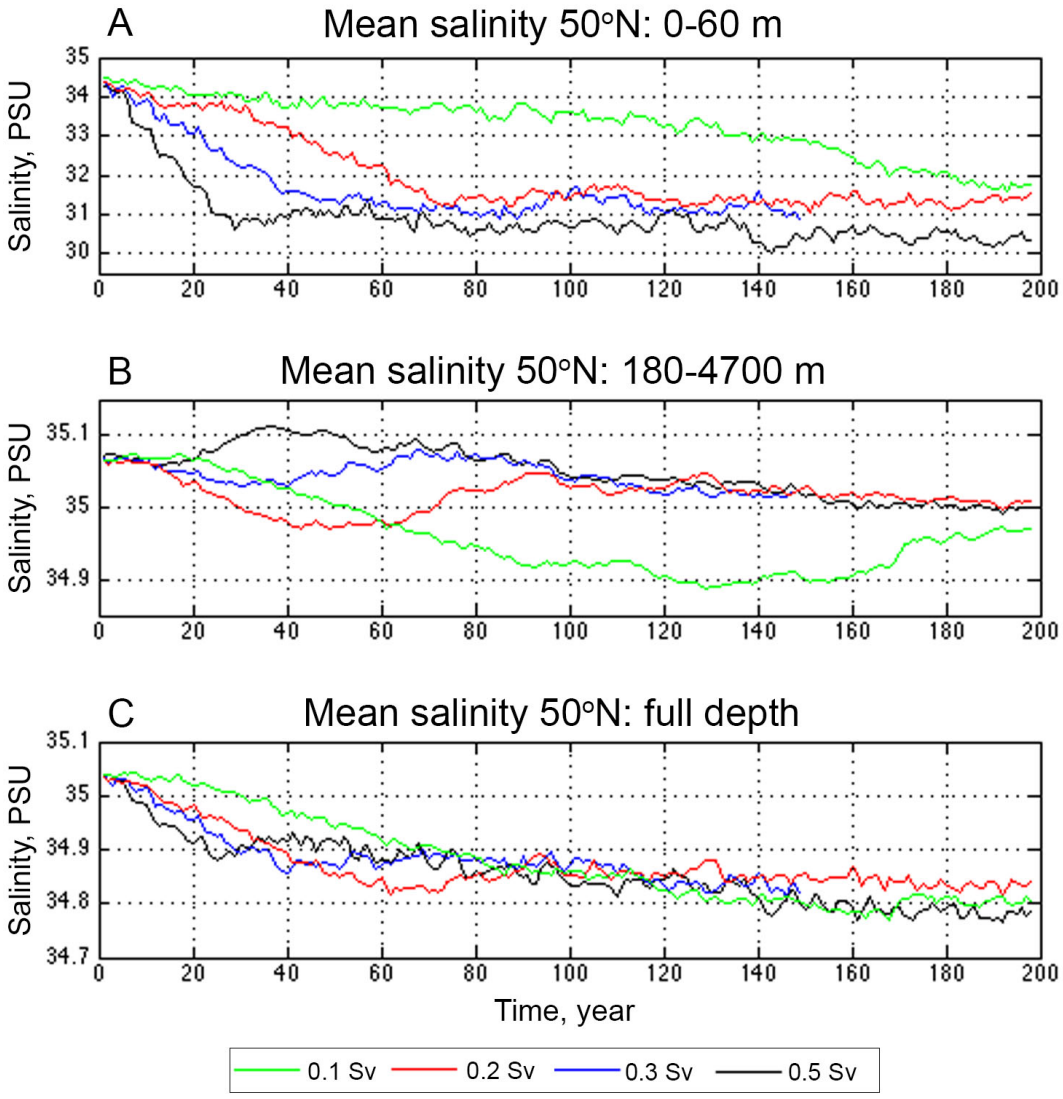

Fig. 3.12 Volume mean salinity (PSU) over a box 45-55˚N over the full width of the Atlantic for the HadGEM3-GC2 runs. **A:** from 0-60 m, **B:** 180-4700 m, and **C:** the full depth. Legend applies to all plots

3.7 Discussion

At the onset of hosing in the HadGEM3-GC2 hosing simulations, the freshwater is transported downwards by the AMOC, reducing the density through a significant depth of the water column and thereby reducing the strength of the AMOC. The

mixed layer shoals, which reduces the mixing down of surface properties, enabling the formation of a fresh surface cap. The surface cap acts as a barrier between the subsurface ocean and atmosphere, preventing the warm northward ocean transports from being able to release their heat, causing a warm temperature anomaly to develop beneath the cap. The heat anomaly further reduces the density of the ocean. In all of our simulations, the temperature contribution eventually dominates over salinity in driving AMOC decline in response to freshwater hosing.

Both the depth-dependent method and the volume mean density approach were able to reconstruct the strength of the AMOC. However, the volume mean density approach gave greater perturbation to AMOC strength from changes in North Atlantic salinity, since the volume mean values give equal weightings to density changes at the surface and at depth and hence were dominated by strong surface anomalies. The depth-dependent method showed greater temperature dominance of AMOC weakening, as it was more responsive to dynamically important variations in pressure gradients at depth, where temperature changes dominate. AMOC theory suggests that surface anomalies are not directly dynamically significant in determining the strength of the AMOC and that the depth-dependent method is a more theoretically sound technique for identifying the physical mechanisms of AMOC weakening (Oliver et al. 2005; de Boer et al. 2010). In our experiments the volume mean approach acts as a proxy by indicating the extent of the fresh surface cap, which is well correlated with AMOC decline. This suggests that while the volume mean approach can be used to reconstruct the AMOC and can be used alongside density budget analysis, understanding the vertical distribution of density changes is also important.

Previous freshwater forcing studies have also found high latitude subsurface temperature increase to result from suppression of ventilation, destabilising the water column (Mignot et al. 2007; Krebs and Timmermann 2007). Our work indicates that this temperature anomaly is not merely a by-product of the hosing, but is the dominant mechanism by which the AMOC is weakened in response to strong and/or long-term hosing.

For the weakest hosing rates examined, which are more relevant for past and future climate change, this study suggests that salinity would initially dominate AMOC weakening, and that tracking the depth of the MLD could be used as an indicator of mechanistic change, after which heat would dominate. In climate change scenarios forced with radiative forcing, which allow for Greenland ice mass loss, the weakening of the AMOC has been suggested to be dominated 60% by changes in North Atlantic temperature, 40% by salinity (Thorpe et al. 2001). In such simulations the AMOC is primarily weakened by thermally stratifying the upper ocean. This study has suggested that the formation of a surface cap in response to surface freshening may also contribute to North Atlantic subsurface warming. This suggests that both hosing and radiative forcing ultimately act in the same way, by preventing heat loss from the subsurface North Atlantic. It is unclear how these two forcing mechanisms would interact, whether later local surface heating would be mixed down to the upper ocean, impacting AMOC strength, or whether it would remain above the shallow MLD reinforcing the isolation of a warm and fresh surface cap, and preventing AMOC recovery. Either way, in terms of AMOC weakening they may be expected to reinforce rather than mitigate each other.

An interesting result of this study is that freshwater forcing can result in a weakening of the AMOC whether or not the freshwater propagates down the water column. When the freshwater does mix downwards, the increased buoyancy of the freshened region leads to AMOC weakening. While freshwater that does not mix downwards collects to form a barrier to surface fluxes, causing the development of a temperature anomaly below, which in turn reduces the buoyancy and weakens the AMOC. The formation of a surface cap does not qualitatively alter the rate of AMOC weakening, and the AMOC weakening was not found to be sensitive to whether the weakening is dominated by salinity or temperature changes.

Chapter 4: Mechanistic investigation of AMOC recovery and non-recovery in response to the removal of freshwater forcing

Abstract

The Atlantic meridional overturning circulation (AMOC) is projected to weaken due to anthropogenic climate change, partially due to ice melt freshening the North Atlantic Ocean. In order to successfully mitigate climate change it is important to consider the reversibility of temporary forcing and explore longer-term changes to the ocean state. We use temporary freshwater forcing in a prototype CMIP6 global climate model to investigate the roles of temperature and salinity in the AMOC response. Of a range of 11 temporarily forced simulations, 5 showed no signs of recovery within 100 years of the removal of forcing. We use salinity and temperature budget analysis to understand the role of surface and ocean advective feedbacks in the recovering and non-recovering ocean states. A positive salt advective feedback was found for the region 30°N in the Atlantic to the Bering Strait. However more locally to the region of convection, changes in the surface freshwater flux resulted in a positive freshwater feedback – which partially compensated for the removal of hosing and so supported the weak AMOC state. This suggests that a North Atlantic net evaporation reanalysis time series could be used as an indicator that the AMOC resilience to forcing had been exceeded.

4.1 Introduction

The Atlantic meridional overturning circulation (AMOC) is projected to weaken due to anthropogenic climate change (Collins et al. 2013). The North Atlantic is expected to freshen due to ice melt, reducing local density, and weakening the AMOC by reducing the meridional density gradient. Various studies have explored the resilience of the AMOC to temporary freshwater forcing (hosing), some finding that after sufficient hosing the AMOC did not recover when hosing was removed (Stouffer et al. 2006; Yin and Stouffer 2007; Brunnabend and

Dijkstra 2017). AMOC non-recovery has been associated with a salt advective feedback (Stommel 1961; de Vries and Weber 2005; Jackson 2013), where the weakening AMOC transported less salinity into the Atlantic basin, causing the basin salinity to decrease, further weakening the AMOC. Whether or not a model exhibits this bistability may be dependent on the representation of atmospheric feedbacks and ocean resolution (Yin et al. 2006; den Toom et al. 2012). A prototype CMIP6 eddy-permitting model was able to maintain a weak AMOC for 440 years after the removal of hosing (Mecking et al. 2016). This was attributed to a greater northward salinity transport in higher resolution models within the Atlantic, achieved with greater resolution of eddy transports and boundary currents, enabling a stronger salt advective feedback throughout the basin. The greater salt transport into the Atlantic Basin found in bistable models is closer to the observed transports (Garzoli et al. 2013), suggesting that the modern ocean is in a bistable state.

In this study we further explore previously presented freshwater forcing experiments to better understand how mechanisms found in the permanently hosed experiments (Haskins et al. 2019) relate to those experiments' capacity for recovery and hysteresis (Jackson and Wood 2018b). In the permanently hosed experiments, changes in AMOC strength were strongly dominated by changes in North Atlantic temperature and salinity, which were well represented by values at 50°N. Haskins et al. (2019) found that a fresh surface cap that developed in the North Atlantic acted as a barrier for surface fluxes. This isolated the subsurface from the atmosphere, and allowed for subsurface warming to become the dominant driver of AMOC weakening. Jackson and Wood (2018b) presented post-hosing continuations that 'stepped off' these long hosing experiments after various hosing durations. They found the AMOC to demonstrate hysteresis, with non-recovery resulting from a salt advective feedback over the region 30°N in the Atlantic to the Bering Strait.

We explore the response of the AMOC to the removal of freshwater forcing, and the mechanisms that govern the AMOC capacity for recovery within decades of the removal of forcing. By considering the model response in multiple latitudinal regions, we bring together the findings of the 2 previous studies to give a greater understanding of controls on AMOC recovery. Experiment duration is often

limited by the high computational expense of long GCM experiments. We therefore also ask what the ocean state associated with non-recovery can tell us about the timescale on which a longer-term recovery may occur.

4.2 Model and Experiments

We used the Hadley Centre Global Environmental Model version 3 global configuration version 2 (HadGEM3-GC2), an eddy permitting fully coupled ocean atmosphere general circulation model (Williams et al. 2015), which uses the Global Ocean v5 model from NEMO (Megann et al. 2014) and the Global Atmosphere v6 model of the Met Office UM. The 75 vertical ocean levels have a resolution of 0.25˚, and the 85 level atmosphere has resolution ~135 km at mid-latitudes. Freshwater forcing was applied from 50˚N in the Atlantic to the Bering Strait at hosing rates of 0.1, 0.2, 0.3, 0.5 and 1.0 Sv (see Jackson and Wood (2018a) and Jackson and Wood (2018b) for further discussion of these experiments). There is a long hosed run for each hosing rate, along with runs continued without hosing after various hosing durations, **Table 4.1**. The experiments are initiated from a preindustrial control run. This was previously spun up for 146 years from a present day control. Although the AMOC strength is steady at ~14 Sv, deep ocean temperature and salinity have not had time to reach equilibrium **Figure 4.1**. As the resultant model drift in temperature and salinity is transported by the AMOC, the drift strength may be expected to vary with the AMOC strength. The AMOC does not fully collapse in any run presented here, suggesting that the drifts remain active. We have therefore chosen to linearly remove the drift seen in the control run from all figures presented in this study.

Table 4.1 Details of hosing runs (full duration or number of years).

Hosing		Total length (yrs)	Recovering?	Final AMOC (Sv)
Hosing rate	Duration (yrs)			
0.1 Sv	Full	250	-	4
	20	101	Yes	15
	150	300	Borderline yes	12
0.2 Sv	Full	200	-	3
	20	111	Yes	15
	30	82	Yes	14
	40	119	Borderline yes	12
	50	149	No	6
0.3 Sv	Full	150	-	3
	20	120	Yes	14
	50	150	No	6
0.5 Sv	Full	200	-	2
	20	200	No	6
1.0 Sv	Full	200	-	1
	10	141	No	7
	20	150	No	7

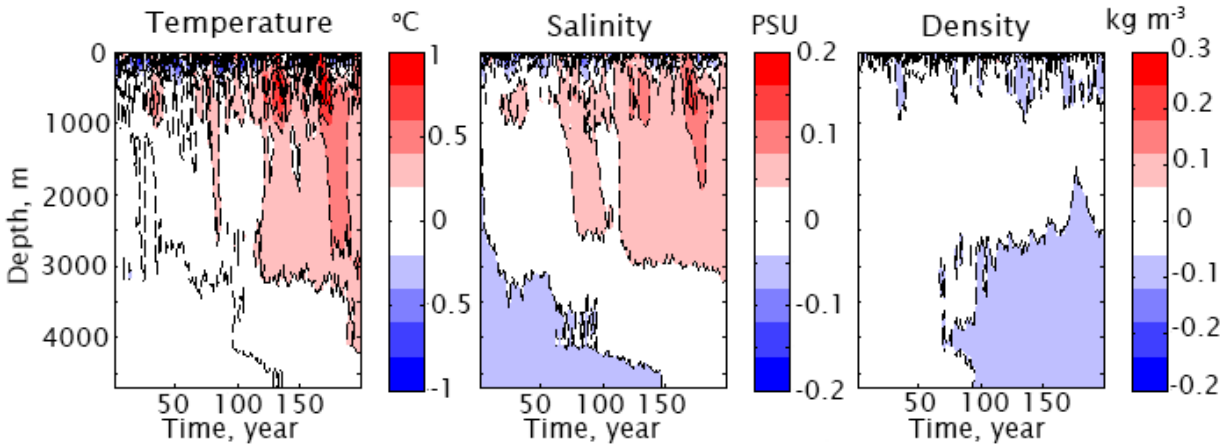

Fig. 4.1 Temperature (˚C), salinity (PSU), and density (kg m^{-3}) hovmoller anomaly plots for 50˚N in the control run. Anomalies are taken with reference to the first year. Note that the control run is longer than most temporarily hosed runs, and there is minimal anomaly within the first 100 years

4.3 Response to hosing

The greater the hosing rate the quicker the AMOC weakened, with the AMOC eventually weakening to <4 Sv for all permanently hosed runs **Figure 4.2**. Post-hosing runs starting from an AMOC stronger than 8 Sv mostly recovered, while those starting from a weaker AMOC generally did not, as has been previously observed (Jackson and Wood 2018b). Jackson and Wood (2018b) explored the changing relationship between water bodies as the AMOC became weak. They found that with sufficient continuous hosing the Atlantic overturning cell is largely eradicated and a shallow reverse cell develops. Unlike other freshwater forcing studies, there was no strengthening of the Antarctic bottom water cell (Haskins et al. 2018) or upper-ocean Antarctic Intermediate water cell (Gregory 2003; Jackson 2013).

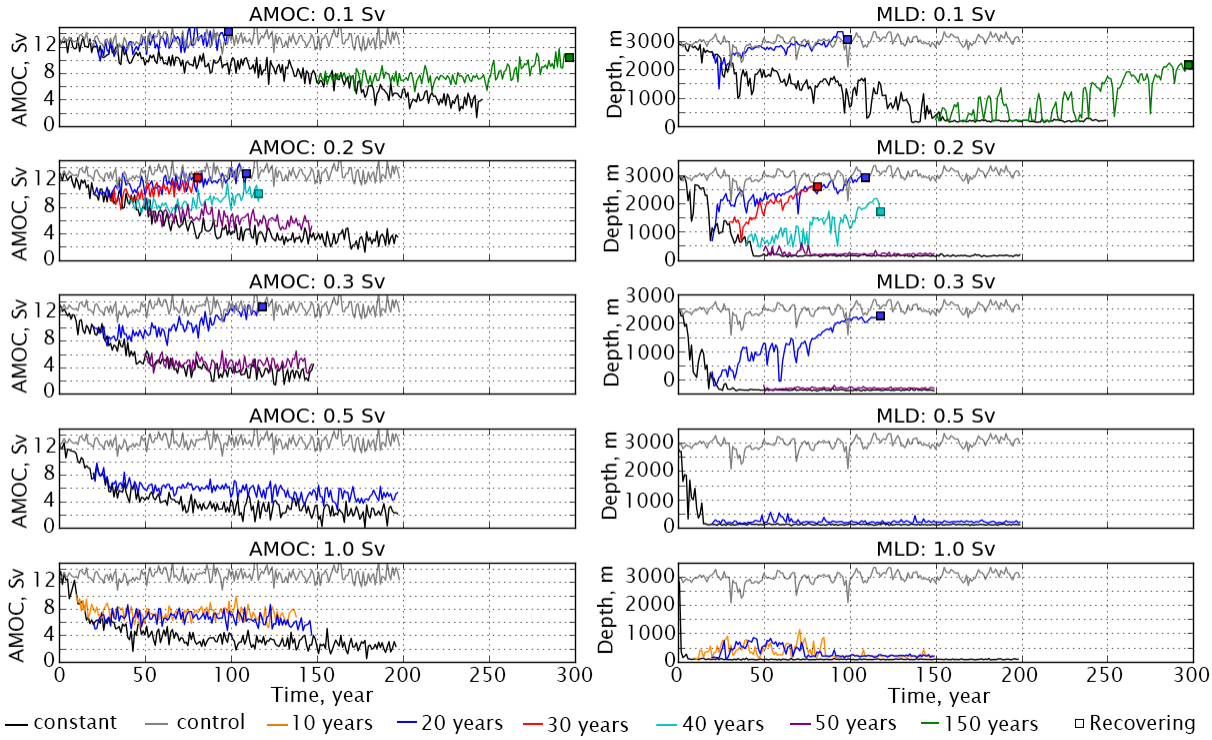

Fig. 4.2 AMOC at 30˚N (Sv) and the March Labrador Sea mixed layer depth (m) for all runs. In runs ending with a square the AMOC is considered to recover

We use the March Labrador Sea mixed layer depth (MLD) as an indicator of Atlantic convection. As the freshwater forcing causes North Atlantic stratification to increase, the MLD reduces and vertical mixing between the surface and subsurface ocean decrease. During hosing the MLD reduces to ~140 m and becomes steady, weakening faster the greater the hosing rate. However in

strongly hosed runs we see a jump in the MLD when hosing is first removed – suggesting a short lived convective event. Jackson and Wood (2018b) suggested that the MLD can be used as an indicator of non-recovery, with experiments unable to recover if the region of significant convection (MLD > 500 m) in the North Atlantic was sufficiently reduced (< 20,000 km^2) during hosing. Haskins et al. (2019) found that the MLD reduced while North Atlantic freshening drove AMOC weakening. When the MLD was collapsed, subsurface warming below the MLD dominated the continuing AMOC weakening.

4.4 Exploration of the non-recovering AMOC ocean state

We have seen that the AMOC is able to recover from limited forcing (hosing), and that runs with greater forcing do not recover when forcing is removed. We now want to explore the behaviour of the ocean state in AMOC non-recovery, and assess whether the weak AMOC state is likely to be long lived. Central to understanding how long the AMOC could remain weak post-freshwater forcing, is understanding how the new ocean dynamics keep the AMOC weak. To do this we will examine the exchanges of salinity and temperature through the longest non-recovering run (hosed with 0.5 Sv for 20 years) as a case study. The results will be contrasted with the results for both the control run and for the recovering run hosed with 0.3 Sv for 20 years. In **Section 4.3** we will consider whether these results are generally applicable to the other recovering and non-recovering runs.

4.4.1 Temperature and salinity budget for a non-recovering run

The transports of salinity and temperature into a region from 30°N in the Atlantic to the Bering Strait, **Figure 4.3**, have previously been used to understand the density changes related to AMOC non-recovery (Jackson and Wood 2018b, including supplementary materials). Jackson and Wood (2018b) found a strong correlation between local salinity and AMOC strength. The region is strongly freshened during hosing, with greater freshening in the more heavily hosed non-recovering run. The region also warms, with the non-recovering run warming more strongly, due to greater reduction in the surface heat flux.

Following the removal of hosing the total salinity is dominated by changes in the advective term, with little change in the surface flux. The changes in surface heat flux largely mirror the changes in heat advection, suggesting that as less heat is transported into the region, less is available to be released to the atmosphere. The primary differences between the net impacts in the recovering and non-recovering run are driven by differences in salinity advection. Here, the recovering AMOC increases the salinity of the region, increasing density, reinforcing AMOC recovery. In the non-recovering run, weakened advection strongly reduces the import of salinity, allowing the North Atlantic density to stay weak and keeping the AMOC weak in a positive advective feedback. Jackson and Wood (2018b) found this advective feedback to be the primary determinant of AMOC non-recovery.

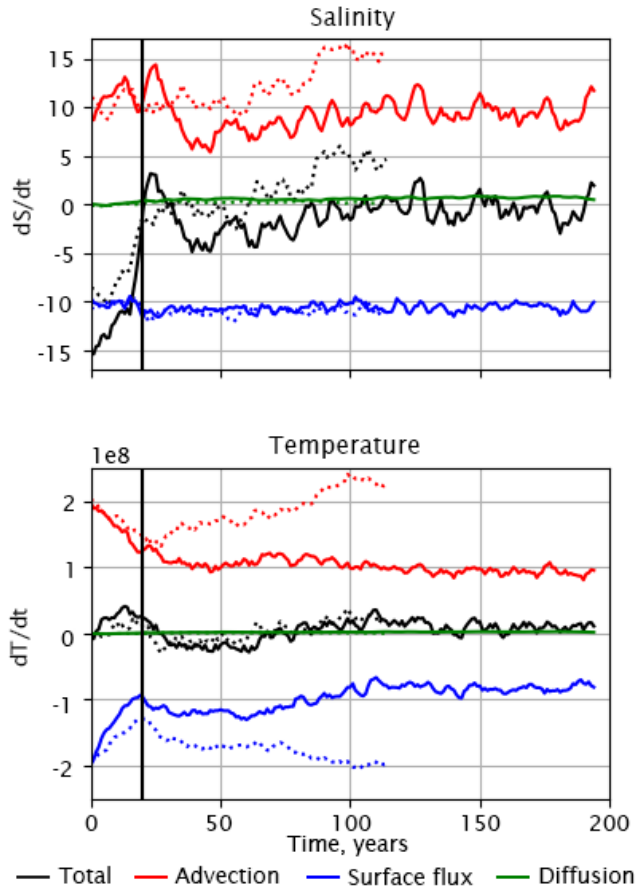

Fig. 4.3 Rate of change of temperature (10^8 K m^3 s^{-1}) and salinity (PSU m^3 s^{-1}) from 30˚N in the North Atlantic to the Bering Strait. **Solid lines**: show the non-recovering run (0.5 Sv hosing), **dashed lines**: recovering line (0.3 Sv hosing). 5-year rolling means have been applied for clarity. The black vertical marks the end of hosing at year 20. Hosing input is not included in the surface flux

However, Haskins et al. (2019) found that as hosing increased in the long hosing runs, the AMOC weakening was driven by subsurface temperature changes

resulting from the weakening of surface fluxes, due to the development of a surface cap in the northern Atlantic. We therefore want to explore further what happens in more detail within this region. We split the total region (30˚N to the Bering Straits) into two regions: a high North Atlantic (30-60˚N) region (able to directly influence the strength of the AMOC), and an Arctic region (60˚N to the Bering Straits). We also consider the low North Atlantic (0-30˚N). These latter regions represent external forcing and buoyancy stores, **Figure 4.4**.

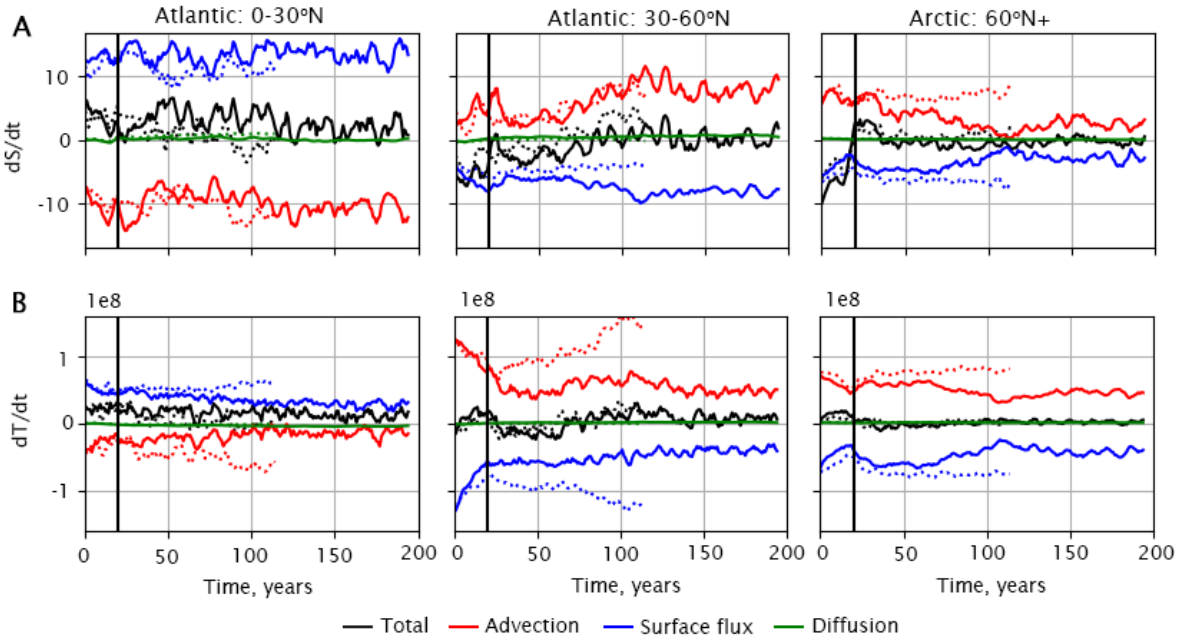

Fig. 4.4 Rate of change of **A**: salinity (PSU m^3 s^{-1}) and **B**: temperature (10^8 K m^3 s^{-1}) over the North Atlantic (0-30˚N and 30-60˚N) and Artic (60˚N+) regions, due to surface fluxes and ocean convergences by advection and diffusion. All data shown as 5-year rolling means. **Solid lines**: non-recovering run, **dashed lines**: recovering run. Black vertical marks the end of hosing at year 20. All lines have had the linear control run drift removed. Note that dS/dt total includes impact due to hosing, while the surface flux does not

The temperature and salinity balance north of 30˚N is between advection, which imports heat and salt, and surface fluxes that freshen and cool **Figure 4.4**. South of 30˚N they have the reverse impacts. The magnitudes of salinity change by advection and surface fluxes become stronger in the non-recovering run than in the control run in the high North Atlantic (30-60˚N), and weaker in the Arctic.

During hosing all of the Arctic and part of the high North Atlantic region are being forced with freshwater, and both regions net freshen. For the non-

recovering run, although the previous analysis showed no changes in surface freshwater fluxes, we see that there are compensating changes in the high North Atlantic and Arctic. These surface flux changes salinify the Arctic and freshen the Atlantic. There are also compensating changes in advection with exchange across 60˚N acting to freshen the Arctic and salinify the Atlantic. In the recovering run there are negligible changes in surface fluxes, and the high Atlantic salinity increases due to advection. Both regions warm in the non-recovering run when hosing is applied, due to having a faster/greater reduction in surface heat loss than the reduction in ocean heat convergence. The recovering run has less Arctic warming, and no net high North Atlantic warming, primarily due to differences in the surface flux.

Following the removal of hosing, the high North Atlantic continues to freshen due to a reduced advective import of salinity. In the recovering run this freshening is later balanced by salinity increase (from year 80) as freshwater is exported southwards. However, in the non-recovering run the salinity increase due to altered exchanges with the Arctic is largely balanced by increased surface freshening – resulting in the high North Atlantic remaining fresh.

After hosing ends, the high North Atlantic cools in the recovering run due to the continuing reduction of advective heat import in line with the AMOC continuing to weaken, while the surface heat flux remains steady. After year 80, the high North Atlantic warms. The multi decadal timescale form of dT/dt is dominated by the variability of the heat advection, due to changes in net meridional velocity, while a background warming trend comes from the gradually reducing surface heat flux. The Arctic is initially cooled by a temporary strengthening of surface heat loss. After year 70 magnitudes of both advective warming and surface cooling reduce, continuing until ~year 110.

By the final 50 years of the non-recovering run, the low latitude North Atlantic shows a steady increase in both temperature and salinity. While the salinity and temperature in the high North Atlantic and Arctic regions appear to have become stable **Figure 4.4**. However, a steady temperature or salinity volume mean over these regions does not mean that the density distribution is steady within each

region. The distribution of salinity and temperature within each region can be explored using the zonal mean values **Figure 4.5**. Each region contains contrasting anomalies, primarily occurring at different depths. If the vertical dependence of the meridional density is considered mechanically important, we need to understand how movement and mixing of density anomalies between depths may impact the ocean state.

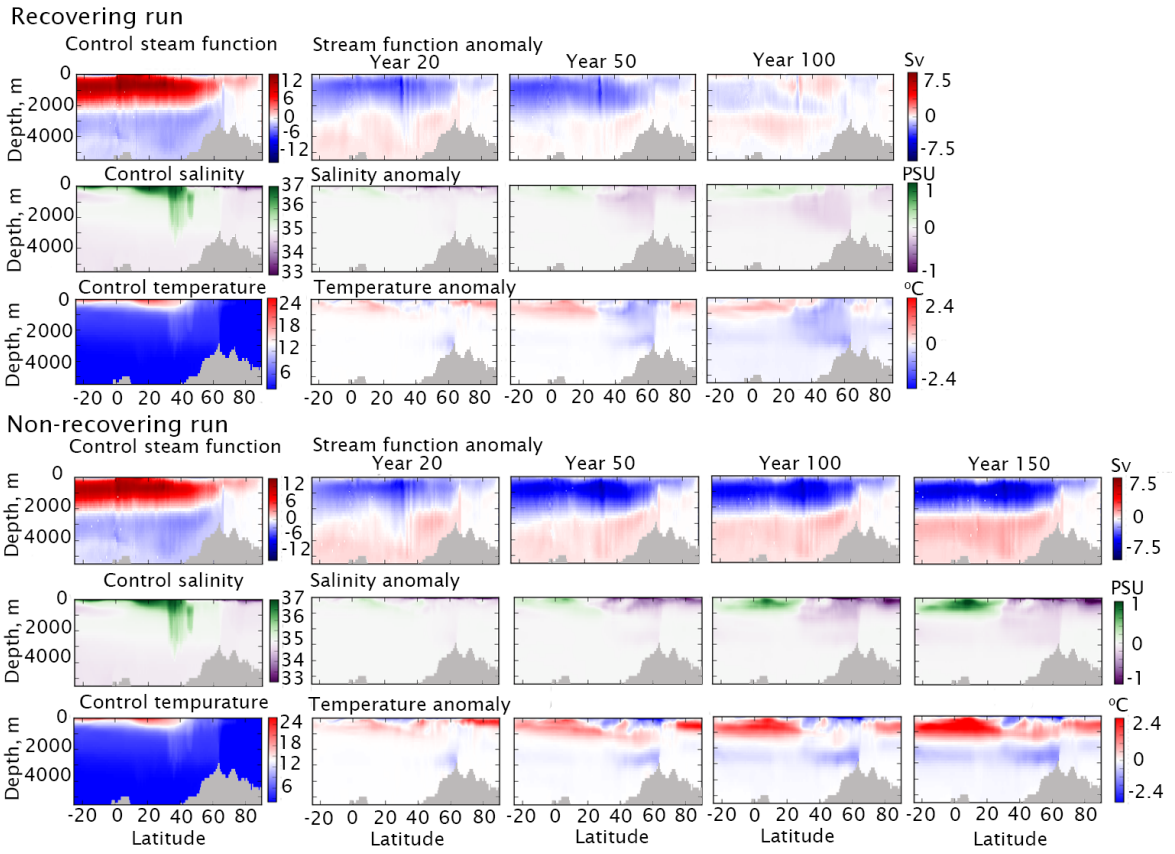

Fig. 4.5 Zonal mean Atlantic (30˚S-90˚N) stream function (Sv), salinity (PSU) and temperature (˚C) for both the recovering and non-recovering run. The leftmost panel shows control run values, from which the following panels show anomalies. All anomaly plots show detrended decadal means

4.4.2 Role of vertical structure

We are particularly interested in whether the negative density anomalies of the surface cap are being dissipated, exchanging properties with the subsurface, or remaining intact. In order to explore any vertical redistribution of temperature and salinity, we calculate the mean salinity and temperature for the North Atlantic (30-60˚N) and Arctic (60˚N+) regions each split between a surface box (0-200 m) and lower box (200 m – full depth), **Figure 4.6**. The surface box may be

considered as a store for buoyancy and a control on surface fluxes, which does not directly alter AMOC strength. The density of the lower box, which impacts AMOC strength (Haskins et al. 2019), will in part be determined by the exchanges with the surface box.

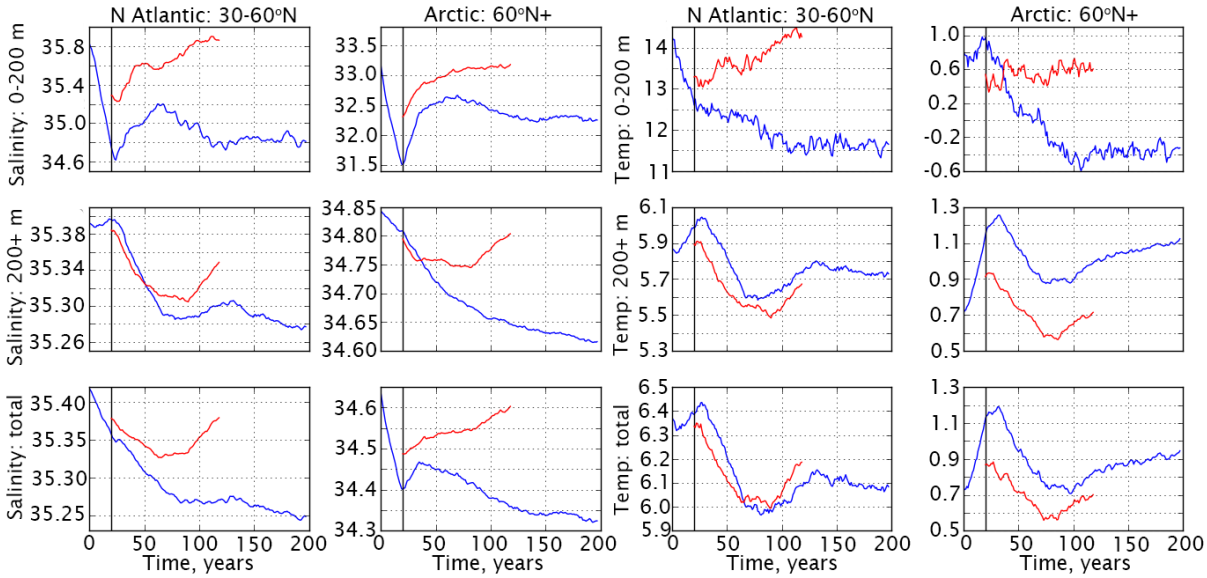

Fig. 4.6 Volume mean salinity (PSU) and temperature (˚C) for the North Atlantic (30-60˚N) and Artic (60˚N+) regions, for a surface box (0-200 m), lower box (200 m – full depth) and the full depth. **Blue line**: non-recovering run (0.5 Sv hosing), **red line**: recovering run (0.3 Sv hosing). Vertical line marks the end of hosing at year 20. Model drift has been removed

The surface boxes are strongly linearly freshened during hosing, with some of this freshening impacting the deep Arctic box. When hosing is removed, the salinities and the deep temperatures of the recovering and non-recovering runs respond in similar ways. The deep ocean is more strongly warmed during hosing in the non-recovering run, particularly in the Arctic. When hosing is removed, salinity rapidly increases at the surface, while decreasing in the deep box – suggesting convection weakening the surface cap in both the recovering and non-recovering runs.

The salinity of the recovering and non-recovering runs begin to diverge 10 years after hosing ends in the deep Arctic box, where the values of the recovering run start to recover, while the non-recovering run continues to freshen. This comes from a combination of the recovering run having greater advective convergence of salinity and weaker impact from the freshwater surface flux, via the surface

box, **Figure 4.4**. Note that the surface box for the non-recovering run gains salinity faster than that for the recovering run, despite having greater freshwater surface flux. This suggests that the convective event implied by the MLD in **Figure 4.2** is enabling a mixing down of properties from the surface cap. In the North Atlantic, the deep box is freshening more strongly than for the recovering run, the majority of this difference coming from the greater surface freshening in the non-recovering run, **Figure 4.4**.

At about the same time we see divergence in the surface box temperature of the North Atlantic. Recall **Figure 4.4**, where we saw the advective heat transport recover, with a greater/more rapid recovery of the surface heat flux, resulting in an overall cooling of the region. Here, we can see that the deep ocean net cools despite the subsurface warm anomaly, enhancing the strength of the AMOC. In the recovering run the surface ocean warms allowing for the recovery of the surface fluxes, while in the non-recovering run the surface continues to cool. The MLD of the recovering run ceases to strongly fluctuate and the surface boxes return to their initial values **Figure 4.6**. The MLD of the non-recovering run again becomes steady at year ~75 **Figure 4.2**, with the surface remaining cooled and freshened.

At the end of the recovering run, the cool fresh anomalies of the surface boxes have declined. The deep boxes remain broadly freshened and cooled **Figure 4.5**. The non-recovery run surface boxes appears to have become steady by the final 50 years of the run. The cold fresh surface cap continues to impact surface fluxes. The deep Atlantic and Arctic continue to freshen, alongside subsurface warming and deep cooling. The subsurface warming is stronger in the Arctic region, driving net warming **Figure 4.6** while in the North Atlantic the warming and cooling are more balanced **Figure 4.5**. The freshening is primarily responsible for the increased buoyancy, weakening the meridional density gradient and stratification, and keeping the AMOC weak. However, the subsurface warming has created a subsurface buoyancy store, primarily in the Arctic, coupled with surface cooling that may help to weaken stratification.

4.4.3 Surface freshwater flux and feedbacks

We have seen that a non-linear increase in freshening of the North Atlantic, due to changes in surface freshwater fluxes, prevents the salinity recovery seen in the recovering runs, **Figure 4.4**. In this section we want to identify the physical mechanisms responsible for the changes in the surface freshwater flux. We begin by splitting the surface freshwater flux into the flux from the ocean to the atmosphere and the surface flux related to ice physics over a region 45-55°N across the Atlantic, **Figure 4.7**. Neither of these components include the imposed freshwater hosing. There is some ice growth during the hosing run, near the western boundary and south of Greenland (not shown), which acts to extract some freshwater from the ocean. However, the negative freshwater flux from the open water to the atmosphere dominates the sign and form of the total flux. The surface ocean is increasingly freshened during hosing due to changes at the air-sea boundary, with the extent of the freshening modulated by ice growth. Once hosing is removed these 2 components continue to act in opposition, with smaller magnitude changes in the ice physics component.

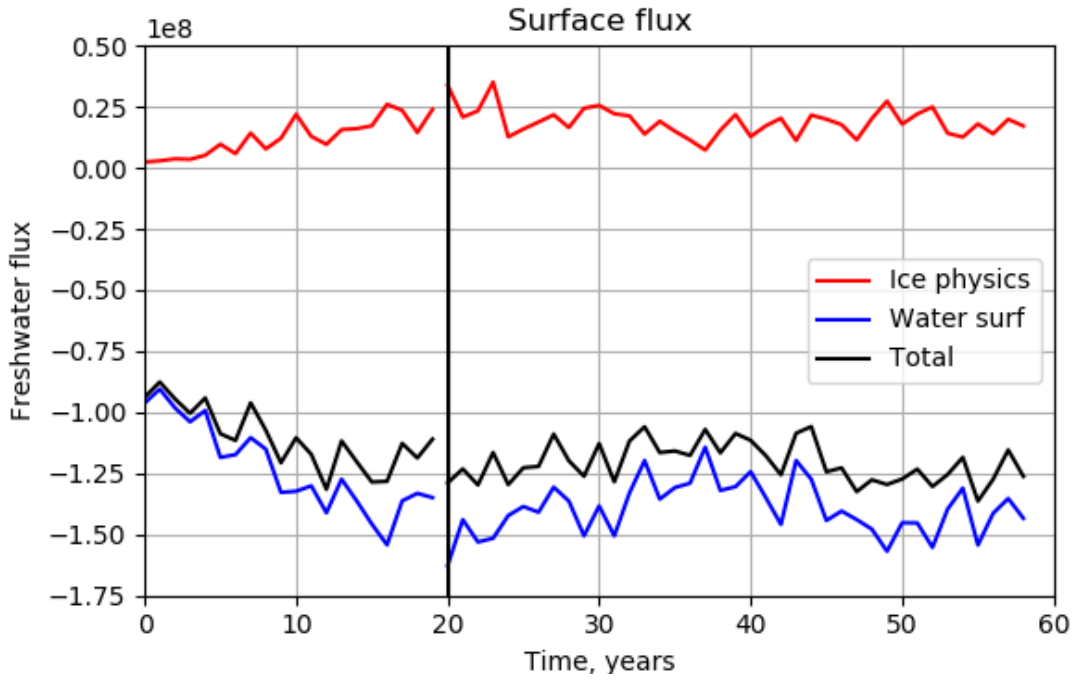

Figure 4.7 Surface freshwater flux, kg m^{-2} s^{-1}, integrated over a region 45-55°N across the Atlantic. Data shows a run hosed with 0.5 Sv of freshwater for 20 years, followed by 40 year post-hosing. **Black**: total freshwater surface flux, **Blue**: Freshwater flux from water surface to atmosphere, **Red**: Freshwater flux from water into ice. Black vertical marks the end of hosing

The freshwater flux from the water to the atmosphere is now broken down into precipitation and evaporation components, **Figure 4.8**. There is a strong reduction in evaporation over the high latitude North Atlantic and into the Nordic seas. This is likely due to cooled surface temperatures from both reduced northward transport of heat, and reduced convection leading to less warm subsurface water being mixed upwards into the sub-polar gyre. The reduction in North Atlantic evaporation results in there being less atmospheric moisture available to the wider area, which reduces the net precipitation both locally and over the Arctic region. The high North Atlantic and Arctic regions see a broad reduction in precipitation – seen in **Figure 4.4** as the weakened freshening in the Arctic region.

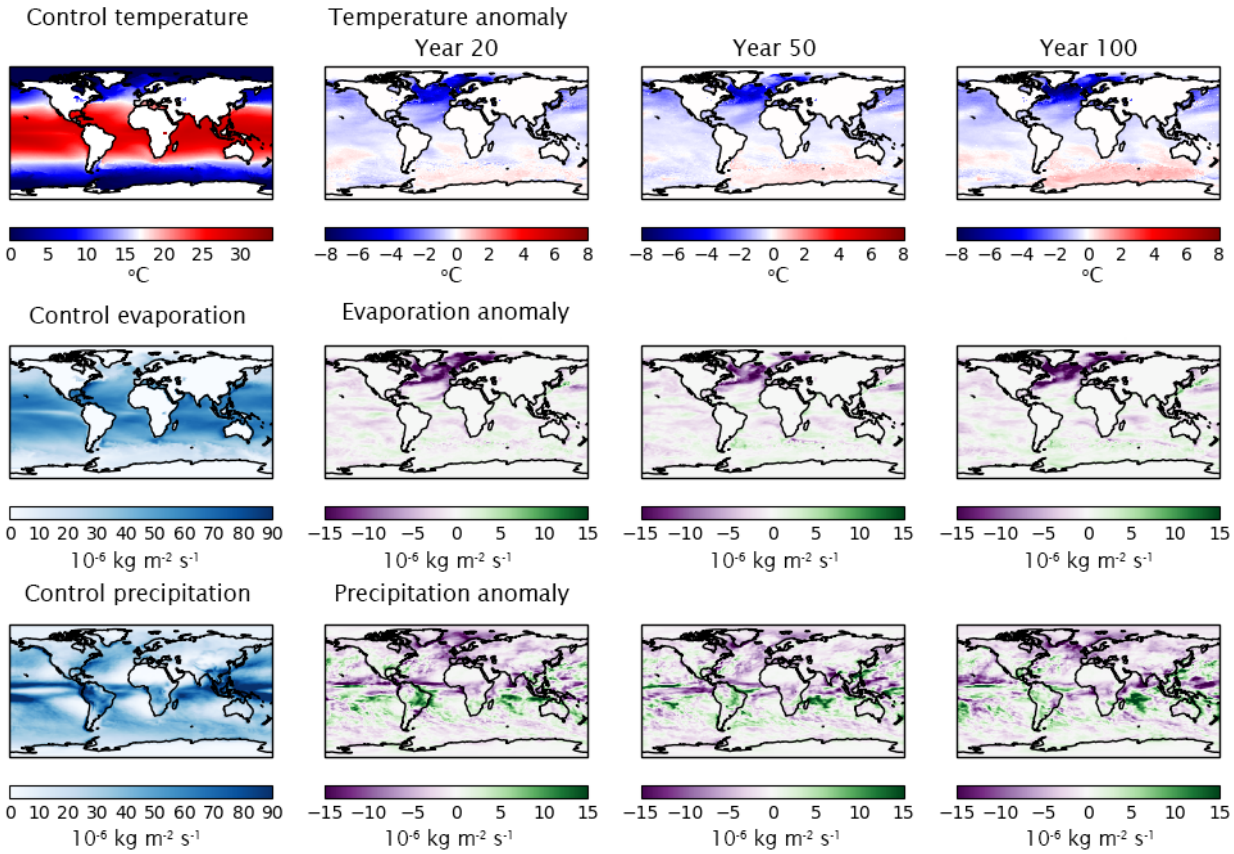

Fig. 4.8 Left: Control global surface temperature (˚C), evaporation and precipitation (10^{-6} kg m^{-2} s^{-1}), followed by 5-year mean anomaly plots (from the initial values) at years 20 (end of hosing), 50, and 100. All panels are for the run hosed with 0.5 Sv for 20 years

The evaporation anomaly dominates over the precipitation anomaly in the North Atlantic (30-60˚N), giving a net increase in freshening by surface fluxes – which partly compensates for the removal of hosing as a fresh forcing on the North

Atlantic. These changes to the surface freshwater flux act as a positive feedback: the AMOC is weakened by reduced North Atlantic density and so transports less warmth northwards, leading to less North Atlantic evaporation, increasing the regions freshness, further increasing buoyancy and keeping the AMOC weak.

4.5 Pattern of behaviour in recovering and non-recovering runs

We have so far explored the differences between one recovering and one non-recovering run, and established how their behaviour differs. We now want to consider whether these findings are representative of the full range of hosing experiments presented in **Figure 4.2**. The robust responses of the recovering and non-recovering runs will be described, along with 2 borderline runs that were slow to recover, suggesting that hosing ended while the ocean state was near the tipping point for non-recovery. This section will focus on controls on density at 50˚N in the Atlantic. Haskins et al. (2019) found this latitude to be representative of changes in North Atlantic density and therefore of AMOC strength, which is here supported by the meridional coherence over 30-60˚N **Figure 4.5**.

4.5.1 Recovering runs

The surface of the North Atlantic at 50˚N is initially freshened and cooled by hosing in all runs **Figure 4.9**. While AMOC strength remains > 8 Sv, the form of the net density anomaly is dominated by changes in salinity, with the extent of density reduction modulated by cooling **Figures 4.9** and **4.10**. Through the depth of the North Atlantic **Figure 4.11A**, this salinity driven reduction in density dominates AMOC weakening. However, reduced convection, with a rapidly shallowing MLD **Figure 4.2**, causes the cool fresh anomaly to be increasingly concentrated near the surface **Figure 4.9**. This gradually reduces the upward surface heat flux **Figure 4.12**.

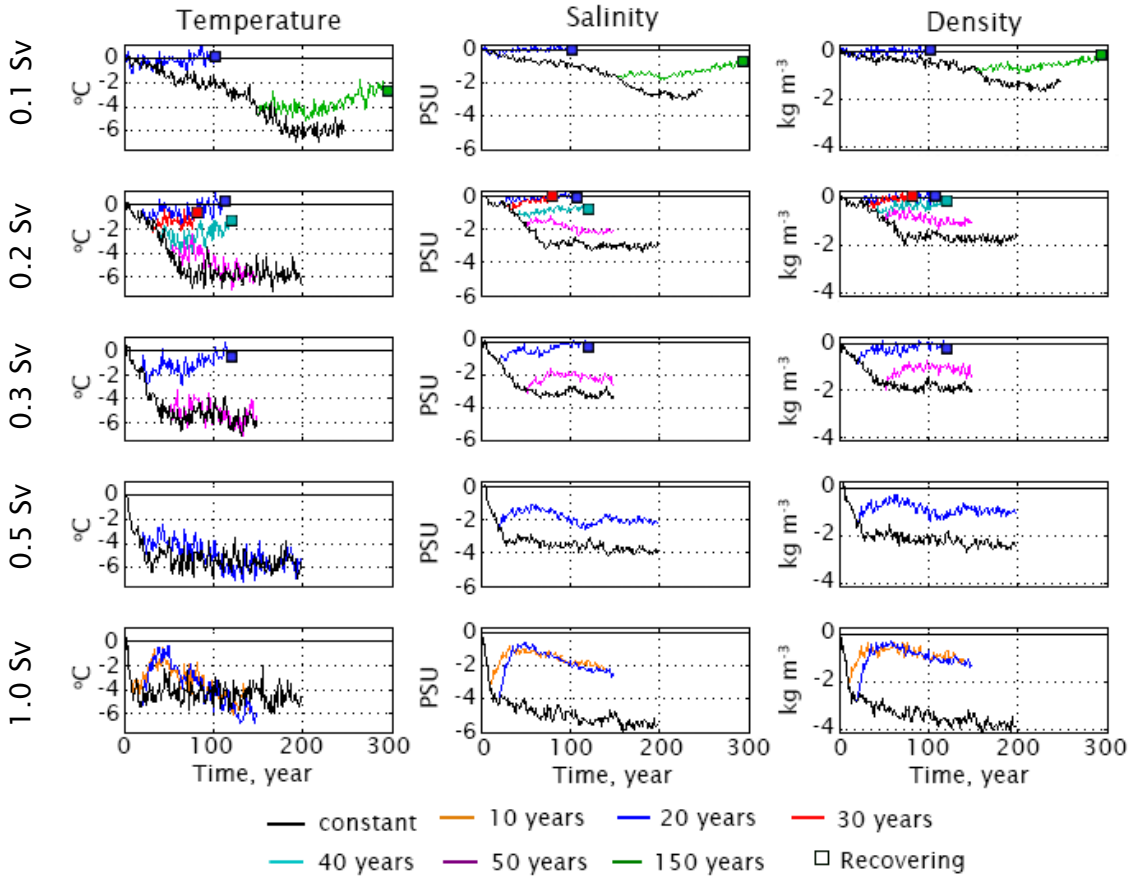

Fig. 4.9 Temperature (˚C), salinity (PSU), and density (kg m^{-3}) anomalies, depth 50 m, at 50˚N in the North Atlantic. In runs ending with a square the AMOC is considered to recover. Permanent hosing run is given in black, with hosing rate stated on the far left

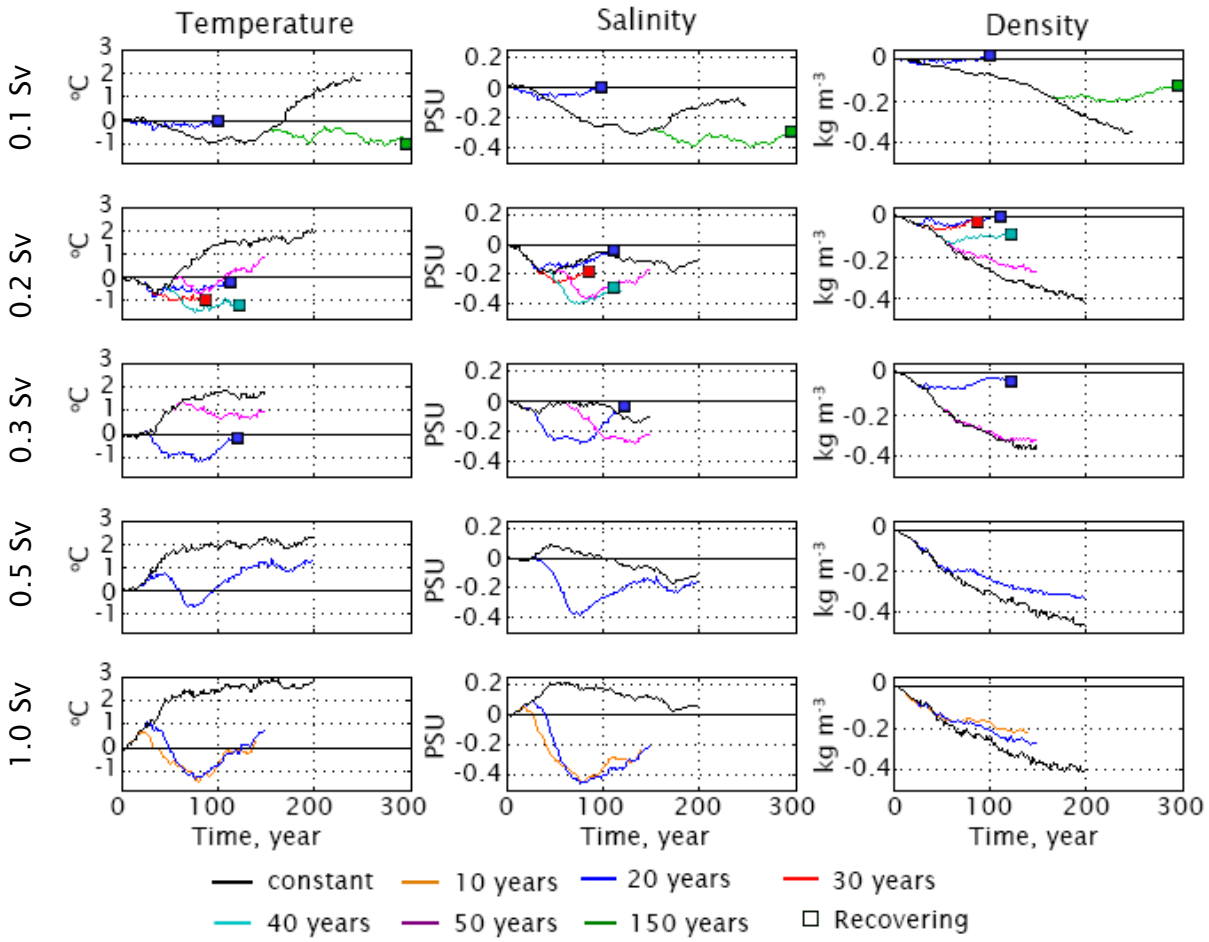

Fig. 4.10 Temperature (°C), salinity (PSU), and density (kg m^{-3}) anomalies, depth 1000 m, at 50°N in the North Atlantic. In runs ending with a square the AMOC is considered to recover. Permanent hosing run is given in black, with hosing rate stated on the far left

After hosing ends, convection enhances allowing for greater exchange between the atmosphere and ocean subsurface, allowing the surface heat flux to gradually recover **Figure 4.12**, and mixing surface anomalies down through the water column **Figure 4.11A**. The opposing impacts on the net density of temperature and salinity changes can be large, though mostly balance one another **Figures 4.9** and **4.10**. The temperature and salinity impacts level off as the MLD deepens to 2500 m and the AMOC recovers **Figure 4.2**. The recovering AMOC warms the region and feeds the surface heat flux. The temperature and salinity anomalies recover more slowly than the AMOC, which initially recovers due to a balance of anomalous coolness and freshness **Figure 4.11A**.

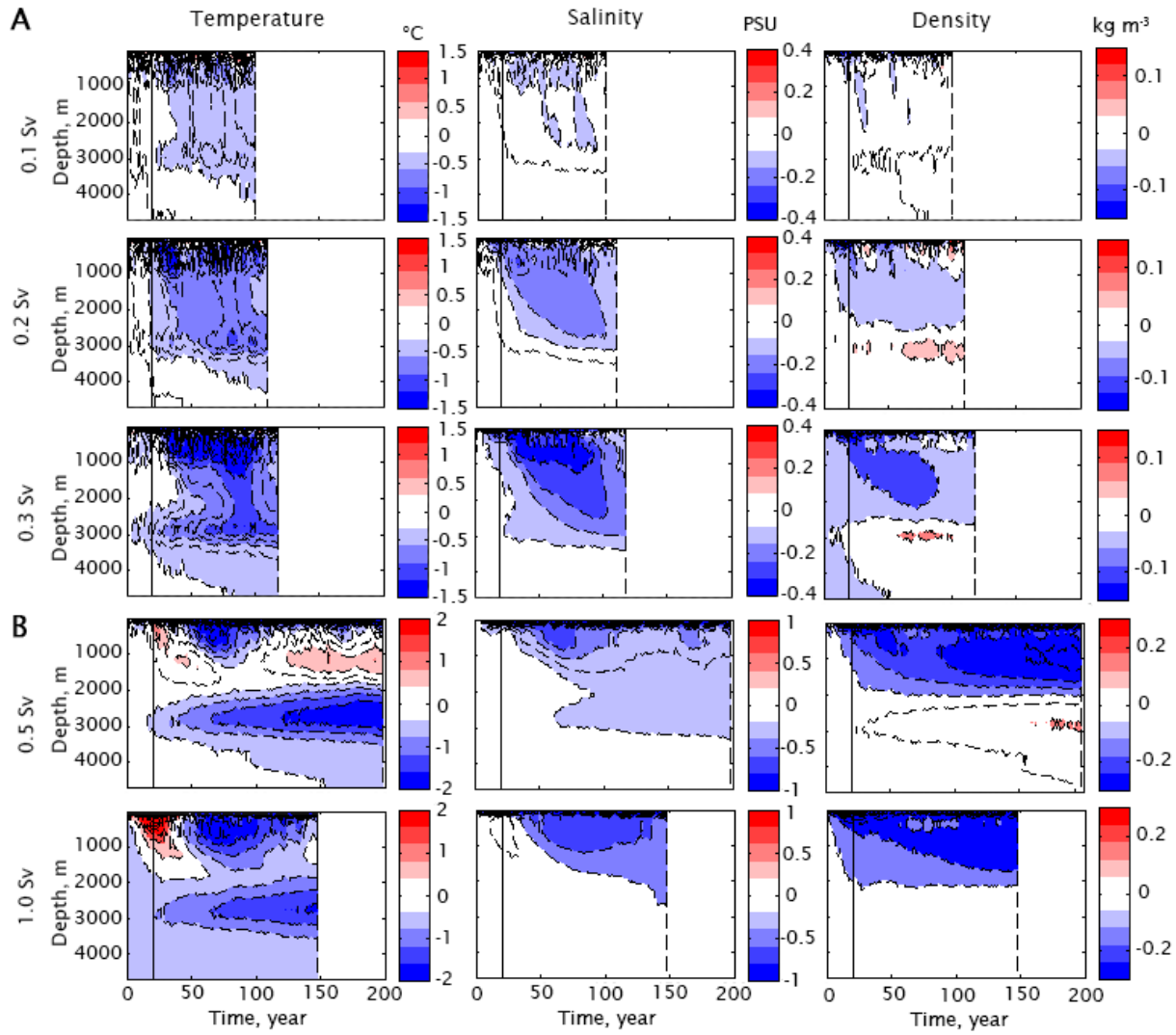

Fig. 4.11 Detrended anomaly hovmollor plots of temperature (˚C), salinity (PSU), and density (kg m^{-3}) at 50˚N. Each row is for a different hosing rate (0.1, 0.2, 0.3, 0.5 and 1.0 Sv of freshwater). All runs were hosed for 20 years, marked by the black vertical. **A**: The upper 3 runs recover, **B**: the lower 2 do not. Note different colour ranges are used in **A** and **B**.

4.5.2 Non-recovering runs

In the runs that did not recover post-hosing, the AMOC had already been significantly weakened, and the MLD had reduced to a depth of ~140 m, by the time that hosing was removed **Figure 4.2**. The cool fresh surface anomalies are more weakly convected downwards, becoming isolated within the shallow MLD **Figure 4.11B**. This limits the depth of their impact on subsurface density, and therefore on the AMOC strength (Haskins et al. 2019). The formation of a buoyant surface cap **Figure 4.9** strongly reduces the surface heat flux **Figure**

4.12, leading to the development of a subsurface warm anomaly **Figure 4.10**. As total forcing increases, this warm anomaly strongly reduces North Atlantic density, weakening the AMOC. For all non-recovering runs, the ocean surface at 50˚N is sufficiently cool for the ocean to be taking up heat from the atmosphere. Having so far reduced quite weakly, the net evaporation undergoes a more rapid decline. The net surface freshwater flux into the ocean thus increases **Figure 4.12**, reinforcing the hosing input. These changes in the surface fluxes suggest that in all non-recovering runs there is a positive surface freshwater feedback over the North Atlantic and Arctic regions, as described in **Section 4.3**. This relationship is further explored in **Figure 4.13,** which contrasts AMOC strength and surface freshwater flux for the start of all post-hosing runs. The more negative the surface freshwater flux (integrated over 45–55˚N across the Atlantic) has become by the time that hosing is removed, the less able was the AMOC to recover. The strength of the AMOC is less robustly related to the capacity of the AMOC to recover. This is partly due to the significant interannual variability, but also potentially due to different timescales of ocean response to the different hosing rates.

During the post-hosing phase the surface cap does not recover **Figure 4.9**. In the more strongly hosed runs, the surface anomalies show an initial decrease in the cool fresh anomalies – with salinity responding more strongly than temperature, and all runs later redeveloping their low-density cool fresh surface cap. This can be seen as the removal of hosing making the surface less fresh, which weakens the stratification and allows temporary convection **Figure 4.2**. This brings warm water to the surface, increasing heat loss and evaporation **Figure 4.12**. This releases some trapped subsurface heat, and freshens and cools the subsurface **Figure 4.11B**. Fluctuations in the subsurface temperature and salinity anomalies largely compensate for each other **Figure 4.10**, leaving little change in net density. The subsurface salinity anomaly remains fresher in the non-recovering runs than in the recovering runs, which contributes to keeping the AMOC weak. This is consistent with the findings for the North Atlantic (30-60˚N) below 200 m in the case studies **Figure 4.6**, again supporting the use of values at 50˚N as representative of values over the convective region.

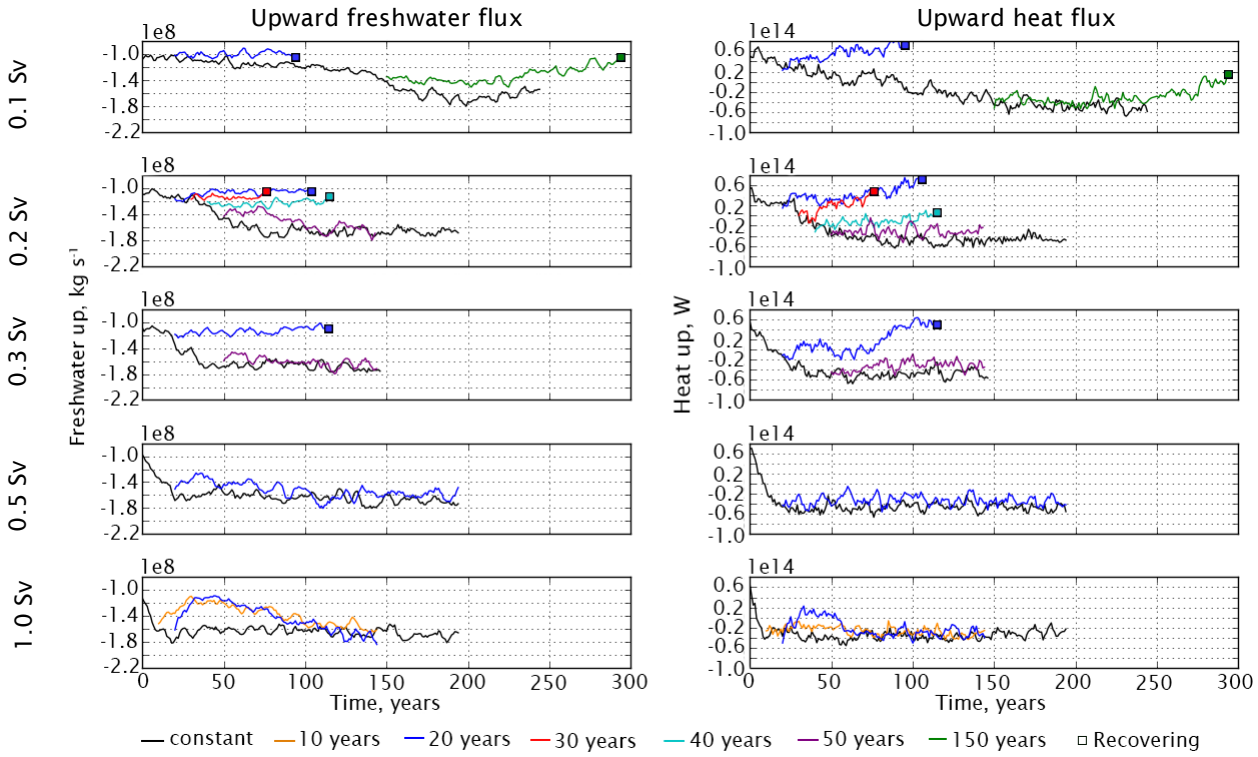

Fig. 4.12 Surface fluxes of upward freshwater (kg s^{-1}) and upward heat (W). Fluxes were calculated for the full width of the Atlantic Basin, from 45–55°N. A 5-year rolling mean has been applied to all lines for clarity. In runs ending with a square the AMOC is considered to recover. Permanent hosing run is given in black, with hosing rate stated on the far left

4.5.3 Borderline recovering runs

Two runs appear to be very close to the tipping point for non-recovery, in that they are slow to begin to recover when hosing is removed (one hosed with 0.1 Sv for 150 years and the other hosed with 0.2 Sv for 40 years). We are therefore expecting their responses to be intermediate between the recovering and non-recovering cases. In these runs, we can see that the AMOC enhancing influence of the initial subsurface cool anomaly is already in decline by the end of hosing **Figure 4.10**. The MLD has already significantly shallowed and the upward surface heat flux is significantly reduced **Figure 4.12**. While the subsurface has begun to warm under the beginning of a surface cap, there is still a negative subsurface temperature anomaly **Figure 4.10**. As the subsurface is not strongly isolated from the surface, we see less surface cooling and the net evaporation has not yet reached a point of sudden decline **Figure 4.12**, with freshwater surface flux being reduced to intermediate values **Figure 4.13**. This suggests that these runs do not

experience the surface freshwater feedback associated with altered surface fluxes. Once hosing is removed it takes the MLD some time to make clear signs of recovery **Figure 4.2**. These borderline recovering runs suggest that the tipping point for AMOC non-recovery is linked to the extent of the surface cap, and the resultant surface freshwater feedback.

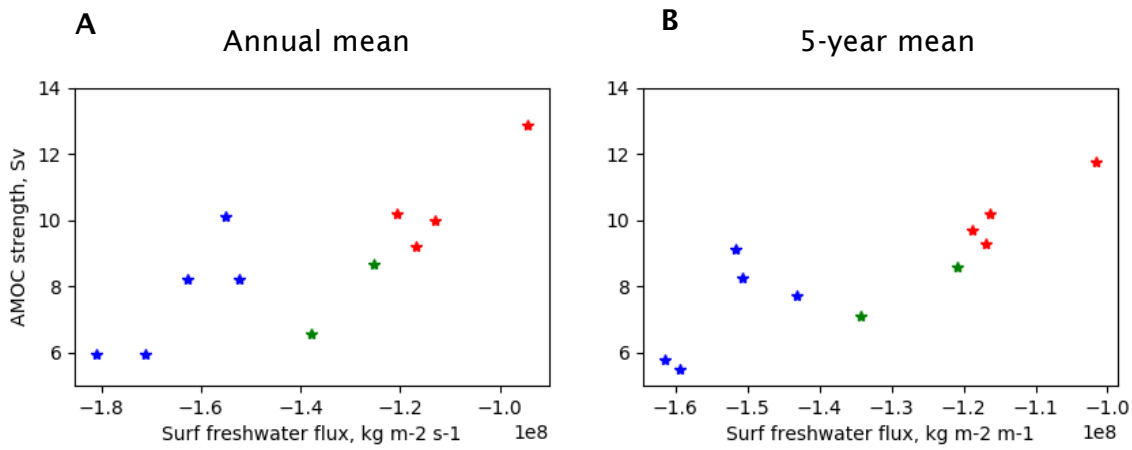

Figure 4.13 AMOC strength, Sv, plotted against surface freshwater flux (excluding ice physics), 10^8 kg m^{-2} s^{-1}, integrated over 45–55°N across the Atlantic for **A**: the first annual mean of the post-hosing simulations, and **B**: the 5-year mean at the start of the post-hosing runs. **Red**: recovering runs, **Green**: Borderline runs, **Blue**: non-recovering runs

4.6 Discussion

We have robustly identified ocean states associated with AMOC recovery and non-recovery in response to temporary freshwater forcing in HadGEM3-GC2. We have tried to understand not just what can cause the AMOC to initially remain weak, but also to consider the long-term impacts of the temporary hosing. Here, we will discuss the possible consequences of the built-up anomalies and feedbacks, before giving a summary of our primary findings in **Section 4.7**.

In the recovering runs, the distribution of temperature and salinity in the North Atlantic recover on a much longer timescale than is implied by AMOC strength alone. This is due to North Atlantic density first recovering as a balance between freshening and cooling, with the values of salinity and temperature being slower to recover, as previously noted (Haskins et al. 2018). Throughout this time the

ocean is in a different state to the control run, and may therefore be expected to respond differently to further forcing, making the resilience of the recovered AMOC to moderate renewed forcing unclear.

The convective event following the removal of hosing in the heavily hosed non-recovering runs is linked to the rapid release of subsurface heat. In previous studies this has be associated with rapid AMOC recovery (Mignot et al. 2007; Haskins et al. 2018). However, this upward convection of heat can be paired with a downward convection of freshwater, slowing the AMOC recovery to the timescales of ocean export of the fresh anomaly (Brady and Otto-Bliesner 2011). Our experiments also show this exchange of subsurface heat for surface freshness due to a convective event. However the following reformation of the surface cap, partially fed by the altered surface freshwater fluxes, allows the subsurface warm anomaly to later reform, a phenomenon not apparent in Brady and Otto-Bliesner (2011). Kleinen et al. (2009) stressed that subsurface warming is likely highly model dependent, and while it is encouraging to see these responses in a high-resolution model, a multi-model comparison that tracks the long-term behaviour of subsurface warming would add confidence.

The surface cool freshwater cap appeared stable above the warm anomaly at the end of the non-recovering runs. This raises the question of whether the increased buoyancy below would eventually drive convective mixing by vertical instability. However, a radiative forcing study found subsurface warming below freshening to lock in surface stratification, preventing the resumption of deep convection (Brodeau and Koenigk 2016). Their study did not include freshwater forcing from Greenland ice melt, which would likely have enhanced both surface freshening and subsurface warming, potentially further enhancing stratification.

The cooling of North Atlantic surface temperatures resulted in a positive surface freshwater feedback, due to reducing the surface export of freshwater by evaporation. This feedback would continue to freshen the North Atlantic surface as long as the ocean surface remains cool. These altered heat and freshwater transports would have further consequences for the surrounding landmasses. Previous hosing studies have reported similar North Atlantic surface cooling

reducing North Atlantic evaporation and North Atlantic and Arctic precipitation, acting to freshen the North Atlantic (Vellinga and Wood 2002, Figures 3 and 4; Jackson et al. 2015 and references within). They both found this to lead to cooling and reduced precipitation on the landmasses surrounding the North Atlantic, resulting in a decline in primary production. These findings were supported by Jacob et al. (2005), who found that weakening the AMOC resulted in reduced precipitation, cooling, and increased snow cover over continental as well as coastal Europe. Due to the impact on albedo, this led to a positive feedback on European cooling.

The warm saline anomaly that developed at the equator in the non-recovering run could dynamically impact overturning if transported northwards (Yin and Stouffer 2007; Wan et al. 2010). Increased low latitude salinity due to changes in the hydrological cycle and southward shift of the ITCZ have been suggested to help reinvigorate the AMOC once hosing is removed (Stouffer et al. 2006; Krebs and Timmermann 2007). However, in higher resolution models such as HadGEM3-GC2 the stronger salinity transport can result in a greater reduction in transport convergence with an AMOC weakening, and hence cause a freshening that can oppose the salinification (Mecking et al. 2016). In our study, the salinity anomaly is significant and continuing to build, suggesting that it could eventually be transported northwards by advection or diffusion. Paleoclimate studies have suggested that warm salty subsurface waters that collect in the subtropical Atlantic during periods of weak AMOC are gradually transported northwards, leading to the destabilisation of ice shelves. This allows the high latitude subsurface warm anomaly to be released to the atmosphere, reintensifying the AMOC (Hernández-Almeida 2015). Sgubin et al. (2015) found that the transport/dispersal of this high salinity anomaly was model dependent, and could define the recovery behaviour.

4.7 Conclusion

The North Atlantic was freshened with various hosing rates, for various durations, leading to a progression of changes in the distribution of density. With limited hosing, the AMOC is resilient to forcing and recovers once hosing is removed. However, with greater hosing and significant reduction in MLD, a buoyant surface

cap forms. This isolates the subsurface ocean from the atmosphere, causing a subsurface warm anomaly to develop and altering the surface fluxes, giving a positive feedback on freshening over the high latitude North Atlantic surface. The subsurface warm anomaly was shown to eventually become the dominant driver of AMOC weakening in Haskins et al. (2019). This change in ocean state coincides with the limit for AMOC recovery in HadGEM3-GC2.

As was found by Jackson and Wood (2018b), we saw a positive salt advective feedback over a region 30°N in the Atlantic to the Bering Strait as the AMOC weakened. However, Haskins et al. (2019) had found AMOC weakening to be ultimately driven by North Atlantic density changes resulting from a surface freshwater cap, motivating us to explore more regional density exchanges. By considering the density transfers between the high North Atlantic and Arctic regions we identified a surface freshwater positive feedback on AMOC weakening (also seen in Stouffer et al. 2006 and Mecking et al. 2016). As the AMOC weakened and North Atlantic convection reduced, the surface of the North Atlantic cooled, reducing local evaporation. This reduced the air moisture available for precipitation both locally and over the Arctic region, giving a net freshening of the North Atlantic and increasing the surface salinity of the Arctic. In the runs where this feedback had been established the AMOC did not recover, partly as this net freshening partially compensated for the removal of hosing. Due to the rapid reduction in North Atlantic net evaporation as the AMOC strength became unrecoverable, this study suggests that tracking reanalysis precipitation minus evaporation data could be used as an indicator of the AMOC exceeding its resilience to forcing.

Chapter 5: Discussion

In this thesis I have sought to explore the response of the AMOC to permanent and temporary North Atlantic freshwater forcing. I have examined the drivers of change in temperature and salinity throughout the full depth of the water column to understand what controls North Atlantic density, and the impact this has on the strength of the AMOC. In the **Introduction** 3 questions were raised from the existing literature which I have endeavoured to explore throughout this work. Firstly, I sought to explore the asymmetry between the weakening and recovery processes of the AMOC. This was largely addressed in **Chapter 2**, where I found the recovery process to be mechanically distinct from the weakening process. I then asked whether the subsurface warming qualitatively present in some freshwater forcing studies was significantly impacting North Atlantic density, and thereby AMOC strength, and whether the vertical structure of density anomalies were important in understanding changes in AMOC strength and resilience. I began exploring the subsurface warming in **Chapter 3**, where I found the subsurface warming to become not just significant but dominate in weakening the AMOC. The process enabling this was related to changes in the vertical structure of temperature and salinity, which lead to the isolation of the ocean subsurface from the atmosphere. Once this change in vertical structure was in place, I found it to not just weaken the AMOC but to also signify the limit of AMOC resilience in **Chapter 4**.

To conclude this thesis I will give a summary of the overall findings in **Section 5.1**, in **Section 5.2** I will give a deeper level of discussion into the results, and offer some further interpretations of these findings. Finally, I outline some of the potential future work inspired by this research in **Section 5.3**.

5.1 Summary of work

In **Chapter 2** I explored the asymmetry of the weakening and recovery of the AMOC, using 10-member ensembles in FAMOUS. Following 200 years of freshwater forcing with 0.2 or 0.5 Sv of freshwater, the AMOC took 100 years to first recover initial strength, before overshooting for the following 100 years. In

order to identify the impact of changes to the Atlantic meridional density gradient, I reconstructed the AMOC using the depth dependent Butler et al. (2016) method. While changes in the North Atlantic density were responsible for the weakening behaviour of the AMOC, the recovery process was more complex. As others have previously reported, when the AMOC was weak the surface waters in the low-latitude North Atlantic became anomalously dense. As the AMOC recovered these high-density waters were transported into the deep convection regions causing short-lived pulses of AMOC enhancement. However, the magnitude of the overshoot in these experiments resulted from density changes in the South Atlantic.

Chapter 2 focused on AMOC 'weakening' and 'recovery', as opposed to 'collapse'. This is not to imply that the AMOC could not have been collapsed with further freshwater hosing – but simply that this study was focused on the different mechanisms present through AMOC weakening and recovery. Hawkins et al. (2011) found that FAMOUS showed AMOC bistability with a robust hysteresis loop with freshwater forcing in excess of 7.5 Sv. However, this is not directly comparable, as in Hawkins et al. (2011) net freshwater was conserved using 'surface compensation', where the salinity removed from the hosing region to achieve the 'freshening' is returned evenly over the surface of the global ocean. In this study we used 'volume compensation', where the salinity removed from the hosing region is returned evenly over the full volume of the global ocean. The choice of salinity compensation has been shown to impact global density stratification and AMOC response to freshwater forcing in FAMOUS (Jackson et al. 2017). If compensation is applied throughout the volume of the global ocean, rather than at the surface, the region of hysteresis is much narrower (in fact the AMOC is virtually mono-stable – see Fig. 2b of Jackson et al. 2017). We used volume compensation because it does not introduce spurious dynamics, its principle effect being due to the small non-linearity in haline contraction, comparable to the effect of surface compensation on stratification. Therefore, we were not expecting our simulations to behave as in Hawkins et al. (2011). Given this, we did not expect any threshold behaviour in our results.

While the usual interpretation in freshwater forcing studies suggests that the AMOC is directly weakened by the freshening of the North Atlantic reducing local

density, some of the findings in FAMOUS challenged this assumption. There was a strong increase in basin mean temperature during hosing (apparent in **Figure 2.5**) and the North Atlantic temperature hovmoller in **Figure 2.12** showed that while the surface at 50˚N was cooled, below this a warm anomaly developed. The zonal mean plots of **Figure 5.10** showed that despite subsurface salinity increasing, local density was decreasing due to warming.

In order to investigate this further, in **Chapter 3** I again used the depth dependent approach to reconstructed the strength of the AMOC, now splitting the contribution down between both changes in the North and South of the Atlantic and also between changes in temperature and salinity. To establish whether the strong subsurface warm anomaly was a model dependent feature, resultant from FAMOUS relatively low resolution, I included data from similar experiments using the 1/4˚ eddy-permitting model HadGEM3-GC2.

This analysis supported the theory of the dominant impact of subsurface warming on AMOC weakening. However, HadGEM3-GC2 responded less simply to freshwater forcing than did FAMOUS. Initially the lower hosing rates in HadGEM3-GC2 showed that the AMOC was weakened by the freshwater input itself. The heaviest hosing rate in HadGEM3-GC2 was the most similar to the response seen in FAMOUS (at all hosing rates). The role of temperature and salinity at 50˚N was made clearer by considering the impact in terms of the total freshwater added. This established the approximate pattern that the AMOC was weakened by freshwater for the first 10 Sv yrs, after which subsurface warming led to temperature domination. This occurred when the AMOC was reduced to a strength of about 8 Sv – which Jackson and Wood (2018b) had found to correlate with the tipping point for AMOC non-recovery.

This raised the question of whether there was a relationship between the mechanistic change leading to temperature domination of AMOC weakening, and the AMOC becoming unable to recover when hosing was removed. In **Chapter 4** this was explored using a series of 11 post-hosing runs, some that recovered and some that did not. By using temperature and salinity budget analysis I was able to identify both a previously observed salt advective feedback at 30˚N (Jackson and

Wood 2018b), and altered surface freshwater fluxes in the high latitude North Atlantic and Arctic region. Reduced freshwater export by evaporation, seen only in non-recovering runs, acted to freshen the North Atlantic, giving a positive feedback on reducing the density of the North Atlantic and helping to stabilise the weak AMOC state.

It is interesting to consider the differences between the post-hosing experiments in FAMOUS in **Chapter 2** and HadGEM3-GC2 in **Chapter 4**. While the mechanism of AMOC weakening in the recovering FAMOUS runs is similar to the heavily hosed, non-recovering, runs in HadGEM3-GC2 - there is a different response to the removal of forcing. One explanation for this is the greater resolution of HadGEM3-GC2 enabled a stronger salt advective feedback than was seen in FAMOUS. Though the response of the surface freshwater flux was not fully addressed in **Chapter 2**, from **Figure 2.9** it appears that there may have been some North Atlantic freshening, due to changes in the surface fluxes, which recovers with the AMOC. This suggests that in FAMOUS the freshening was responsive to sea surface cooling reducing evaporation, but did not develop an effective freshwater feedback. FAMOUS may therefore have lacked both the advective and surface freshwater feedbacks that enabled non-recovery in HadGEM3-GC2. This suggests that the mechanisms controlling AMOC weakening do not directly control the AMOC capacity for recovery. Instead, AMOC non-recovery is controlled both by background ocean state (salinity fluxes) and surface feedbacks relating to atmosphere/ice – which may be dependent on model complexity. The modern ocean has the strong northward salinity transport seen in HadGEM3-GC2, and the atmospheric physics is better described by HadGEM3-GC2. This suggests that lower resolution models such as FAMOUS may be overestimating the stability of the AMOC, and showing recovery after mechanistic changes which would be associated with non-recovery in the real ocean.

5.2 Discussion of results

Throughout the course of this research there has been a range of interesting findings, some of which appear to be in conflict with the existing literature. Some of the implications of these findings will here be considered, along with some of my own views.

The asymmetry of the weakening and recovery process of the AMOC was considered in **Chapter 2**. The process of applying freshwater forcing can be compared to steadily applying an increasing force to the surface of the ocean, with the ocean state below being increasing altered by the applied pressure. Once the pressure is removed there are 2 possibilities for a recovering ocean. We could see an 'undoing' of the consequences of the forcing, where recovery would resemble the 'weakening process in reverse'. Alternatively, changes in ocean state could mean that the recovery process follows a mechanically different pathway. In FAMOUS, we saw an initial shock response to the removal of hosing followed by the working out of developed anomalies by the recovering ocean transports. This gave asymmetry in rate of change of AMOC strength either side of the removal of forcing. Initially, the removal of freshwater forcing allowed for a rapid export of subsurface warmth, accumulated while the AMOC was weak. This increased North Atlantic densities compared to the South, enabling enhanced overturning. The enhanced overturning was then able to transport developed density anomalies around the basin, and readjust surface fluxes, returning the basin towards the initial balance of meridional density difference. The asymmetry present in the maximum magnitude of the AMOC either side of the removal of forcing is due to the AMOC overshoot, which originated from the different timescales of recovery in the north and south of the Atlantic. In the North Atlantic the presence of freshwater forcing in itself stabilised the vertical structure, preventing the release of subsurface warmth. In the South Atlantic the density changes were related to both a deepening of the pycnocline and changes in the wind fields and latitude of the South Atlantic gyre.

Together these asymmetries raise some really interesting questions in terms of managing the real world climate system. Studies considering what constitutes acceptable or unacceptable decline in the AMOC generally consider the climate

impact of the weakening process. However this research suggests that the recovery process could be more challenging in terms of societal resilience and infrastructure demands, in that there could be a greater rate of change and total magnitude of change during the recovery phase.

In these simulations the freshwater forcing was removed in one time step, while in the natural world changes in rate of ice melt would most likely be gradual. It is unclear how a melting Greenland ice sheet could be restabilised, however assuming that it was, we could expect that restabilisation to result in a tapering off of freshwater input into the surrounding ocean surface. This would mean that the surface freshwater would disperse, and the surface fluxes re-establish, more gradually (in relation to the behaviour seen in FAMOUS). This suggests that in the natural world we may not see the same shock behaviour in the release of subsurface warmth and rapid early recovery. There would be a slower surface response to more gradually changing rates of ice melt run off – whether this would enable a slower recovery of surface fluxes, or whether subsurface warmth would still drive rapid vertical instability at a tipping point giving rapid AMOC recovery, is unclear.

In **Chapter 3**, the reconstruction of AMOC strength using the volume mean method was able to give a good estimate of the AMOC time series. This supports its use for practical estimates of AMOC strength that can be used alongside volume mean budget analysis of the North Atlantic. However, in this study we wanted to break this region down further, including vertically, in order to understand how the changing distribution of temperature and salinity impacted the behaviour of the AMOC. The Butler et al. (2016) method is important for being able to examine the impact of density changes within the ocean. It enables insight into the density changes that directly impact deep pressure gradients and can thereby directly drive changes in overturning.

By taking the Butler depth-dependent approach we are better able to assess and quantify the relative impacts of temperature and salinity on the strength of the AMOC, and also to understand the significance of both their individual and combined vertical structures. While the use of ‘rotated geostrophy’ in the Butler

method cannot in and of itself establish causality, it can take us a step in the right direction by enabling us to quantitatively identify the significance of changes in density at depth within the ocean, giving a more direct understanding of what drives change in ocean overturning. The AMOC in HadGEM3-GC2 was found to weaken linearly with increased freshwater input (in Sv yr), with no qualitative change in rate of AMOC weakening between times dominated by freshening, and those dominated by warming. However, through the different hosing rates, there was a spread in the relative influence of temperature and salinity for any given total freshwater input, **Figure 3.10**. When using the volume mean approach this detail in the changing dynamic of the ocean is lost.

All of the new analysis presented in the thesis is based on data from 2 global climate models. The lower resolution model FAMOUS dominated the experiment design, as it set the more significant limitations. In particular the choice of such as broad hosing region was made in respect to previous FAMOUS studies that showed that more selective hosing regions resulted in down-welling starting outside of the hosing region in physically unrealistic locations (Smith and Gregory 2009). This is partially due to the fact that the bathymetry in FAMOUS was altered in various was, including the removal of Iceland and deepening of North Atlantic overflow channels, to enhance and thereby better represent meridional ocean transports. However, it would clearly be unhelpful to find that freshwater forcing near Greenland resulted in ocean down-welling down through Iceland. We therefore used a broad hosing region to ensure that our analysis would focus on the mechanisms and implications of a weakening of the AMOC.

In many ways FAMOUS was less representative of the real Earth-system than was HadGEM3-GC2. I have previously described FAMOUS as having a compensation of errors enhancing AMOC strength, the sign of the freshwater flux at 30˚S in the Atlantic not being in agreement with the modern ocean, the issues of representing eddy transports with the Gent-McWilliams scheme. However, I do think that it is both useful and important to repeat experiments using a hierarchy of climate models. To my mind there are 3 main reasons for this. Firstly, every new study has a context within the literature, and when trying to unpick why a model behaves in a different way it can be helpful to know whether the model response is determined by a change in methodology or by the

resolution/complexity of your model. Secondly, FAMOUS was a much more computationally affordable model to run. This not only allowed me to develop ensemble results, but it also allowed me to more fully explore the parameter space and analyse a far wider range of variables to get a better feel for the knock on effects of the primary features of the study. This helped to develop the analytical approach which was then applied to the HadGEM3-GC2 data. Finally, contrasting between the 2 models gave a continual reminder to not become overconfident of the results of the higher-resolution, more complex, model. It was not just the assumptions and biases in FAMOUS that I needed to consider, but the impact of the different assumptions and biases between the 2 models. Ultimately, the results of model analysis describe the model used not the real Earth-system. However, they are a profoundly useful tool for exploring our knowledge of Earth-system physics, and supply a laboratory in which to test theory.

During the introduction, we referred to the finding in Driesschaert et al. (2007) that at the end of a 1000-year simulation radiative forcings of 4 Wm^{-2} and 7 Wm^{-2} gave additional freshwater fluxes into the North Atlantic of approximately 0.01 Sv and 0.05 Sv, respectively. However, in our simulations we used 0.1 to 1.0 Sv of freshwater forcing. This raises the question of whether these simulations explore more extreme cases than could be considered realistic. Estimates of both current freshwater input to the North Atlantic due to ice melt (sea ice and Greenland ice sheet) and future projections vary significantly and are not well constrained, though tend to be of order magnitude 10^{-2} Sv (Frajka-Williams et al. 2016, and references within). It is likely that the response seen in GCM simulations to freshwater forcing is both model and resolution dependent. As we saw in **Chapter 3**, 0.2 Sv of hosing reduced the strength of the AMOC in FAMOUS by 50%, while the same forcing in HadGEM3-GC2 gave a 75% reduction in AMOC strength. The quantity of freshwater added and resultant magnitude of AMOC weakening should therefore not necessarily be taken too literally, instead the focus should be on dynamics and relationships observed within the models. Due to concerns that climate models may be artificially stable and less responsive to forcing as compared with the real Earth-system, it is logical to use exaggerated forcing scenarios in order to understand the mechanical processes possible. While the 1.0 Sv run is perhaps best considered as testing the parameter space,

the consequences of the lower hosing rate scenarios need to be given careful consideration.

In the observational and paleoclimatological literature AMOC hysteresis has only been associated with glacial periods (see **Section 1.2.1.1)**. The idea of anthropogenic climate change being able to induce interglacial AMOC hysteresis therefore requires extreme additional forcing – significantly beyond that which is projected. In **Chapter 2**, there was no indication of hysteresis in FAMOUS despite a previous study using FAMOUS having identified hysteresis (Hawkins et al. 2011). This is partly explained by the focus in **Chapter 2** on AMOC weakening and recovery. Hosing rates of 0.2 and 0.5 Sv were used while Hawkins et al. (2011) continued to significantly higher hosing rates. In addition there was an important methodological difference. Hawkins et al. (2011) conserved net freshwater using 'surface compensation', where the salinity removed from the hosing region to achieve the 'freshening' is returned evenly over the surface of the global ocean. In this study we used 'volume compensation', where the salinity removed from the hosing region is returned evenly over the full volume of the global ocean. The choice of salinity compensation has been shown to impact global density stratification and AMOC response to freshwater forcing in FAMOUS (Jackson et al. 2017). If compensation is applied throughout the volume of the global ocean, rather than at the surface, the region of hysteresis is much narrower (in fact the AMOC is virtually mono-stable – see Fig. 2b of Jackson et al. 2017). We used volume compensation because it does not introduce spurious dynamics, its principle effect being due to the small non-linearity in haline contraction, comparable to the effect of surface compensation on stratification. Therefore, we were not expecting our simulations to behave as in Hawkins et al. (2011).

In **Chapter 4** the non-recovering HadGEM3-GC2 runs remained weak for a significant time after hosing was removed. It is important here to highlight the distinction between the non-recovering runs and the permanently hosed runs. From an initial strength of 14 Sv, permanent hosing at all hosing rates reduced the AMOC to below 4 Sv, however the non-recovering runs remained at intermediate strengths of ~7 Sv. As we have seen, the reason for the AMOC remaining weak was due to changes in atmospheric forcing on the ocean, and the

result of a feedback. This does not evidence the existence of a second attractor or bistability, and the non-recovering state is therefore likely to be only quasi-stable.

5.3 Future work

As is the nature of science, for every result new questions arise. Over the course of my doctoral research there have been many interesting results and questions which given more time I would have liked to investigate further. Below I will discuss some of my ideas for directions that I would like to take my research in. Some of the interesting findings presented in this thesis would benefit from further investigation of robustness and validation of methodology, so I have also suggested some ways that this could be approached.

It is possible that heavier hosing rates in FAMOUS (0.6 Sv and greater) may have been able to result in AMOC non-recovery (Jackson et al. 2017). However, it may in addition require alteration of the Atlantic salinity transports – to alter the salt advective feedback through the Atlantic basin. In the FAMOUS simulations presented, F_{ov} at 30˚S remained positive throughout the hosing part of the simulations, while non-recovery is associated with negative F_{ov}. This could be adjusted by applying a flux correction in the South Atlantic, to push the AMOC into a bistable regime. It has previously been found that adding such a salinity flux adjustment changes the freshwater flux being imported into the Atlantic basin, and the response of the AMOC to hosing (De Vries and Weber 2005; Cimatoribus et al. 2012). This may be considered as moving the initial position of the simulation on the hysteresis diagram, from a stable to a bistable state. Jackson (2013) found that applying such a flux adjustment in HadGEM3 resulted in the AMOC recovering later and at a slower rate than it did without flux adjustment.

All experiments, in both models, used the same broad hosing region and design, making it easier to compare between runs. It would be interesting to experiment

with varying the hosing regime and setup in both models to explore the how this would impact the mechanisms and feedbacks which were seen. Initial exploration of the parameter space in FAMOUS indicated that the AMOC recovered at the same rate following the removal of hosing after 200, 400, or 600 years of hosing – with larger overshoots for longer durations of hosing, it would be interesting to see if these results could be replicated in HadGEM3-GC2. If the freshwater hosing in HadGEM3-GC2 were limited to the Greenland coastline, mimicking the input from Greenland ice melt, this could impact the area that became covered by a fresh surface cap. This questions whether North Atlantic convection would still be widely reduced or whether the region of maximum convection would shift elsewhere (as Smith and Gregory (2009) found it to in FAMOUS). This would have strong implications for the development of subsurface warming and changes to the surface freshwater flux. It would also be interesting to explore whether the relationship between total freshwater added and impact of changes in temperature and salinity seen in **Chapter 3** would hold if the freshwater hosing had been increased with time in a ramp-up experimental design.

Experimenting with different forcing, including altering radiative and wind forcing and using more localised freshwater forcing, could be used to compare the effectiveness of the Butler et al. (2016) method and volume mean density method in attributing control of AMOC weakening to salinity or temperature. Where, if the Butler et al. (2016) method was genuinely better at representing the impact of density changes on the deep pressure gradients it would reconstruct the AMOC well regardless of the forcing approach, whereas the volume mean approach may respond differently to different forcing approaches. The impact of changes in temperature and salinity on the strength of the AMOC could also be estimated from geostrophy at 50˚N, comparing the results of this with the results presented in **Chapter 3**. This comparison may favour one method over the other. A preliminary look at the changes in temperature and salinity across the Atlantic basin at 50˚N suggest that the pycnocline was flattened (not shown), suggesting that this could be an effective approach.

The recovering runs in HadGEM3-GC2 generally end when the AMOC first recovers its initial strength, or a little before. While this was sufficient for the analysis in **Chapter 4**, it would be very interesting to run these experiments on

further to see whether the AMOC overshoots. If there was an overshoot, I would want to break down the contribution of AMOC enhancement between the North and South Atlantic, to see whether a southern contribution similar to that seen for FAMOUS in **Chapter 2** is also present in HadGEM3-GC2. While this was lead by South Atlantic freshening in FAMOUS, there is indication of southern warming in HadGEM3-GC2 that may play a similar role. This would be very helpful for understanding the full consequences of temporary forcing, and examining the timescales of recovery for density distribution and pycnocline depths.

Previous studies have identified damaging European climate impacts of AMOC weakening. **Chapter 2** shows that due to asymmetry and overshoot, the recovery phase could result in faster and stronger climate changes than the weakening phase. Some of the changes in ocean state and atmospheric response seen in these studies are significant and would be expected to impact weather and climate, with consequences for society. It would therefore seem important to explore these further. The need for climate change mitigation has generally been seen here in relation to avoiding non-recovery of the AMOC. The importance of avoiding non-recovery can be exemplified by studies of the climate impact of a long-term weak AMOC (Vellinga and Wood 2002, 2008; Jackson et al. 2015). However, the climate impacts of a weakening and recovery of the AMOC may also be significant – especially in terms of 'rate of change' of meridional heat transport in the event of an AMOC overshoot. It would be particularly interesting to look at this with reference to 'critical thresholds' in infrastructure and agricultural adaptation – to understand what rate/extent of weakening would be manageable, and whether there is an 'ideal' rate of mitigation, which would effectively prevent damaging levels of AMOC weakening without resulting in damaging impacts from an overly rapid recovery.

To explore the full series of impacts from initial forcing to societal impact, a regional climate model could be 'nested' within a GCM of reasonably high complexity, such as HadGEM3-GC2. In this way, the GCM could be used to represent the full global impacts, including the longer-timescale readjustments, such as changes in the pycnocline depths. The output would be used to give time-varying boundary conditions for a high-resolution regional climate model – to form a 'street level' view of how changes in precipitation, temperature, and

storm activity would vary over a region such as the UK through the weakening and recovery of the AMOC. These ‘street level’ results could then be used with vulnerability and loss models used by the reinsurance sector, in order to understand the economic impact associated with different AMOC forcing regimes. This work would have 2 primary benefits: firstly, it would give a numerical basis in terms of human impact to help guide an understanding of acceptable/unacceptable changes in the AMOC. Secondly, it would enable the communication of AMOC research in terms more meaningful to policy makers, making findings both more approachable and more actionable.

List of References

Adkins JF (2013) The role of deep ocean circulation in setting glacial climates. 28(September):539–561. http://doi.org/10.1002/palo.20046

Ahn J, Brook E (2014) Siple Dome ice reveals two modes of millennial CO_2 change during the last ice age. Nature Communications https://doi.org/10.1038/ncomms4723, 5(1), 3723

Ansorge IJ, Baringer M, Campos EJD, Dong S, Fine RA, Garzoli SL, Goni G, Meinen CS, Perez RC, Piola AR, Roberts MJ, Speich S, Sprintall J, Terre T, Van den Berg MA (2014) Basin-wide oceanographic array bridges the South Atlantic. Eos 95: 53–54.

Bakker P, Schmittner A, Lenaerts JTM, Abe-Ouchi A, Bi D, Broeke MR, Chan W-L, Hu A, Beadling RL, Marsland SJ, Mernild SH, Saenko OA, Swingedouw D, Sullivan A, Yin J (2016) Fate of the Atlantic Meridional Overturning Circulation – Strong decline under continued warming and Greenland melting. Geophys Res Lett 43(23):12252–12260. http://doi.org/10.1002/2016GL070457

Bitz CM, Chiang JCH, Cheng W, Barsugli JJ (2007) Rates of thermohaline recovery from freshwater pulses in modern, Last Glacial Maximum, and greenhouse warming climates. Geophys Res Lett 34:L07708. http://doi:10.1029/2006GL029237.

de Boer AM, Nof D (2004) The exhaust valve of the North Atlantic. J Clim 17(3):417–422.

de Boer AM, Gnanadesikan A, Edwards NR, Watson AJ (2010) Meridional Density Gradients Do Not Control the Atlantic Overturning Circulation. J Phys Oceanogr 40(2):368–380. http://doi.org/10.1175/2009JPO4200.1

Boulton CA, Allison LC, Lenton TM (2014) Early warning signals of Atlantic Meridional Overturning Circulation collapse in a fully coupled climate model. Nat Commun 5. http://doi.org/10.1038/ncomms6752.

Bouttes N, Gregory JM, Lowe JA (2013) The reversibility of sea level rise. J Clim 26:2502–2513. doi:10.1175/JCLI-D-12-00285.1

Bouttes N, Good P, Gregory JM, Lowe JA (2015) Non-linearity of ocean heat uptake during warming and cooling in the FAMOUS climate model. Geophys Res Lett 42:2409–2416.

Brady EC, Otto-Bliesner BL (2011) The role of meltwater-induced subsurface ocean warming in regulating the Atlantic meridional overturning in glacial climate simulations. Clim Dyn 37(7–8):1517–1532. http://doi.org/10.1007/s00382-010-0925-9

Brodeau L, Koenigk T (2016) Extinction of the northern oceanic deep convection in an ensemble of climate model simulations of the 20th and 21st centuries. Clim Dyn 46(9):2863–2882. http://doi.org/10.1007/s00382-015-2736-5

Brunnabend SE, Dijkstra HA (2017) Asymmetric response of the Atlantic Meridional Ocean Circulation to freshwater anomalies in a strongly-eddying global ocean model. Tellus A: Dynamic Meteorology and Oceanography 69:1:1299283. DOI: 10.1080/16000870.2017.1299283

Bryan F (1987) Parameter sensitivity of primitive equation ocean general circulation models. J Phys Oceanogr 17:970–985.

Bryden HL, Longworth HR, Cunningham SA (2005) Slowing of the Atlantic meridional overturning circulation at 25 degrees N. Nature 438:655-657. doi:10.1038/nature04385

Bryden H (2011) South Atlantic overturning circulation at 24 S. J Mar Res 69(1):38–55(18).

Buckley MW, Marshall J (2016) Observations, inferences, and mechanisms of Atlantic Meridional Overturning Circulation variability: A review. Rev Geophys 54. doi:10.1002/2015RG000493

Butler ED, Oliver KIC, Hirschi JJM, Mecking JV (2016) Reconstructing global overturning from meridional density gradients. Clim Dyn 46(7–8):2593–2610. http://doi.org/10.1007/s00382-015-2719-6.

Cao L, Duan L, Bala G, Caldeira K (2016) Simulated long-term climate response to idealized solar geoengineering. Geophys Res Lett 43(5):2209–2217. http://doi.org/10.1002/2016GL068079.

Cimatoribus AA, Drijfhout SS, den Toom M, Dijkstra HA (2012) Sensitivity of the Atlantic meridional overturning circulation to south Atlantic freshwater anomalies. Clim Dyn 39:2291–2306.

Cimatoribus AA, Drijfhout SS, Dijkstra HA (2014) Meridional overturning circulation: Stability and ocean feedbacks in a box model. Clim Dyn 42:311–328.

Clark PU, Pisias NG, Stocker TF, Weaver AJ (2002) The role of the thermohaline circulation in abrupt climate change. Nature 415(6874):863–869.

Collins M, Knutti R, Arblaster J, Dufresne J-L, Fichefet T, Friedlingstein P, Gao X, Gutowski WJ, Johns T, Krinner G, Shongwe M, Tebaldi C, Weaver AJ Wehner M (2013) Long-term Climate Change: Projections, Commitments and Irreversibility. In: Climate Change 2013: The Physical Science Basis. Contribution of Working Group I to the Fifth Assessment Report of the Intergovernmental Panel on Climate Change Cambridge University Press, Cambridge, United Kingdom and New York, NY, USA.

Crowley T (1992) North Atlantic Deep Water Cools the Southern Hemisphere. Paleoceanography 7:489–497.

Dansgaard W, Johnsen SJ, Clausen HB, Dahl-Jensen D, Gundestrup NS, Hammer CU, Hvidberg CS, Steffensen JP, Sveinbjornsdottir AE, Bond G (1993) Evidence for general instability of past climate from a 250-kyr ice-core record. Nature 364(6434):218–220

Delaney CA (2003) The Last Glacial Stage (the Devensian) in Northwest England. Northwest Geography 3:1476-1580.

Dijkstra, HA (2007) Characterization of the multiple equilibria regime in a global ocean model. Tellus 59A 695-705.

Dima, M., Lohmann, G., Knorr, G. (2018) North Atlantic Versus Global Control on Dansgaard- Oeschger Events, 991–998. http://doi.org/10.1029/2018GL080035

Driesschaert E, Fichefet T, Goosse H, Huybrechts P, Janssens I, Mouchet A, Munhoven G, Brovkin V, Weber SL (2007) Modeling the influence of Greenland ice sheet melting on the Atlantic meridional overturning circulation during the next millennia. Geophys Res Lett 34(10):1–5. http://doi.org/10.1029/2007GL029516.

Drijfhout S, van Oldenborgh GJ, Cimatoribus A (2012) Is a decline ofAMOC causing the warming hole above the North Atlantic in observed and modeled warming patterns? J Clim. 25:8373–79.

Emile-Geay J, Madec G (2008) Geothermal heating, diapycnal mixing and the abyssal circulation. Ocean Science 5(2):203–217. http://doi.org/10.5194/osd-5-281-2008

Feng QY, Viebahn JP, Dijkstra HA (2014) Deep ocean early warning signals of an Atlantic MOC collapse. Geophys Res Lett 41:6008–6014. doi:10.1002/2014GL061019

Frajka-Williams E, Bamber JL, Vaage K (2016) Greenland melt and the Atlantic meridional overturning circulation. Oceanogr 29(4):22–33. https://doi.org/10.5670/oceanog.2016.96.

Ganachaud A, Wunsch C (2000) Improved estimates of global ocean circulation, heat transport and mixing from hydrographic data. Nature 408(6811):453–457.

Garzoli SL, Baringer MO, Dong S, Perez RC, Ya Q (2013) South Atlantic meridional fluxes. Deep-Sea Res I 71:21-32.

Gent PR, McWilliams JC (1990) Isopycnal mixing in ocean circulation models. J Phys Oceanogr 20(1):150–155

Gierz P, Lohmann G, Wei W (2015) Response of Atlantic overturning to future warming in a coupled atmosphere-ocean-ice sheet model. Geophys Res Lett 42(16):6811–6818. http://doi.org/10.1002/2015GL065276.

Gillett NP, Arora VK, Zickfeld K, Marshall SJ, Merryfield, WJ (2011) Ongoing climate change following a complete cessation of carbon dioxide emissions. Nat Geosci 4:83–87. doi:10.1038/ngeo1047

Gnanadesikan A (1999) A simple predictive model for the structure of the oceanic pycnocline. Science 283:2077–2079.

Gordon C, Cooper C, Senior CA, Banks H, Gregory JM, Johns TC, Mitchell JFB, Wood R (2000) The simulation of SST, sea ice extents and ocean heat transports in a version of the Hadley Centre coupled model without flux adjustments. Clim Dyn 16:147–168.

Gregory JM, Saenko OA, Weaver AJ (2003) The role of the Atlantic freshwater balance in the hysteresis of the meridional overturning circulation. Clim Dyn 21(7-8):707–717. http://doi.org/10.1007/s00382-003-0359-8.

Gregory JM, Huybrechts P, Raper SCB (2004) Threatened loss of the Greenland ice-sheet. Nature 428(April):2513–2513. http://doi.org/10.1038/nature02512.

Gregory JM, Dixon KW, Stouffer RJ, Weaver AJ, Driesschaert E, Eby M, Fichefet T, Hasumi H, Hu A, Jungclaus JH, Kamenkovich IV, Levermann A, Montoya M, Murakami S, Nawrath S, Oka A, Sokolov AP, Thorpe RB (2005) A model

intercomparison of changes in the Atlantic thermohaline circulation in response to increasing atmospheric CO_2 concentration. Geophys Res Lett 32(12):1–5. http://doi.org/10.1029/2005GL023209.

Gregory JM, Tailleux R (2011) Kinetic energy analysis of the response of the Atlantic meridional overturning circulation to CO_2-forced climate change. Clim Dyn 37(5):893–914. http://doi.org/10.1007/s00382-010-0847-6.

Hand E (2016) New scrutiny for a slowing Atlantic conveyor. Science 352:751-752. doi: 10.1126/science.352.6287.751

Haskins RK, Oliver KIC, Jackson LC, Drijfhout SS, Wood RA (2018) Explaining asymmetry between weakening and recovery of the AMOC in a coupled climate model. Clim Dyn 0(0):1–13. http://doi.org/10.1007/s00382-018-4570-z

Haskins RK, Oliver KIC, Jackson LC, Wood RA, Drijfhout SS (2019) Temperature domination of AMOC weakening due to freshwater hosing in two GCMs. Clim Dyn 0(0):1–14. https://doi.org/10.1007/s00382-019-04998-5

Hawkins E, Smith RS, Allison LC, Gregory JM, Woollings TJ, Pohlmann H, De Cuevas B (2011) Bistability of the Atlantic overturning circulation in a global climate model and links to ocean freshwater transport. Geophys Res Lett 38(10):1–6.

Heinrich H (1988) Origin and consequences of cyclic ice rafting in the northeast Atlantic Ocean during the past 130,000 years. Quat Res 29:142–152.

Held H, Kleinen T (2004) Detection of climate system bifurcations by degenerate fingerprinting. Geophys Res Lett 31:L23207. http://doi.org/10.1029/2004GL020972

Henry LG, Henry LG, McManus JF, Curry WB, Roberts NL, Piotrowski AM, Keigwin LD (2016) North Atlantic ocean circulation and abrupt climate change during the last glaciation. Science 5529:470-474. http://doi.org/10.1126/science.aaf5529

Hofmann M, Maqueda MAM (2009) Geothermal heat flux and its influence on the oceanic abyssal circulation and radiocarbon distribution. Geophys Res Lett 36(3):1–4. http://doi.org/10.1029/2008GL036078.

Hogg AM, Dijkstra HA, Saenz JA (2012) The Energetics of a Collapsing Meridional Overturning Circulation. Journal of Physical Oceanography 43:1512-1524. http://doi.org/10.1175/JPO-D-12-0212.1

Hu, A, Meehl GA, Otto-Bliesner BL, Waelbroeck C, Han W, Loutre MF, Lambeck K, Mitrovica JX, Rosenbloom N (2010) Influence of Bering Strait flow and North Atlantic circulation on glacial sea level changes. Nat. Geosci., 3, 118–121, doi:10.1038/ngeo729

Hu A, Meehl GA, Han W, Abe-Ouchi A, Morrill C, Okazaki Y, Chikamoto MO (2012a) The Pacific-Atlantic seesaw and the Bering Strait. Geophys Res Lett 39(3):1–6. http://doi.org/10.1029/2011GL050567

Hu A, Meehl GA, Han W, Timmermann A, Otto-Bliesner B, Liu Z, Washington WM, Large W, Abe-Ouchi A, Kimoto M, Lambeck K, Wu B (2012b) Role of the Bering Strait on the hysteresis of the ocean conveyor belt circulation and glacial climate stability. Proc Nat Acad Sci 109(17):6417–6422. https://doi.org/10.1073/pnas.11160 14109.

Huisman SE, den Toom M, Dijkstra HA, Drijfhout SS (2010) An indicator of the multiple equilibria regime of the Atlantic meridional overturning circulation. J Phys Oceanogr 40:551–567.

Jacob D, Goettel H, Jungclaus J, Muskulus M, Podzun R, Marotzke J (2005) Slowdown of the thermohaline circulation causes enhanced maritime climate influence and snow cover over Europe. Geophys Res Lett 32(21):1–5. http://doi.org/10.1029/2005GL023286

Jackson LC (2013) Shutdown and recovery of the AMOC in a coupled global climate model: The role of the advective feedback. Geophys Res Lett 40(6):1182–1188. http://doi.org/10.1002/grl.50289.

Jackson LC, Schaller N, Smith RS, Palmer MD, Vellinga M (2014) Response of the Atlantic meridional overturning circulation to a reversal of greenhouse gas increases. Clim Dyn. doi:10.1007/s00382-013-1842-5.

Jackson LC, Kahana R, Graham T, Ringer MA, Woollings T, Mecking JV, Wood RA (2015) Global and European climate impacts of a slowdown of the AMOC in a high resolution GCM. Clim Dyn 45:3299–3316. http://doi:10.1007/s00382-015-2540-2.

Jackson LC, Peterson KA, Roberts CD, Wood RA (2016) Recent slowing of Atlantic overturning circulation as a recovery from earlier strengthening. Nature Geoscience 9(7):518–522. http://doi.org/10.1038/ngeo2715.

Jackson LC, Smith RS, Wood RA (2017) Ocean and atmosphere feedbacks affecting AMOC hysteresis in a GCM. Clim Dyn 49: 173. https://doi.org/10.1007/s00382-016-3336-8

Jackson LC, Wood RA (2018a) Timescales of AMOC decline in response to fresh water forcing. Clim Dyn 51(4):1333–1350. http://doi.org/10.1007/s00382-017-3957-6

Jackson LC, Wood RA (2018b) Hysteresis and resilience of the AMOC in an eddy-permitting GCM. Geophys Res Lett 45:8547-8556. https://doi.org/10.1029/2018GL078104

Johnson HL, Marshall DP, Sproson DAJ (2007) Reconciling theories of a mechanically driven meridional overturning circulation with thermohaline forcing and multiple equilibria. Clim Dyn 29:821–836.

Jones C (2003) A fast ocean GCM without flux adjustments. J Atmos Oceanic Technol 20:1857–1868. doi:10.1175/1520-0426(2003)020<1857:AFOGWF>2.0.CO;2

Jungclaus JH, Haak H, Esch M, Roeckner E, Marotzke J (2006) Will Greenland melting halt the thermohaline circulation? Geophys Res Lett 33(17):1–5. http://doi.org/10.1029/2006GL026815.

Jungclaus JH, Lohmann K, Zanchettin D (2014) Enhanced 20th-century heat transfer to the Arctic simulated in the context of climate variations over the last millennium. Climate of the Past 10(6):2201–2213. https://doi.org/10.5194/cp-10-2201-2014

Koenigk T, Brodeau L (2014) Ocean heat transport into the Arctic in the twentieth and twenty-first century in EC-Earth. Clim Dyn 42(11):3101–3120. https://doi.org/10.1007/s00382-013-1821-x

Körper J, Spangehl T, Cubasch U, Huebener H (2009) Decomposition of projected regional sea level rise in the North Atlantic and its relation to the AMOC. Geophys Res Lett 36(19):1–5. http://doi.org/10.1029/2009GL039757.

Kleinen T, Osborn T, Briffa K (2009) Sensitivity of climate response to variations in freshwater hosing location. Ocean Dyn 59(3):509–521. http://doi.org/10.1007/s10236-009-0189-2.

Krebs U, Timmermann A (2007) Fast advective recovery of the Atlantic meridional overturning circulation after a Heinrich event. Paleoceanography 22(1):1–9. http://doi.org/10.1029/2005PA001259

Lambeck K, Chappell J (2001) Sea level change through the last glacial cycle. Science 292:679–686. doi:10.1126/science.1059549.

Levermann A, Griesel A, Hofmann M, Montoya M, Rahmstorf S (2005) Dynamic sea level changes following changes in the thermohaline circulation. Clim Dyn 24(4):347–354. http://doi.org/10.1007/s00382-004-0505-y.

Liu W, Liu Z (2013) A diagnostic indicator of the stability of the Atlantic meridional overturning circulation in CCSM3. J Clim 26 1926-1938.

Liu W, Liu Z, Hu A (2013) The stability of an evolving Atlantic meridional overturning circulation. Geophys Res Lett 40 1562-1568.

Liu W, Liu Z (2014) A Note on the Stability Indicator of the Atlantic Meridional Overturning Circulation. J Clim 27 969-975.

Liu W, Xie S-P, Liu Z, Zhu J (2017) Overlooked possibility of a collapsed Atlantic Meridional Overturning Circulation in warming climate. Sci Advances 3 e1601666.

Liu W, Fedorov AV (2019) Global impacts of Arctic sea ice loss mediated by the Atlantic meridional overturning circulation. Geophys Res Lett 46:944–952. https://doi.org/ 10.1029/2018GL080602

Lozier MS, Li F, Bacon S, Bahr F, Bower AS, Cunningham SA, de Jong MF, de Steur L, deYoung B, Fischer J, Gary SF, Greenan BJW, Holliday NP, Houk A, Houpert L., Inall ME, Johns WE, Johnson HL, Johnson C, Karstensen J, Koman G, Le Bras IA, Lin X, Mackay N, Marshall DP, Mercier H, Oltmanns M, Pickart RS, Ramsey AL, Rayner D, Straneo F, Thierry V, Torres DJ, Williams RG, Wilson C, Yang J, Yashayaev I, Zhao J (2019) A sea change in our view of overturning in the subpolar North Atlantic. Science 363(6426): 516-521. https://doi.org/ 10.1126/science.aau6592

Lumpkin R, Speer K (2003) Large-scale vertical and horizontal circulation in the North Atlantic Ocean. J Phys Oceanogr 33(9):1902–1920. https://doi.org/ 10.1175/1520-0485(2003)033<1902:LVAHCI>2.0.CO;2.

Lumpkin R, Speer K (2007) Global ocean meridional overturning. J Phys Oceanogr 37(10):2550–2562. https://doi.org/ 10.1175/JPO3130.1.

Manabe S, Stouffer RJ (1997) Coupled ocean-atmosphere model response to freshwater input: Comparision to Younger Dryas event. Paleoceanography 12(2):321–336.

Marotzke J (1997) Boundary mixing and the dynamics of three-dimensional thermohaline circulations. J Phys Oceanogr 27:1713–1728.

Marotzke J (2000) Abrupt climate change and thermohaline circulation: mechanisms and predictability. Proceedings of the National Academy of Sciences of the United States of America 97(4):1347–1350. http://doi.org/10.1073/pnas.97.4.1347.

McCarthy GD, Smeed DA, Johns WE, Frajka-Williams E, Moat BI, Rayner D, Baringer MO, Meinen CS, Collins J, Bryden HL (2015) Measuring the Atlantic Meridional Overturning Circulation at 26°N. Prog Oceanogr 130:91–111. doi:10.1016/j.pocean.2014.10.006.

McManus JF, Francois R, Gherardi J-M, Keigwin LD, Brown-Leger S (2004) Collapse and rapid resumption of Atlantic meridional circulation linked to deglacial climate changes. Nature 428(6985):834–837. http://doi.org/10.1038/nature02494

Mecking JV, Drijfhout SS, Jackson LC, Graham T (2016) Stable AMOC off state in an eddy-permitting coupled climate model. Clim Dyn 47(7):2455–2470. http://doi.org/10.1007/s00382-016-2975-0

Meehl GA, Washington WM, Collins WD, Arblaster JM, Hu A, Buja LE, Strand WG, Teng H (2005) How much more global warming and sea level rise? Science 307:1769–1772. doi:10.1126/science.1106663

Megann A, Storkey D, Aksenov Y, Alderson S, Calvert D, Graham T, Hyder P, Siddorn J, Sinha B (2014) GO5.0: the joint NERCMet Office NEMO global ocean model for use in coupled and forced applications. Geosci Model Dev 7(3):1069–1092. http://doi:10.5194/gmd-7-1069-2014

Mignot J, Ganopolski A, Levermann A (2007) Atlantic subsurface temperatures: Response to a shutdown of the overturning circulation and consequences for its recovery. J Clim 20(19):4884–4898. http://doi.org/10.1175/JCLI4280.1

Mikolajewicz U, Vizcaíno M, Jungclaus J, Schurgers G (2007) Effect of ice sheet interactions in anthropogenic climate change simulations. Geophys Res Lett 34(18):1–5. http://doi.org/10.1029/2007GL031173.

Nakashiki N, Kim D-H, Bryan FO, Yoshida Y, Tsumune D, Maruy- ama K, Kitabata H (2006) Recovery of thermohaline circulation under CO_2 stabilization and overshoot scenarios. Ocean Model 15:200–217. doi:10.1016/j.ocemod.2006.08.007

Negre C, Zahn R, Thomas AL, Masque P, Henderson GM, Martinez-Mendez G, Hall IR, Mas JL (2010) Reversed flow of Atlantic deep water during the Last Glacial Maximum. Nature 468(7320):84–88. http://dx.doi.org/10.1038/nature09508

Oka A, Hasumi H, Abe-Ouchi A (2012) The thermal threshold of the Atlantic meridional overturning circulation and its control by wind stress forcing during glacial climate. 39:1–6. http://doi.org/10.1029/2012GL051421

Oldenburg D, Armour KC, Thompson L, Bitz C (2018) Distinct mechanisms of ocean heat transport into the Arctic under internal variability and climate change. Geophys Res Lett 45:7692–7700. https://doi.org/10.1029/2018GL078719

Oliver KIC, Heywood KJ (2003) Heat and Freshwater Fluxes through the Nordic Seas. Journal of Physical Oceanography 33(5):1009–1026. http://doi.org/10.1175/1520-0485(2003)033<1009:HAFFTT>2.0.CO;2

Oliver KIC, Watson AJ, Stevens DP (2005) Can limited ocean mixing buffer rapid climate change? Tellus, Series A: Dynamic Meteorology and Oceanography 57(4):676–690. http://doi.org/10.1111/j.1600-0870.2005.00119.x

Oltmanns M, Karstensen J, Fischer J (2018) Increased risk of a shutdown of ocean convection posed by warm North Atlantic summers. Nat Clim Change 8:300–304. https://doi.org/10.1038/s41558-018-0105-1

Otterå OH, Drange H, Bentsen M, Jiang D (2003) The sensitivity of the present-day Atlantic meridional overturning circulation to freshwater forcing. Geophys Res Lett 30(17):1–4. http://doi.org/10.1029/2003GL017578.

Peltier WR, Vettoretti G (2014) Dansgaard-Oeschger oscillations predicted in a comprehensive model of glacial climate: A “kicked” salt oscillator in the Atlantic. Geophys Res Lett 41(20):7306–7313. http://doi.org/10.1002/2014GL061413

Pu B, Vizy EK, Cook KH (2012) Warm season response over North America to a shutdown of the Atlantic meridional overturning circulation and CO_2 increases. J Clim 25(19):6701–6720. http://doi.org/10.1175/JCLI-D-11-00611.1

Rahmstorf S (1996) On the freshwater forcing and transport of the Atlantic thermohaline circulation. Clim Dyn 12:799–811.

Rahmstorf S, Marotzke J, Willebrand J (1996) Stability of the thermohaline circulation, in The warm water sphere of the North Atlantic ocean, W. Krauss, Editor. Borntraeger: Stuttgart. p. 129-158.

Rahmstorf S (2000) The thermohaline ocean circulation: A system with dangerous thresholds? An Editorial Comment. Climatic Change 46:247–256.

Roberts WHG, Valdes PJ, Payne AJ (2014) Topography's crucial role in Heinrich Events. Proceedings of the National Academy of Sciences of the United States of America 111(47):16688–93. http://doi.org/10.1073/pnas.1414882111.

Robinson AR (1960) The general thermal circulation in equatorial regions. Deep-Sea Res 6:311–317.

Robinson A, Calov R, Ganopolski A (2012) Multistability and critical thresholds of the Greenland ice sheet. Nat Clim Change 2(6):429–432.

Rugenstein MAA, Winton M, Stouffer RJ, Griffies SM, Hallberg R. (2012) Northern high-latitude heat budget decomposition and transient warming. J Clim 26:609–21.

Saenko OA, Schmittner, A Weaver AJ (2004) The Atlantic-Pacific seesaw. J Clim 17:2033–2038. doi:10.1175/1520-0442(2004)017<2033: TAS>2.0.CO;2

Saenko OA (2013) Energetics of weakening and recovery of the Atlantic overturning in a climate change simulation. Geophys Res Lett 40(5):888–892. http://doi.org/10.1002/grl.50101

Saenz JA, Hogg AM, Hughes GO, Griffiths RW (2012) Mechanical power input from buoyancy and wind to the circulation in an ocean model. Geophys Res Lett 39:L13605. doi:10.1029/2012GL052035

Schmittner A, Latif M, Schneider B (2005) Model projections of the North Atlantic thermohaline circulation for the 21st century assessed by observations. Geophys Res Lett 32:L23710. http://doi:10.1029/2005GL024368.

Sévellec F, Huck T (2016) Geostrophic Closure of the Zonally Averaged Atlantic Meridional Overturning Circulation. J Phys Oceanogr 46(3):895–917. http://doi.org/10.1175/JPO-D-14-0148.1

Sévellec F, Fedorov AV, Liu W (2017) Arctic sea-ice decline weakens the Atlantic Meridional Overturning Circulation. Nat Clim Change 7 604-610.

Sgubin G, Swingedouw D, Drijfhout S, Hagemann S, Robertson E (2015) Multimodel analysis on the response of the AMOC under an increase of radiative forcing and its symmetrical reversal. Clim Dyn 45(5–6):1429–1450. http://doi.org/10.1007/s00382-014-2391-2.

Sijp WP, England MH, Gregory JM (2012a) Precise calculations of the existence of multiple AMOC equilibria in coupled climate models. Part I: Equilibrium states. J Clim 25 282-298.

Sijp WP, Gregory JM, Tailleux R, Spence P (2012b) The key role of the western boundary in linking the AMOC strength to the north-south pressure gradient. J Phys Oceanogr 42:628– 643. http://doi:10.1175/JPO-D-11-0113.1

Skinner LC, Elderfield H (2007) Rapid fluctuations in the deep North Atlantic heat budget during the last glacial period. Paleoceanography 22:PA1205. doi:10.1029/2006PA001338. 1

Smith RS, Gregory JM, Osprey A (2008) A description of the FAMOUS (version XDBUA) climate model and control run. Geosci Model Dev 1(1):53–68. http://doi.org/10.5194/gmd-1-53-2008.

Smith RS, Gregory JM (2009) A study of the sensitivity of ocean overturning circulation and climate to freshwater input in different regions of the North Atlantic. Geophys Res Lett 36(15):1–5. http://doi.org/10.1029/2009GL038607.

Smith RS (2012) The FAMOUS climate model (versions XFXWB and XFHCC): Description update to version XDBUA. Geosci Model Dev 5(1):269–276. http://doi.org/10.5194/gmd-5-269-2012.

Srokosz MA, Bryden HL (2015) Observing the Atlantic Meridional Overturning Circulation yields a decade of inevitable surprises. Science 348(6241):1255575–1255575. http://doi.org/10.1126/science.1255575

Stommel H (1961) Thermohaline convection with two stable regimes of flow. Tellus 13:224–230.

Stouffer RJ, Manabe S (1999) Response of a coupled ocean–atmosphere model to increasing atmospheric carbon dioxide: Sensitivity to the rate of increase. J Clim 12:2224–2237.

Stouffer RJ, Yin J, Gregory JM, Dixon KW, Spelman MJ, Hurlin W, Weaver AJ, Eby M, Flato GM, Hasumi H, Hu A, Jungclaus JH, Kamenkovich IV, Levermann A, Montoya M, Murakami S, Nawrath S, Oka A, Peltier WR, Robitaille DY, Sokolov A, Vettoretti G, Weber SL (2006) Investigating the causes of the response of the thermohaline circulation to past and future climate changes. J Clim 19:1365-1387. http://doi.org/10.1175/JCLI3689.1

Swingedouw D, Braconnot P (2013) Effect of the Greenland Ice-Sheet Melting on the Response and Stability of the AMOC in the Next Centuries. Ocean Circulation: Mechanisms and Impacts - Past and Future Changes of Meridional Overturning, 383–392. http://doi.org/10.1029/173GM24

Timmermann A, Gildor H, Schulz M, Tziperman E (2003) Coherent resonant millennial-scale climate oscillations triggered by massive meltwater pulses. J Clim 16:2569–2585. doi:10.1175/1520-0442(2003)016<2569:CRMCOT>2.0.CO;2

Thibodeau B, Not C, ZHu J, Schmittner A, Noone D, Tabor C, Zhang J, Liu Z (2018) Last century warming over the Canadian Atlantic shelves linked to weak Atlantic meridional overturning circulation. Geophys Res Lett 45:12376–12385. https://doi. org/10.1029/2018GL080083

Thorpe RB, Gregory JM, Johns TC, Wood RA Mitchell JFB (2001) Mechanisms determining the Atlantic thermohaline circulation response to greenhouse gas forcing in a non-adjusted coupled climate model. J Clim 14:3102–3116.

den Toom M, Dijkstra HA, Cimatoribus AA, Drijfhout, SS (2012) Effect of atmospheric feedbacks on the stability of the Atlantic meridional overturning circulation. J Clim. http://doi.org/10.1175/JCLI-D-11-00467.1

Vellinga M, Wood RA (2002) Global climatic impacts of a collapse of the Atlantic thermohaline circulation. Clim Change 54(3):251–267. http://doi.org/10.1023/A:1016168827653.

Vellinga M, Wood RA, Gregory JM (2002) Processes governing the recovery of a perturbed Thermohaline Circulation in HadCM3. J Clim 15:764–780

Vellinga M, Wood RA (2008) Impacts of thermohaline circulation shutdown in the twenty-first century. Climatic Change 91(1-2):43–63. http://doi.org/10.1007/s10584-006-9146-y

Vettoretti G, Peltier WR (2016) Thermohaline instability and the formation of glacial North Atlantic super polynyas at the onset of Dansgaard-Oeschger warming events. Geophys Res Lett 43:5336–5344. doi:10.1002/2016GL068891

de Vries P, Weber SL (2005) The Atlantic freshwater budget as a diagnostic for the existence of a stable shut down of the meridional overturning circulation. Geophys Res Lett 32:L09606.

Wan X, Chang P, Schmidt MW (2010) Causes of tropical Atlantic paleo-salinity variation during periods of reduced AMOC. Geophys Res Lett 37:L04603. doi:10.1029/2009GL042013

Wary M, Eynaud F, Swingedouw D, Masson-Delmotte V, Matthiessen J, Kissel C, Zumaque J, Rossignol L, Jouzel J (2017) Regional seesaw between the North Atlantic and Nordic Seas during the last glacial abrupt climate events. Clim Past 13:729–739. https://doi.org/10.5194/cp-13-729-2017

Weijer W, de Ruijter W, Dijkstra H, van Leeuwen P (1999) Impact of interbasin exchange on the Atlantic overturning circulation. J Phys Oceanogr 29 2266-2284.

Weijer W, De Ruijter W, Dijkstra H (2001) Stability of the Atlantic Overturning Circulation: Competition between Bering Strait Freshwater Flux and Agulhas Heat and Salt Sources. Journal of Physical Oceanography 31:2385–2402.

Williams KD, Harris CM, Camp J, Comer RE, Copsey D, Fereday D, Graham T, Hill R, Hinton T, Hyder P, Ineson S, Masato G, Milton SF, Roberts MJ, Rowell DP, Sanchez C, Shelly A, Sinha B, Walters DN, West A, Woollings T, Xavier PK (2015) The Met Office Global Coupled model 2.0 (GC2) configuration. Geosci Model Dev 88:1509–1524. http://doi.org/10.5194/gmd-88-1509-2015

Wu P, Jackson L, Pardaens A, Schaller N (2011) Extended warming of the northern high latitudes due to an overshoot of the Atlantic meridional overturning circulation. Geophys Res Lett 38:L24704. doi:10.1029/2011GL049998.

Wunsch C, Ferrari R (2004) Vertical Mixing, Energy, and the General Circulation of the Oceans. Annu Rev Fluid Mech 36:281– 314.

Yin J, Schlesinger ME, Andronova NG, Malyshev S, Li B (2006) Is a shutdown of the thermohaline circulation irreversible? J Geophys Res 111(D12):D1104. doi:10.1029/2005jd006562

Yin J, Stouffer RJ (2007) Comparison of the Stability of the Atlantic Thermohaline Circulation in Two Coupled Atmosphere–Ocean General Circulation Models. J Clim 20(17):4293–4315. http://doi.org/10.1175/JCLI4256.1

Yu L, Gao Y, Otterå OH (2016) The sensitivity of the Atlantic meridional overturning circulation to enhanced freshwater discharge along the entire, eastern and western coast of Greenland. Clim Dyn 46(5–6):1351–1369. http://doi.org/10.1007/s00382-015-2651-9

Zhang X, Prange M, Merkel U, Schulz M (2014) Instability of the Atlantic overturning circulation during Marine Isotope Stage 3. Geophys Res Lett 41:4285–4293. doi:10.1002/ 2014GL060321

Zhang R (2015) Mechanisms for low-frequency variability of summer Arctic sea ice extent. Proceedings of the National Academy of Sciences. 112(15):4570–4575. https://doi.org/10.1073/pnas.1422296112 7700

Zhang X, Knorr G, Lohmann G, Barker S (2017) Abrupt North Atlantic circulation changes in response to gradual CO_2 forcing in a glacial climate state. Nature Geoscience 10(7):518–523. https://doi.org/10.1038/ngeo2974